University of applied Sciences Hamburg
Faculty Life Sciences

Master Thesis

Economic optimization of combined electricity feed in and hydrogen production

Study program “Renewable Energy Systems - Environmental and Process Engineering”

Submitted by

Max, Lüdemann

[redacted]

Hamburg

22.12.2023

1. Supervisor: Prof. Dr.-Ing. Sebastian Timmerberg

2. Supervisor: M. Sc. Carsten Schütte

Abstract

This master's thesis introduces a Python-based optimization tool for maximizing annual profits in energy systems. Core components include photovoltaic (PV) systems and inverters, supplemented by modules addressing grid limitations, wind turbines, batteries, hydrogen generation, and daily hydrogen demand. Applying Mixed-Integer-Linear-Programming, the tool ensures practical design sizes, guided by techno-economic parameters drawn from reputable sources.

A case study on the Baltic Sea island of Rügen at a 50-hectare area, reveals that integrating electricity feed in with hydrogen production can be economically advantageous. The optimal system design, achieving an ROI exceeding 5%, features PV, inverters, wind turbines, electrolyzers, compressors, and H2 storage tanks. In every simulated scenario wind turbines are included in the optimized solutions, which indicates an economic advantage of wind turbines over PV in such systems.

Exclusive PV-based hydrogen production is economically viable without daily demand constraints. While limited grid capacity modestly impacts economic indicators, it significantly influences system design. Fluctuations in electricity and H2 prices, along with market data changes, reveal the importance of extended simulations.

Battery systems remain economically unviable, and PV systems with alternative orientations fail to enhance economic outcomes. The conclusion emphasizes the economic feasibility of combining electricity feed-in and hydrogen production, contingent on favorable electricity prices or higher returns from selling renewable H2. A sensitivity analysis highlights the impact of decreasing H2 sales prices, emphasizing the need for comprehensive simulations over extended plant lifetimes for accurate results.

Acknowledgement

I would like to thank everyone who helped and supported me on the way to my degree and my master's thesis. You have all contributed to the successful completion of my thesis.

Special thanks go to my supervisors Prof. Dr. Timmerberg and Carsten Schütte for their dedicated support and the discussions we had together, which always helped to motivate me and take my work to a higher level. Despite many uncertainties, especially at the beginning, Prof. Dr. Timmerberg, gave me the decisive impetus to keep going and to ultimately implement the thesis as it became. I also appreciate the support of Carsten Schütte, who invested a lot of his own time, especially at the end of the editing period, to give me feedback for the final polish of the thesis.

Jens Meincke, I would like to thank you for the freedom you gave me. This enabled me to create my master's thesis in my own individual way. I am also grateful to the staff at Ecovis F&D for the discussions, which have always motivated me.

A big thank you also goes to my friends, who always had an open ear for my thoughts and concerns. I would particularly like to mention Tobias Eichelmann, with whom I was able to have numerous discussions about my thesis. I would also like to thank Amber Kandhari, with whom I spent countless hours in the library.

My family deserves sincere thanks for their unconditional support. Without their encouraging words, patience, and constant encouragement, I would not have been able to pursue my studies the way I did.

And finally, I would like to thank my girlfriend, Hannah Roitsch. Her loving support, her understanding of the many hours I spent in the library and her encouragement have always given me support during the stressful phases of my work, especially in the last days. Her belief in my abilities has made a significant contribution to my success.

Thank you all once again for your valuable help and support!

Table of content

List of Abbreviations

Abbreviation	Explanation
a	Ano
AEL	Alkaline Electrolyzer
CAPEX	Capital Expenditure
°C	Degrees Celsius
EU	European Union
GW	Gigawatt
GWh	Gigawatt hour
h	Hour
H_2	Hydrogen
HHV	Higher Heating Value
IRENA	International Renewable Energy Agency
j	Joule
kg	Kilogram
kW	Kilowatt
kWh	Kilowatt hour
LCOE	Levelized Cost of Electricity
$LCOH_2$	Levelized Cost of Hydrogen
LHV	Lower Heating Value
m	Meter
MILP	Mixed-Integer Linear Programming
MIPNNI	Mixed-Integer Programming
MW	Megawatt
MWh	Megawatt hour
NNI	Non-Negative Integer
NNR	Non-Negative Reals
η	Efficiency
OPEX	Operating Expenditure
PEMEL	Proton Exchange Membrane Electrolyzer
PT	Payback Time
PYOMO	Python Open-Source Modeling and Optimization
PPA	Power Purchase Agreement
PV	Photovoltaic
RE	Renewable Energy
ROI	Return on Investment
SoC	State of Charge
SOEC	Solid Oxide Electrolyzer

SP	Selling Price
TWh	Terawatt hour
w	work

List of Figures

List of Tables

1 Introduction

In the following, the motivation and background, the objective, and the research questions of the conducted master thesis are presented.

1.1 Motivation and Background

In 2015, a total of 195 countries agreed to significantly reduce their emissions that are responsible for climate change as part of the Paris Climate Agreement. The goal is to limit the temperature increase to 1.5 °C compared to pre-industrial times (European Commission, 2016). Renewable hydrogen (H_2) is expected to be a key component in implementing the needed energy transition to achieve this goal, both nationally and globally. In Germany, the goal is to install a total electrolyzer (Ely) capacity of up to 10 GW until 2030 (BMWK, 2023). The operation of these electrolyzers must be economically feasible and fit into the current legal framework. Only then can companies and investors develop H_2 projects and invest to drive the energy transition forward (Staiger and Tanțău, 2020).

Techno-economic studies, model-based simulations, and optimizations of energy systems consisting of renewable energies (RE), electrolyzers, battery and H_2 storage systems, and the electricity grid offer further investment security and ensure the economic viability and thus the successful implementation of H_2 projects (Odenweller et al. 2022). For economic optimization, current techno-economic parameters describing the analyzed energy system must be integrated into an appropriate mathematical model. Such models allow the simulation of different scenarios to understand the impact of different assumptions and parameters on the economic viability of H_2 projects. This holistic approach allows early identification of potential challenges and bottlenecks to ensure long-term economic viability (Urbanucci, 2018).

As part of the master's thesis, an optimization tool is being developed that combines the feed in of electricity from RE into the power grid with the production of H_2 from the same RE in a limited area. The system design that generates the maximum annual profit is determined by the tool. To apply the developed optimization tool, a case study with an area of fifty hectares on the Baltic Sea island of Rügen will be evaluated. In addition, the parameters that have the greatest influence on the results and how strong this influence is will be identified. The knowledge gained from the thesis should enable practice-relevant conclusions to be drawn for the implementation of such energy systems in the future.

1.2 Objective and Research Questions

The goal of the master thesis is to develop a Python-based optimization tool that is able to determine the optimal system design of an energy system that can combine renewable electricity feed in into the power grid and renewable H_2 production under consideration of current techno-economic data. The profitability of the energy system, in terms of profit per year, should be the parameter to be optimized. The tool will be used to analyze different scenarios. The focus will be on identifying scenarios that yield the highest annual profit and evaluating the economic feasibility of integrating electricity feed-in and hydrogen production into a single energy system. Moreover, it is investigated to what extent the integration of individual or combined components, such as wind turbines and batteries, can increase the profitability of an energy system that uses only PV. In addition, the effect of a grid restriction, which limits the input of electricity feed in and the condition that a daily H_2 demand must be covered will be included. Furthermore, it will be analyzed how these different components and constraints affect the solution of the optimization tool related to the system design and the economic feasibility. Finally, the impact of the

electricity price, the Capital Expenditures (*CAPEX*) of the different components, and the H_2 price on the optimization solution will be examined. Overall, the following research questions can be derived from this:

1. Does it economically make sense to integrate electricity feed in with H_2 production in a single energy system?
2. To what extent does the integration of wind turbines and/or batteries into exclusive PV use, along with the constraints of a grid restriction and/or a daily H_2 demand, influence the economic profitability and system design of an energy system that combines renewable electricity feed in and H_2 production?
3. How do the prices of electricity and H_2, as well as the *CAPEX* of individual system components, impact the economic viability and system design of the analyzed energy systems combining electricity feed in and H_2 production?

2 Theoretical Background

In this chapter, the needed theoretical background for the thesis is explained. The chapter covers topics such as requirements for the integration of RE and H_2 in the current energy system, production of RE with a focus on PV and wind turbines, batteries, H_2 production, compressor and storage systems, energy system optimization, and economic assessments of energy systems.

2.1 Requirements for Renewable Energy and Hydrogen

To explain the requirements for integrating RE into the current energy system, it is first necessary to clarify the definition of RE. It can be divided into different areas: electricity, heat, H_2, and other energy carriers. In the following, the focus will be on electricity and H_2. In general, renewable electricity means environmentally friendly energy sources, typically derived from renewable resources such as solar, wind, hydro, geothermal, tidal, biomass, and biofuels (Androniceanu and Sabie, 2022). H_2 produced from renewable electricity sources is also known as green H_2 (BMWi, 2020).

The EU published the Delegated Act on a methodology for renewable fuels of non-biological origin in 2023 to provide a legal framework to produce renewable fuels such as renewable H_2. This issued Delegated Act is a complement to the 2018 issued Directive (EU) 2018/2001 of the European Parliament and the Council on the promotion of the use of energy from renewable sources. The Delegated Act contains, among other things, the definitions that state that H_2 is called renewable H_2 if it is produced in one of the following ways (European Commission, 2023):

Direct connection
If the electrolyzer is directly powered by RE plants without the use of the power grid to produce renewable H_2. Additionally, starting on January 1st, 2028, the RE plant responsible for H_2 production must be built specifically for the operation of the electrolyzer to ensure that existing RE capacity is not used for H_2 production (European Commission, 2023).

Share of RE over 90 % in power grid
Electricity from the power grid can be used to operate an electrolyzer for H_2 production if the grid electricity in this electricity bidding zone has had a RE share of more than 90 % in the last five years. However, the electrolyzer is not allowed to exceed a certain number of operating hours, calculated based on the share of RE in the electricity mix and the annual operating hours (European Commission, 2023).

Using RE from Power Purchase Agreement (PPA)
Electricity can be used from the grid to produce H_2, even if the percentage of RE in the grid is below 90 %, if a PPA contract is established between the operator of the RE plant and the H_2 producer. To be classified as renewable, temporal and geographical correlation principles must be met. This requires that the electricity to be used by the electrolyzer be supplied to the grid by the RE plant in the same month. If the electrolyzer begins operation after December 31, 2029, the electricity consumed from the electrolyzer must have been fed into the grid during the same hour. Additionally, the RE plant needs to be located in the same bidding zone, in a neighboring area with higher electricity prices, or in a neighboring offshore bidding zone (European Commission, 2023).

Avoiding the shutdown of RE plants

If electricity is used, which would be shut off due to the redispatch mechanism, to produce H_2, it will be considered renewable H_2. To prevent power grid overloads, electrolyzers can utilize the amount of electricity that would usually be shut off by the redispatch mechanism. It guarantees the most effective use of accessible RE capability, thereby helping to ensure grid stability.

Another requirement to integrate RE is the location of the plants. This includes the necessary available area for the plants, and there must be a suitable possibility to connect the plants to the power grid (Quaschning, 2019).

The demand for land for RE is high, and in Germany, land is only available in limited quantities. For this reason, for each potential area, the demand should be exactly examined to see how it can be used for RE. This means how much capacity can be installed and how much power can be fed into the grid on site with the installed capacity. (Ponitka and Boettner, 2020). In addition, the operation of RE plants must be economical in order to reduce emissions in the long term and successfully drive forward the energy transition (Androniceanu and Sabie, 2022). The electricity market price and how it is set is one of the key factors in the economic operation of RE systems, as it has a direct impact on the plant's profit. Therefore, a brief explanation of the electricity market and how it works is provided in the following.

In Europe, the electricity market is segmented into regions with uniform prices, known as price zones. In this thesis takes a closer look at the German island of Rügen. So, the German and Luxembourg price zone plays an important role because the prices in this price zone are valid for everyone who wants to buy electricity on the exchange market in this area (Bundeskartellamt and Bundesnetzagentur, 2022). The exchange market seeks to create a balance between supply and demand. To achieve that, the different electricity suppliers are sorted according to their provision costs, which creates the so-called merit order. Now it depends on how much electricity the suppliers can supply. All suppliers, sorted from the cheapest upwards, can sell their electricity until the energy demand is covered. Consequently, the electricity exchange price corresponds to the cost required by the most expensive producer involved in the supply to meet the energy demand. In the electricity market, this principle is used to set electricity prices at the exchange market. This leads to variable electricity prices throughout the day and throughout the year, depending on the supply and demand of electricity, and gives incentives to produce cheap energy (Bundesnetzagentur, 2023).

However, it is essential to acknowledge that there are numerous additional requirements and complexities associated with the complete integration of RE into the current energy system. While these considerations are significant in the broader context of the sustainable energy transition, it is beyond the scope of this thesis to go into all of them comprehensively.

2.2 Electricity Production: Photovoltaic and Wind turbine

In this section, the principles of RE production will be explained. The focus will be on the generation of electricity via PV systems and wind turbines, because these are the technologies used in the thesis.

Photovoltaic (PV)

A PV module consists of many individual solar cells. These solar cells are made of a semiconductor material that absorbs light, thereby releasing electrons and generating an electrical potential. A direct conversion of solar radiation into electricity takes place. The principle behind this phenomenon is based on the photoelectric effect (Quaschning, 2019).

Basically, a PV system consists of solar cells integrated into modules. The modules are mounted on mounting structures, are oriented in a celestial direction, and have a specific tilt angle. Since alternating current is mostly needed, for example, to feed electricity into the grid, the direct current must be converted into alternating current. This is done by inverters, which can convert direct current to alternating current with an efficiency of around 97 % (ABB, 2014; Huawei, 2023; Quaschning, 2019).

This thesis is primarily focused on the combination of renewable power generation plants, inverter, battery storage, and H_2 production. It is essential to scale the components appropriately to achieve optimal overall performance for the system. The maximum total power of the inverters must be adjusted to the total power of the energy system. Therefore, an important aspect is to adapt the right capacity of the inverters and the right capacity of the battery with the appropriate power to the planned PV system in order to not oversize or undersize single parts of the whole system (Hernández-Callejo et al., 2019).

To get a understanding of how much electricity could be harvested from a PV plant at a specific place with a specific angle and orientation of the modules, the full load hours value, or capacity factor, is used. The full-load hours represent the number of hours in a year that a PV system would have to produce at its rated power to achieve the same annual yield as it achieves in real-world operation with frequent part-load and nighttime shutdowns. That means the full load hours differ over the years because of the weather which is different everywhere in the world. Same for the capacity factor, which indicates the ratio of annual full load hours to the 8760 hours of a year (Quaschning, 2019). PV plants in northern Germany have capacity factors of around 10 % over a year. That means the plant works 10 % of the year at full load. A typical value in Germany for full load hours is 900 to 1000 hours per year (Fraunhofer ISE, 2023a). Another point that is relevant for the planning of PV systems is the amount of area required to build it. According to the “Umweltbundesamt”, one hectare of land is needed to install one megawatt peak of PV capacity (Umweltbundesamt, 2023).

Wind Turbine

Another way to generate renewable electricity is by using wind turbines. There, solar energy is used as well, but in an indirect way. The sun creates temperature differences on the earth, which in turn creates wind. This wind can be harvested and converted into electricity with the help of wind turbines. The kinetic energy of the wind spins the rotors of the wind turbine. The rotors rotate and run a generator, which converts the kinetic energy of the rotation into electrical energy. The amount of energy that can be extracted from the wind depends primarily on the wind speed and the area covered by the rotor blades. The wind speed itself depends on the location and the height, as higher wind speeds are available at higher altitudes. In addition to the rotor blades and the generator, a wind turbine consists of several other components, including the tower, the nacelle, the rotor hub, depending on the technology used, a gearbox, control and measurement systems, and a foundation structure. There are also other types of wind turbines with less or more than three rotor blades or a vertical axis of rotation, such as the Darrieus rotor,

but in this thesis, wind turbines with a horizontal axis of rotation are referred to (Almutairi et al., 2021; Quaschning, 2019).

Furthermore, to get an understanding of how much energy could be harvested from a wind turbine at a specific place at a specific height, the full load hours value or the capacity factor is also used. Onshore wind turbines in Germany have capacity factors of 20 to 35 % over a year, depending on the location. That means a wind turbine in Germany has around 1,800 to 3,200 full load hours (Statista, 2021). Each wind turbine requires about 0.4 to 0.5 hectares of land. However, this area requirement is only valid if a wind turbine stands alone. For a wind farm with several wind turbines, the turbines need to be spaced further apart. This distance between the turbines is 3 to 5 times the rotor diameter of the wind turbine (EnBW, 2022; Lütkehus et al., 2013).

2.3 Battery

To realize the energy transition, in addition to renewable power generation, electricity storage systems are also needed that can store the surplus electricity and release it when needed. Batteries are one way to do this. Batteries usually consist of two electrodes embedded in an electrolyte. During the charging process, a voltage is applied, causing electrons to flow from the positive to the negative electrode, converting electrical energy into chemical energy. In the discharging process, the same process takes place in reverse. Nevertheless, there are losses during each charging and discharging cycle, which depend on the efficiency of the battery. Overall, there are several battery technologies that are used in different fields. The best known are lithium ion, lead acid and alkaline batteries (Hannan et al., 2021; Kurzweil and Dietlmeier, 2018) . In this thesis, the technology referred to is the lithium-ion battery.

Lithium-ion batteries have a high energy density of 220 to 250 Wh/kg in relation to other battery technologies. In comparison, lead acid, batteries have an energy density of 25 to 40 Wh/kg. However, the charging and discharging processes cause the lithium-ion battery to lose capacity. How quickly this happens depends primarily on the number of charging cycles and the depth of discharge. (Kurzweil and Dietlmeier; Quaschning, 2019).

2.4 Hydrogen Production, Compression and Storage

H_2 is another important aspect of the energy transition and can help to partly decarbonize the industry, electricity, mobility, and heat sectors. In this section, the needed information for the thesis is supplied for the topics of H_2 production, compression, and storage. These three topics are essential for a power-to-H_2 plant in order to supply H_2 in a sufficient way (Kurzweil and Dietlmeier, 2018; Staiger and Tanțău, 2020).

Hydrogen Production

To produce renewable H_2, the process of electrolysis is mostly used and is the most mature technology. During this process, H_2 is produced by an electrolyzer unit. The term electrolysis is defined as the separation of a solid, liquid or molten ionic conductor (electrolyte) with the use of electric current (Kurzweil and Dietlmeier, 2018). For water electrolysis, water or steam is the electrolyte to be separated, which is separated into oxygen and H_2 with electrical energy. In this process, electrical energy is converted into chemical energy (Ghaib, 2017). The reaction equation is presented in the following formula:

$$H_2O \rightarrow H_2 + \frac{1}{2}O_2 \tag{1.1}$$

Currently, there are three main electrolyzer technologies: Alkaline Electrolysis (AEL), Proton Exchange Membrane Electrolysis (PEMEL), and Solid Oxide Electrolysis (SOEC) (IEA, 2023). In this thesis, the technology of PEMEL will be referred to.

The PEMEL consists of a polymeric solid electrolyte that functions simultaneously as an electrolyte, catalyst, and separator for the reaction gases. A proton exchange membrane is attached to both sides of the solid electrolyte (see Figure 1), which is permeable only to protons (H+) (Kurzweil and Dietlmeier, 2018).

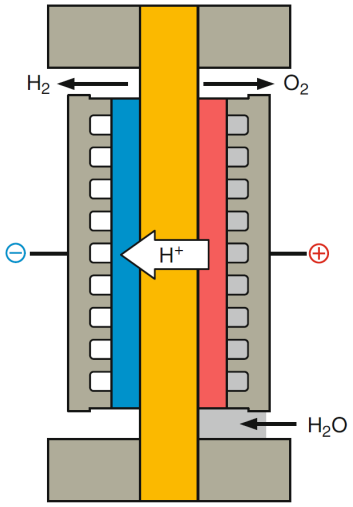

Figure 1: Structure of a PEMEL (Kurzweil and Dietlmeier, 2018, p. 442)

For H_2 production, pure water is supplied at the anode of the PEMEL. There, the water molecule donates two electrons, producing two protons and oxygen. The protons diffuse through the proton-permeable membrane to the cathode. At the cathode, the protons take up two electrons, resulting in the formation of H_2 (Kurzweil and Dietlmeier, 2018). The reaction equations of the PEMEL are shown below:

$$Anode: \quad H_2O \rightarrow \frac{1}{2}O_2 + 2H^+ + 2e^- \tag{1.2}$$

$$Cathode: \quad 2H^+ + 2e^- \rightarrow H_2 \tag{1.3}$$

In recent years, the technology maturity of the PEMEL has increased, and it has an efficiency of 60 to 75 % (Schmidt et al., 2017). In 2022, the technology had a market share of 30 % and the AEL of 60 %, but based on announcements, this will change in the future, and the PEMEL will be gaining market share over the AEL (IEA, 2023). Furthermore, the *CAPEX* decreased as technology maturity increased (Fraunhofer ISE, 2021; Schmidt et al., 2017) . In addition to, the PEMEL has a high current density of almost 2 A/cm^2, which means that the stacks can be built more compactly and consequently have a smaller area requirement than the other electrolyzer technologies. Moreover, the PEMEL has quick start up times and responds significantly more flexibly to load fluctuations than the other electrolyzer technologies, which is important when using fluctuating RE. Another advantage is the possibility of delivering H_2 with up to 50 bar out of the PEMEL (Fraunhofer ISE, 2021).

Compression and Storage

Under normal conditions, H_2 has a high energy density by mass of 39.4 kWh/kg_{H2} (HHV), but a low energy density by volume of 3.54 kWh/Nm^3 H2 (HHV). In comparison, diesel fuel has an energy density of 12.6 kWh/kg (HHV) and 830 kWh/Nm^3 (HHV). Therefore, due to the low energy density of H_2 per volume, H_2 storage systems are required to store H_2 in a compact manner (Kurzweil and Dietlmeier, 2018).

There are a variety of ways to store H_2. The two most technically mature are the pressure storage, where gaseous H_2 is compressed, and liquid storage, where the H_2 is cooled down to -253 °C to liquefy it. Other technologies are material-based storages, which are based on the adsorption or absorption of H_2 molecules (Hassan et al., 2021). In the following, the focus will be on pressure storage in pressure vessels. These pressure vessels are usually made of steel or composite materials and can store H_2 at up to 1,000 bar. For industrial use, low-cost steel storage tanks that can withstand 200 to 300 bar are usually used (Barthelemy et al., 2017).

To store the H_2 at high pressure in á pressure vessel, a compressor is required to compress the H_2 to the desired pressure. There are several compressor technologies that can do that. The piston compressor is currently the most established technology for H_2 compression. The working principle is based on volume reduction, which increases the pressure of the gas (Khan et al., 2021).

The required work of the compressor to compress the H_2 (w_{comp}) depends on the pressure difference it must overcome. This means that as the storage level rises, the pressure inside the tank rises, and so does the energy required to store the H_2 to reach the same pressure level. Equation 4 shows how the compressor work can be calculated in $kWh_{el}/kWh_{comp,H2}$. There, it is assumed that polytropic conditions apply (Bouché and Wintterlin, 1968; Wiegleb, 2016).

$$w_{comp} = \frac{z_m * R + T_{in}}{M_{H2}} * \frac{n}{n-1} * \left[\left(\frac{p_{st}}{p_{ely}} \right)^{\frac{n-1}{n}} - 1 \right] * \frac{1}{\eta_{comp}} \quad (2)$$

Table 1: Parameter for the calculation of the compressor work

z_m	Mean real gas factor
R	Universal gas constant
T_{in}	Temperature inlet gas
n	Polytropic coefficient
M_{H2}	Molar mass of H_2
p_{ely}	Pressure of gas out of the electrolyzer
p_{st}	Pressure in storage
η_{comp}	Efficiency compressor

2.5 Optimization of Energy Systems

For the optimization of energy systems, it must be defined what is to be optimized and what boundary conditions apply. Then an optimization problem can be set up, in which the optimal or best solution can be searched for and found. There are different mathematical methods and approaches for this, which work either deterministically or stochastically. In such models, assumptions must be made to simulate a real system. This means that such a model is only as accurate as the assumptions and boundary conditions that are defined (Bynum et al., 2020). In this thesis, a deterministic mathematical model of an energy system is created. Optimization of virtual energy systems and other technical systems is a common way of checking how the planned system will perform and whether it is economically feasible before major investment decisions are made. In most cases, the variable to be optimized is the profit or production cost of the system. The use of Mixed-Integer-Linear-Programming (MILP) is an appropriate approach for energy systems because it efficiently handles various system variables, such as the number of PV modules or wind turbines (Cuisinier et al., 2021). MILP allows both continuous variables, such as wind speeds, and integer variables, and such as the number of turbines to be installed, to be considered in one mathematical model (Klemm and Vennemann, 2021). Furthermore, MILP is a apropiate method, especially for optimizing investment and operational decisions for energy systems (Urbanucci, 2018). On the other hand, MILP limits the accuracy of the optimization because there are usually some variables that cannot be described by linear equations. In this case, simplifications have to be made even though the accuracy decreases (Cuisinier et al., 2021). To describe such a model, variables, constant parameters, constraints, and an objective function must be defined. These give the optimization the needed framework to find the solution to the optimization problem (Bynum et al., 2020). In the following, the components of an optimization are briefly explained.

Variables
Variables can take on different values and are usually linked to constraints. They are defined at the beginning, where various properties are set. Whether it is a single value or an array of values. It also specifies whether the variable is an integer, float, binary, or other mathematical type, and if it can take on only positive, negative, or all values (Bynum et al., 2020). Only so-called Non-Negative Integers (NNI) and Non-Negative Reals (NNR) are used to describe the model in this thesis.

Constraints
Constraints are used to define the links and dependencies between variables and constant parameters. This means that the variables can only take on the values that the constraints allow. This is an important aspect of achieving reasonable results in optimization (Bynum et al., 2020).

The objective function
The objective function is used to describe the goal of the optimization. This is a mathematical function that is constructed from the previously defined variables to describe the parameter to be optimized. Depending on whether the investigated parameter shall reach the maximum or the minimum, the variables take on values that satisfy all the constraints in order to solve the objective function (Bynum et al., 2020).

Figure 2 shows how linear optimization works in general and how mixed-integer optimization differs from linear optimization. The red, green, and blue functions describe linear equations that represent the constraints for the optimization problem. This creates a feasible region in which the solution to the

optimization problem can be found. In this example, the search is for the minimum. For continuous variables, the solution is the lowest value that fits into the solution space (a). For integer variables, the solution is the lowest integer value that is inside the solution space (b).

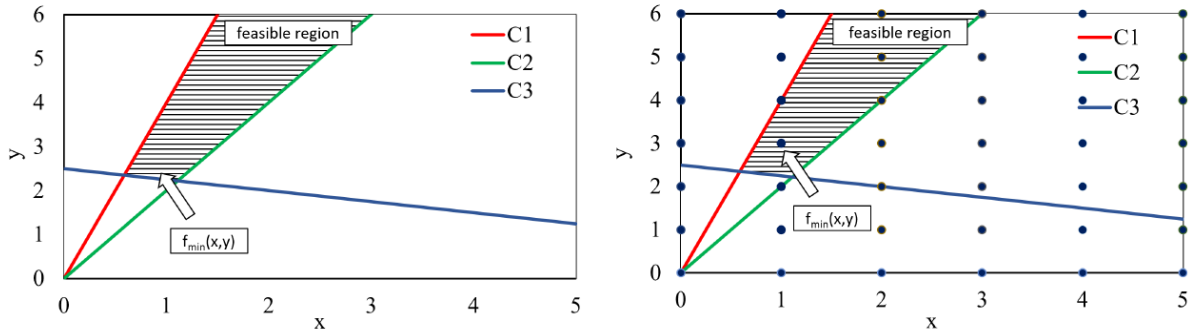

Figure 2: Illustration of linear programming with continuous variables (a) and discrete variables (b) (Neubauer, 2023)

2.6 Economic Assessment

As explained in chapter 2.5, the goal of energy system optimization is usually to reach the minimum or maximum of a certain economic parameter with the set boundary conditions. These help to assess economic viability and ensure that investments provide long-term economic value. Overall, the economic assessment of energy systems is a complex process. It is usually evaluated using several economic variables that take into account all costs incurred, the energy yield of the system, and the expected revenues (Bormann and Johannsmann, 2000). The following formulas have already been adapted to the thesis context.

However, it is important to recognize that there are numerous additional important economic parameters associated with energy systems. While these considerations are significant in the broader context of an economic assessment, it is beyond the scope of this thesis to comprehensively address all of them. This chapter presents all of the key variables used in this thesis and shows how they are calculated.

Profit

The profit of a production plant per year is usually calculated by subtracting all revenues generated per year from all expenses per year. In this thesis, the revenues are the revenues of sold electricity and H_2, and the expenses are the Capital Expenditures per year ($CAPEX_a$) and the Operating Expenditures per year ($OPEX_a$) of the entire plant. The profit per year is determined by the following formula:

$$Profit_a = Revenue_a - CAPEX_a - OPEX_a \tag{3.1}$$

The revenue per year is calculated by the sum of the sold quantities of electricity ($w_{el,h}$) and H_2 ($m_{H2,h}$) per hour multiplied by the Selling Price (SP) at this specific hour. The revenue per year is determined using the following formula:

$$Revenue_a = \sum w_{el,h} \cdot SP_{electricity,h} + \sum m_{H2,h} \cdot SP_{H2} \tag{3.2}$$

The *CAPEX* per year is calculated from the investments of all plant components and their related lifetimes, the annuity factor (*A*), and debt and equity contributions. The following formula is used for this:

$$CAPEX_{total,a} = \sum CAPEX_{comp} \cdot Share\ of\ Debt \cdot A + \frac{CAPEX_{comp} \cdot (1 - Share\ of\ Debt)}{Lifetime_{comp}} \quad (3.3)$$

The annuity factor *A* includes the interest rate *i* and the lifetime of the components of the plant. The annuity factor is calculated for every component using the following formula (Short et al., 1995, p. 14):

$$A = \frac{i \cdot (1+1)^{lifetime_{comp}}}{(1+i)^{lifetime_{comp}} - 1} \quad (3.4)$$

The total *OPEX* per year is calculated by summing the *OPEX* of all components:

$$OPEX_{total,a} = \sum OPEX_{comp} \quad (3.5)$$

Payback Time (PT)

The *PT,* also known as the payback period of an asset, is the time it takes for the accumulated profits to cover the original investments. It indicates how long it takes for the investment to pay for itself. After this period, the profits flow as positive cash flow to the company that owns the assets (Schuster and Rüdt von Collenberg, 2017, p. 121). Formula 3.6 is used in the context of the thesis to determine the *PT*.

$$PT = \frac{CAPEX_{total}}{Revenue_a} \quad (3.6)$$

Return on Investment (*ROI*)

The *ROI* is the rate at which the capital invested in an asset is compounded over its life, assuming a constant rate over all periods. This rate indicates the percentage by which the investment has grown in one year and is also referred to as the overall capital yield in this context. The *ROI* is calculated using the following formula (Schuster and Rüdt von Collenberg, 2017, p. 70):

$$ROI = \left(\frac{Revenue}{CAPEX_a + OPEX_a}\right) \cdot 100\% \quad (3.7)$$

Levelized Cost of Energy (*LCOE*)

The Levelized Cost of Energy is used to illustrate the cost of generating energy. The calculation of the *LCOE* considers the total cost of an energy project over its lifetime and divides it by the amount of energy produced. The types of energy in this thesis will be electricity and H_2. A low *LCOE* indicates that energy production is more economical. The *LCOE* is determined using the following formula (Short et al., 1995, p. 48):

$$LCOE = \frac{CAPEX_{total,a} + OPEX_{total,a}}{produced\ energy\ per\ year} \quad (3.8)$$

3 Design of the Optimization Tool

In this chapter, the optimization tool, which was created to answer the research question, will be explained and presented. Firstly, an overview of the software used will be given, and after that, the structure of the optimization tool will be shown during this chapter. Additionally, each variable and constraint, which were defined to model the virtual energy system, is explained for every component in the model and how they are connected to each other. Lastly, the final objective function is presented.

Software

In order to develop a software that provides detailed insights into the research question outlined in section 1.2, the programming language Python from van Rossom (2023) was used with the 3.11 version. The tool was implemented in the open community version of the PyCharm 2023.2.5 programming interface from JetBrains (2023) which is a freely available. The optimization is based on the Python Open-Source Modeling and Optimization (PYOMO) library. It is used to create the computational representations of the modeled energy system. Within the PYOMO library, the concrete model class is used to define variables and constraints, and it was also used to specify the objective function representing the optimization objective (Bynum et al., 2020). The constructed "concrete model" is then transferred to the solver application, which can solve optimization problems like those explained in chapter 2.5. The solver implemented in the tool is Gurobi Optimization, L.L.C. and is used under an academic license (Gurobi Optimization LLC). MILP has been established as an effective approach for answering questions such as those in Section 1.2 and for finding optimal system designs for technical systems in terms of economic aspects (Klemm and Vennemann, 2021). Numerous scientific publications have already verified the reliability of PYOMO and Gurobi Optimization and used them for similar problems (Cuisinier et al., 2021; Weimann et al., 2021). Furthermore, the matplotlib, the pandas and NumPy libraries are integrated into the tool to work with and illustrate the imported and generated data (Harris et al., 2020; Hunter et al., 2023; Pandas development team, 2023).

Structure

The flow diagram presented in Figure 3 illustrates the structure of the optimization tool. The tool consists of several parts, while all of them are implemented in the PyCharm programming interface. Inside the programming interface, there are different parts that are either imported or programmed within PyCharm. These include external data sets containing technical and economic parameters, which were extracted from the literature and open-source websites. The primary component of the tool is the concrete model that was made with the PYOMO-library to model the energy system. The modeled energy system will be simulated for one year with one-hour time steps. For this reason, the variables are indexed either with "*t*" for variables with hourly values or with no index if the variables are fixed and are not time depending for the entire simulated time. The model distinguishes between basic modules, which the tool always uses, and additional modules that can be added for expansion. Additional modules are identified in Figure 3 by a box with thick red lines and a cursive number in the upper left corner to distinguish them easier. Module one adds a grid limitation, which limits the amount of electricity that can be fed into the grid. Module two adds the option of wind turbines, and module three a battery system to the solution of the optimization. Module four enables the possibility of producing hydrogen. The last module enables a constraint that specifies that a daily H_2 must be covered. The boxes with a green background have integer values, which must be either zero, the later set specified integer number, or a multiple thereof. This approach turns the concrete model from a linear optimization into a MILP (Bynum et al., 2020).

Therefore, the basic model comprises a PV system representing systems of combined east, south, or west orientation or just a single orientation. The system also includes the inverters that convert the electricity from direct current to alternating current and feed it into the grid. The revenue generated by the electricity sold and fed into the grid is dependent on external imported electricity market data. The tool is built to easily add the different modules and all modules can be mixed. For example, if modules two (battery) and three (H_2 production) are added, the electricity can either flow into the battery or directly into the electrolyzer. From there, the electricity can flow to either the electrolyzer or the inverters. After the electrolyzer produces H_2, it is compressed and stored in the H_2 storage unit. Once stored, the H_2 can be sold at the beginning of each day. The total profit of the system is the sum of the profits made with the electricity and the H_2 sold. In addition, this is the variable to be optimized. Depending on which modules are finally selected, the corresponding constraints, assumptions, and variables are passed to the Gurobi solver program. The solver solves the optimization problem with a suitable algorithm and returns the optimal solution and all the corresponding values to reach the optimum, which can then be analyzed in detail.

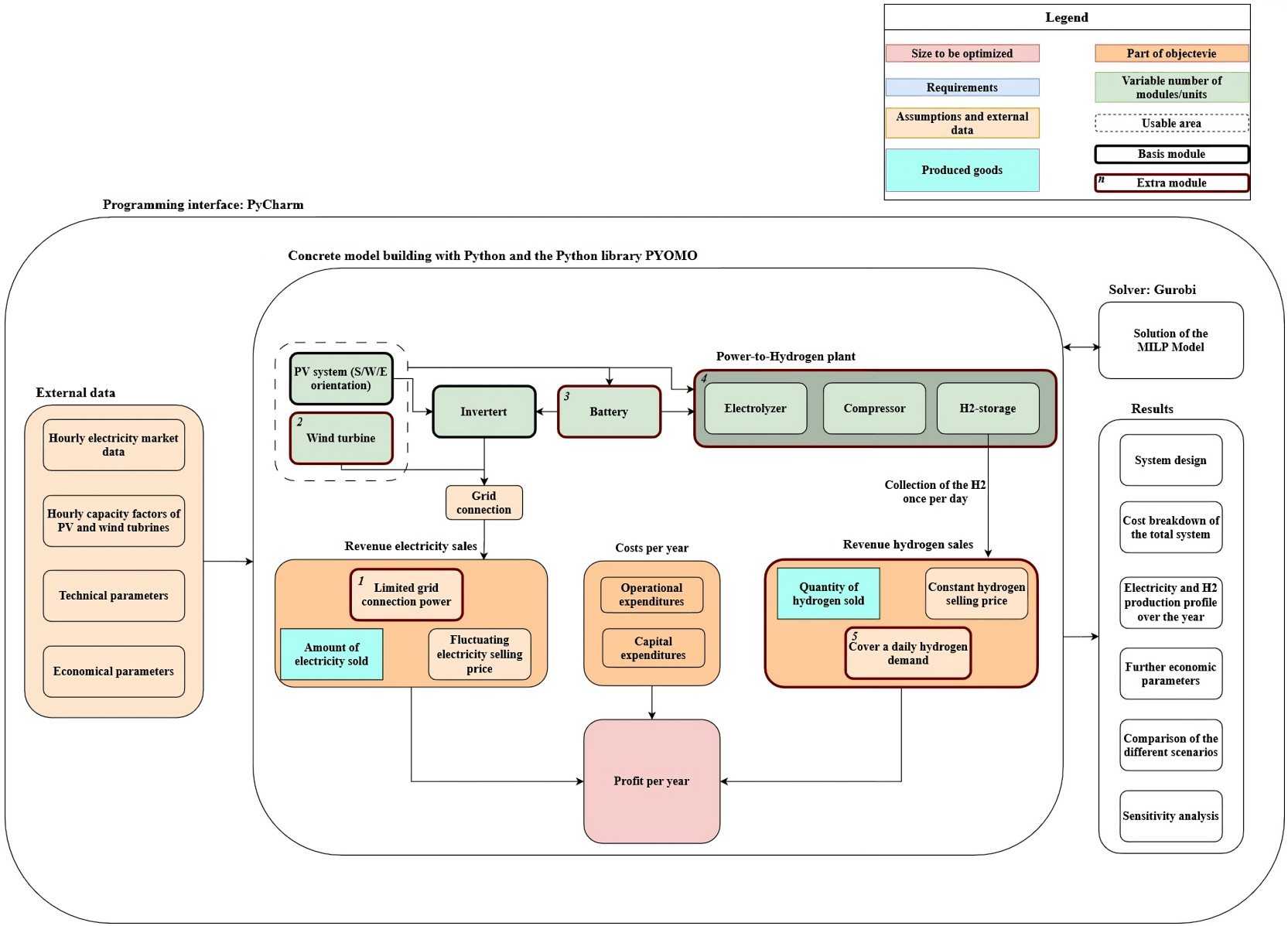

Figure 3: Schematic flow diagram of the optimization tool

3.1 Usable Area and Grid Connection

The area limitation and the grid connection are the variables in the tool that limits the capacity of the power plants and thus prevent infinite power generation. While the usable area is always limiting the number of installed plants, the grid connection can be restricted, but it is not mandatory. The dependencies of the available areas are shown first, followed by the grid connection.

Usable Area

The usable area refers to the area available to build PV systems and wind turbines to generate electricity. It is a user-defined constant variable with the unit hectare and is defined as NNR with the name *usable_area*, so that information with decimal numbers can also be provided depending on the available area. This variable is linked to the required area of the power generation plant by a constraint, which states that the required area from all power generation systems cannot be larger than it. The required area of the PV system and the wind turbines is calculated using a constant literature value of the specific area required by the systems in ha/unit (*wind_area* and *pv_area*) and the number of the respective plants. These are unitless NNI variables named *pv_east_number*, *pv_south_number* and *pv_west_number* as well as *wind_number*. These integer values guarantee that it is a MILP and will also be used for other components later as well. All variables used for this part are shown in Table 2.

$$usable\_area \leq pv\_area \cdot (pv\_east\_number + pv\_south\_number + pv\_west\_number) + wind\_area \cdot wind\_number \quad (4.1)$$

Table 2: Usable area variables

Name	Unit	Type	Known/Unknown
$usable\_area$	ha	NNR	Known
pv_area	ha	NNR	Known
pv_east_number	-	NNI	Unknown
pv_south_number	-	NNI	Unknown
pv_west_number	-	NNI	Unknown
$wind\_area$	-	NNR	Known
$wind\_number$	-	NNI	Unknown

Grid connection

The power grid connects the generation and sale of electricity in the modeled energy system. Table 3 displays all the variables used in this section.

Table 3: Grid connection variables

Name	Unit	Type	Known/Unknown
$ee\_to\_grid_t$	kWh	NNR	Unknown
$inv\_to\_grid_t$	kWh	NNR	Unknown
η_{inv}	%	NNR	Known
$wind\_to\_grid_t$	kWh	NNR	Unknown
max_$grid$	kWh	NNR	Known
$ee\_to\_grid_t$	kWh	NNR	Unknown

The amount of electricity flowing into the grid is determined by the variable $ee\_to\_grid_t$, measured in the unit of kWh, and is calculated for every hour of the year. In the base module, only the electricity produced by the inverters multiplied by their efficiency is fed into the grid. When wind turbines are added, they can also feed electricity into the grid. This is shown in formula 4.2. It is assumed that the wind turbines use their own inverters, which are also included in their *CAPEX*. Therefore, the electricity produced by the wind turbines flows directly into the power grid.

$$ee\_to\_grid_t = inv\_to\_grid_t \cdot \eta_{inv} + wind\_to\_grid_t \tag{4.2}$$

In the case of extra module one from Figure 3, a limiting constraint was defined with the grid restriction. This guarantees that $ee\_to\_grid_t$ never surpasses the maximum limit set by the constant variable *max_grid* as seen in formula 4.3.

$$\max\_grid \geq ee\_to\_grid_t \tag{4.3}$$

3.2 Electricity Production

The electricity in the modeled system can be supplied from PV systems and wind turbines. How they are implemented in the tool will be explained in the following.

PV System

The electricity generated by the PV system depends on several aspects, as explained in section 2.2. As the PV system generates direct current it must be converted to alternating current hence is why the constraints for the inverters are also defined in this section. To define the electricity production in the programmed optimization tool, the hourly capacity factors over the year of the selected site and the given orientation are used. The orientations east ($pv\_east\_capacity_t$), south ($pv\_south\_capacity_t$) and west ($pv\_west\_capacity_t$) have been defined for the tool , causing the combination of the different orientation could possibly be part of the solution, but a single orientation could it be as well. The unit size of the PV plant (*pv_power*) and the inverters (*inv_power*) are set before the optimization process, because of the explained properties of the MILP. As already previously mentioned in Chapter 3.1, this means that only multiples of these values can be a part of the optimization solution. To ensure this, NNI variables are used. Table 4 presents all variables used for power generation by PV systems, including the inverter.

Table 4: Electricity production: PV variables

Name	Unit	Type	Known/Unknown
$usable\_pv\_w_t$	kWh	NNR	Unknown
pv_power	kW	NNI	Known
$pv\_east\_capacity_t$	%	NNR	Known
$pv\_south\_capacity_t$	%	NNR	Known
$pv\_west\_capacity_t$	%	NNR	Known
$pv\_to\_inv_t$	kWh	NNR	Unknown
$pv\_not\_used_t$	kWh	NNR	Unknown
$pv\_to\_ptx_t$	kWh	NNR	Unknown
inv_power	kW	NNI	Known

inv_number	-	NNI	Known

The first step is to calculate the possible usable amount of electricity for each hour *t* (*usable_pv_w*$_t$). This is done by defining the power of the whole PV system by multiplying the NNI variables for each orientation. These values are multiplied by the corresponding capacity factor for each time step to obtain the resulting electricity produced. This is shown in the formula 5.1.

$$usabl\_pv\_w_t = pv\_power \cdot (pv\_east\_number \cdot pv\_east\_capacity_t + pv\_south\_number \cdot pv\_south\_capacity_t + pv\_west\_number \cdot pv\_west\_capacity_t) \quad (5.1)$$

Formula 5.2 describes that the amount of usable electricity is divided into three categories: electricity that flows into the inverter (*pv_to_inv*$_t$) and electricity that remains unused (*pv_not_used*$_t$). If the energy system includes a battery and/or an electrolyzer, the electricity can also flow to these components, which are described as *pv_to_ptx*$_t$.

$$usable\_pv\_w_t = pv\_to\_inv_t + pv\_not\_used_t + pv\_to\_ptx_t \quad (5.2)$$

The inverter can never convert more electricity into alternating current than the total power of the inverter. That means the total power must always be equal or greater than the input flow variable *pv_to_inv*$_t$. The total power is calculated by multiplying the value *inv_power*, which needs to be defined at the beginning, with the NNI variable *inv_number* (Formula 5.3).

$$inv\_power \cdot inv\_number \geq pv\_to\_inv_t \quad (5.3)$$

If the base module operates without electricity flowing from the battery via the inverter, only the PV electricity is fed directly into the grid via the inverter, as shown in formula 5.4.

$$pv\_to\_inv_t = inv\_to\_grid_t \quad (5.4)$$

Wind Turbine

The principle used in the thesis to model electricity in the tool with wind turbines works with the same principle as the just explained PV systems. Table 5 below presents the variables used in this section.

Table 5: Electricity production: wind variables

Name	Unit	Type	Known/Unknown
$usable\_wind\_w_t$	kWh	NNR	Unknown
$wind\_power$	kW	NNI	Known
$wind\_capacity_t$	%	NNR	Known
$wind\_to\_grid_t$	kWh	NNR	Unknown
$wind\_not\_used_t$	kWh	NNR	Unknown
$wind\_to\_ptx_t$	kWh	NNR	Unknown
$total\_wind\_area$	ha/unit	NNR	Known

The amount of electricity from the wind turbines that can be used over the year is represented by the NNR variable *usable_wind_w*$_t$. This is calculated for all timesteps *t* as follows:

$$usable\_wind\_w_t = wind\_power \cdot wind\_number \cdot wind\_capacity_t \quad (6.1)$$

This electricity either flows directly into the power grid (*wind_to_grid*$_t$) or is not used at all (*wind_not_used*$_t$). If there exists a battery or electrolyzer, the electricity may also be directed to these components (*wind_to_ptx*$_t$).

$$usable\_wind\_w_t = wind\_to\_grid_t + wind\_not\_used_t + wind\_to\_ptx_t \quad (6.2)$$

However, there is an additional area constraint that is required when modeling the wind turbines to give the turbines enough space so that they do not interfere with each others power output. Hence why, the additional area required for the turbines is shown in formula 6.3. The variable *total_wind_area* describes the needed area for the turbines to not influence the power output among each other and is used to limit the maximum number of wind turbines.

$$usable\_area \geq total\_wind\_area \cdot wind\_number \quad (6.3)$$

3.3 Battery

By adding the battery module, generated electricity can be stored temporarily and fed into the grid at a later. Additionally, the electricity produced can be used to run the electrolyzer and the compressor to generate and store H_2 if the H_2 generation module is enabled. Table 6 displays the variables that are used for the battery in this chapter.

Table 6: Battery variables

Name	Unit	Type	Known/Unknown
$bat\_capacity$	kWh	NNI	Known
bat_number	-	NNI	Unknown
bat_soc_t	kWh	NNR	Unknown
$ee\_to\_bat_t$	kWh	NNR	Unknown
$ee\_to\_ely_t$	kWh	NNR	Unknown
$ee\_to\_comp_t$	kWh	NNR	Unknown
$bat\_to\_inv_t$	kWh	NNR	Unknown
$bat\_to\_ely_t$	kWh	NNR	Unknown
$bat\_to\_comp_t$	kWh	NNR	Unknown
$bat\_initial\_soc$	%	NNR	Known
soc_max	%	NNI	Known
soc_min	%	NNI	Known
η_{bat}	%	NNR	Known

The electricity generated from the RE plants, which is fed into the battery, depends on the previously introduced variables *pv_to_ptx*$_t$ and *wind_to_ptx*$_t$. These represent the electricity that does not flow directly into the grid but is instead split between the variables *ee_to_bat*$_t$, *ee_to_ely*$_t$ and *ee_to_comp*$_t$, as shown in formula 7.1.

$$pv\_to\_ptx_t + wind\_to\_ptx_t = ee\_to\_bat_t + ee\_to\_ely_t + ee\_to\_comp_t \quad (7.1)$$

The batteries total capacity is defined by multiplying the NNI variables *bat_capacity* and *bat_number*. To reflect the storage function of the battery, it also requires a variable that represents the state of charge (SoC) of it at any given time *t*. This is the purpose of the NNR variable bat_soc_t. To ensure a longer lifetime of the battery limits of the SoC must be in a constrain as well. In formula 7.2 and 7.3 the constrains are defined that the SoC of the battery is always within *soc_min* and *soc_max*.

$$bat\_soc_t \geq soc\_min \cdot bat\_capacity \cdot bat\_number \tag{7.2}$$

$$bat\_soc_t \leq soc\_max \cdot bat\_capacity \cdot bat\_number \tag{7.3}$$

As shown in formula 7.4 the stored energy flows from the battery either to the inverter ($bat\_to\_inv_t$), to the electrolyzer ($bat\_to\_ely_t$) or to the compressor ($bat\_to\_comp_t$). The last two variables are only available if the module is enabled for H_2 generation. The sum of the variables must be always lower than or equal to the SoC of the battery.

$$bat\_soc_t \geq bat\_to\_inv_t + bat\_to\_ely_t + bat\_to\_comp_t \tag{7.4}$$

The SoC for the next time step *t+1* is determined by the energy flowing out of the battery and the energy flowing into the battery. Furthermore, the SoC calculation distinguishes between *t=0* (the beginning of the simulation), the last time step, and all steps in between. At *t=0*, the battery needs to be already charged to a certain percentage of its capacity. This ensures that energy from the battery is already available at the start of the simulation (formula 7.5). Formula 7.6 is used for all further calculations of bat_soc_{t+1} up to the last time step. The final time step is excluded from calculation as it cannot be calculated due to the end of the simulation time.

$$\begin{aligned} bat\_soc_{t+1} = bat\_capacity \cdot bat\_number \cdot bat\_initial\_soc - bat\_to\_ely_t - bat\_to\_comp_t \\ -bat\_to\_inv_t + ee\_to\_bat_t \cdot \eta_{bat} \end{aligned} \tag{7.5}$$

$$bat\_soc_{t+1} = bat\_soc_t - bat\_to\_ely_t - bat\_to\_comp_t - bat\_to\_inv_t + ee\_to\_bat_t \cdot \eta_{bat} \tag{7.6}$$

3.4 Hydrogen Production, Compression and Storage

The extra module four is used to produce, compress, and store H_2. How these steps are modeled for the tool is explained in the following.

Hydrogen Production

Due to the electrolyzer, there is another way to use the generated electricity. Without the extra module for H_2 production, the electricity always ends up flowing into the grid, which no longer needs to be the case. Table 7 displays the variables used to define the constraints for this chapter.

Table 7: Electrolyzer variables

Name	Unit	Type	Known/Unknown
ely_p	kW	NNI	Known
ely_number	-	NNI	Unknown
$ely\_used\_electricity_t$	kWh	NNR	Unknown
$ely\_to\_comp_t$	kWh	NNR	Unknown
η_{ely}	%	NNR	Known

Multiplying the NNI variables *ely_p* and *ely_number* results in the total power of the electrolyzer. Formula 8.1 defines the following constraint in such a way, that the amount of electricity the electrolyzer can use is connected to the power of the electrolyzer. This guarantees that the electrolyzer will never receive more electricity than it can convert to H_2.

$$ely\_p \cdot ely\_number \geq ee\_to\_ely_t + bat\_to\_ely_t \tag{8.1}$$

The total electricity utilized by the electrolyzer, $ely\_used\_electricity_t$, is the sum of the electricity from the PV and wind systems and the amount from the battery at time *t* fed into the electrolyzer. This is displayed in the formula 8.2.

$$ely\_used\_electricity_t = ee\_to\_ely_t + bat\_to\_ely_t \tag{8.2}$$

In the following step, the electricity is converted into H_2 by the electrolyzer and depends on the efficiency of the electrolyzer. The produced amount of H_2 is fed to the compressor and is described by the NNR variable $ely\_to\_comp_t$ in kWh and results, as shown in formula 8.3, from $ely\_used\_electricity_t$ and the selected efficiency of the electrolyzer η_{ely}.

$$ely\_to\_comp_t = ely\_used\_electricity_t \cdot \eta_{ely} \tag{8.3}$$

Hydrogen compression and Storage

In the next step the produced H_2 has to be compressed and fed into the H_2 pressure storage tank. The H_2 stays stored in the vessel until withdrawn for sales purposes, which is possible once per day. The relevant variables for the compressor and the storage tank are illustrated in the Table 8.

Table 8: Hydrogen compressor & storage variables

Name	Unit	Type	Known/Unknown
$comp\_p$	kWh_{H2}/h	NNI	Known
$comp\_number$	-	NNI	Unknown
$comp\_w$	kWh_{el}/kWh_{H2}	NNR	Known
$comp\_to\_storage_t$	kWh	NNR	Unknown
$comp\_losses$	%	NNR	Known
$storage\_capacity$	kWh	NNI	Known
$storage\_number$	-	NNI	Unknown
$storage\_soc_t$	kWh	NNR	Unknown
$storage\_to\_demand_t$	kWh	NNR	Unknown
$storage\_initial\_soc$	%	NNR	Known

As with all previous components of the model, the power of the compressor must be greater than or equal to the amount of input to be processed at any time *t*, which in this case is the H_2 produced. The power of the compressor is again derived from NNI variables. Here it is the set and known variable *comp_p* and the unknown *comp_number*. The corresponding constraint is defined in the formula 9.1.

$$comp\_p \cdot comp\_number \geq ely\_to\_comp_t \tag{9.1}$$

The specific power demand of the compressor (*comp_w*) is defined by formula 2 explained in chapter 2.6. This value is multiplied by the amount of H_2 which needs to be compressed at the timestep *t* and results in the electricity consumption of the compressor, which must be provided directly from the RE or the battery (formula 9.2).

$$ee\_to\_comp_t + bat\_to\_comp_t = comp\_w \cdot ely\_to\_comp_t \tag{9.2}$$

Formula 9.3 defines the amount of H_2 that flows through the compressor into the storage tank at the timestep *t*. This is the amount of H_2 produced ($ely\_to\_comp_t$) minus the loss of the compressor during the compression process (*comp_losses*).

$$comp\_to\_storage_t = ely\_to\_comp_t \cdot (1 - comp\_losses) \tag{9.3}$$

The NNI variables *storage_capacity* and *storage_number* describe the total storage capacity for H_2. Furthermore, a variable is needed to reflect the SoC for the modulated H_2 storage system, which is represented by the NNR variable $storage\_soc_t$. This, along with equation 9.4 and 9.5, ensures that the total capacity of the storage unit is not exceeded at any time. In addition, the amount of H_2 flowing into the storage tank must always be less than or equal to the remaining capacity of the storage tank.

$$storage\_capacity \cdot storage\_number \geq storage\_soc_t \tag{9.4}$$

$$storage\_capacity \cdot storage\_number - storage\_soc_t \geq comp\_to\_storage_t \tag{9.5}$$

The H_2 stored in the storage unit flows from the storage to the demand ($storage\_to\_demand_t$). Therefore, the SoC in the storage tank must be equal to or greater than the H_2 flowing to the demand at any timestep *t* (formula 9.6).

$$storage\_soc_t \geq storage\_to\_demand_t \tag{9.6}$$

As with the battery discussed in chapter 3.3, the SoC for time step *t+1* is calculated for the H_2 storage system at each time step *t*. Again, a distinction is made between time *t=0*, which is the starting point of the simulation, the last time step, and all-time steps in between. At *t=0*, a predetermined percentage value ($storage\_initial\_soc_t$) is already used to partially fill the storage, which is then multiplied by the storage capacity. It guarantees that a demand can supplied right from the start of the simulation if needed. This value is added to the H_2 compressed by the compressor at the first timestep and then subtracted by the demand ($storage\_to\_demand_t$), which results in $storage\_soc_{t+1}$ (formula 9.7). The same calculation is repeated for all subsequent $storage\_soc_{t+1}$ calculations, without determining the initial capacity (formula 9.8). At the final time step this calculation cannot be made, due to the end of the simulation.

$$storage\_soc_{t+1} = storage\_capacity \cdot storage\_number \cdot storage\_initial\_soc + comp\_to\_storage_t - storage\_to\_demand_t \quad (9.7)$$

$$storage\_soc_{t+1} = storage\_soc_t - storage\_to\_demand_t + comp\_to\_storage_t \quad (9.8)$$

3.5 Hydrogen Demand

After production and storage, H_2 is withdrawn from the storage tank from a consumer. The final withdrawal of H_2 from the storage tank does not take place hourly, as in the calculation of the other index variables with the index *t*. The index *t* is still used, but there are two different constraints that regulate the withdrawal process. A distinction is made between the times when there is no demand for H_2 and the times when there is a demand for H_2. As shown in Figure 3, a daily H_2 demand can be defined in the simulation, which is withdrawn from the storage tank. This additional constraint is set as extra module 5 and depends on the set value *demand_day*. To ensure that only once per day H_2 is withdrawn from the vessel, an if condition was defined in the tool that depends on *t*. If *t* is divisible by 24, the formula 10.1 is used, and H_2 flows from the storage tank to the demand. If there is no minimum demand per day, the value of *demand_day* must be set to zero. Otherwise, the value can be any wanted value. At all other times when *t* is not divisible by 24, the formula 10.2 is used, and no H_2 flows out of the storage tank.

$$storage\_to\_demand_t \geq demand\_day \quad (10.1)$$

$$storage\_to\_demand_t = 0 \quad (10.2)$$

3.6 Objective Function

The virtual energy system has been modeled and explained in the chapters 3.1 to 3.5. In this chapter the objective function to be optimized is described. First, it is explained how the profit from electricity and H_2 sales is calculated. Afterwards, the functions for calculating the resulting *CAPEX* and *OPEX* costs are explained and lastly, the resulting objective function is outlined with the variable to optimized value *revenue_total*. Table 9 lists all variables used in this chapter that are not defined in the previous chapters.

Table 9: Objective function variables

Name	Unit	Type	Known/Unknown
$revenue\_total$	€/a	NNR	Unknown
$ee\_selling\_price_t$	€/kWh	NNR	Known
$h2\_revenue_t$	€/a	NNR	Unknown
$h2\_selling\_price$	€/kWh	NNR	Known
$invest\_ely$	€	NNR	Unknown
$capex\_ely$	€/kW	NNR	Known
$operation\_cost\_ely$	€/a	NNR	Unknown
$opex\_ely$	$\%_{CAPEX}$/a	NNR	Known
$profit\_max$	€/a	NNR	Unknown
$invest\_system$	€/a	NNR	Unknown
$operational\_cost\_system$	€/a	NNR	Unknown

Revenue

The tool calculates the total revenue (*revenue_total*) for each time step *t*. The electricity sold is the electricity that is fed into the grid and is defined by the variable $ee\_to\_grid_t$. For each time step, the value $ee\_to\_grid_t$ is multiplied by the current price at timestep *t* ($ee\_selling\_price_t$), which describes the associated revenue $ee\_revenue_t$ (formula 11.1). The electricity price also depends on *t* because the electricity price data fluctuates throughout the year. The calculation of the profit from the sale of H_2 ($h2\_revenue_t$) is defined in the same way (formula 11.2). It multiplies $storage\_to\_demand_t$ by the selected H_2 selling price (*h2_selling_price*). A constant selling price is defined for H_2, which can be changed if desired. The total profit is then calculated in formula 11.3 by adding the two sums of the profits.

$$ee\_revenue_t = ee\_to\_grid_t \cdot ee\_selling\_price_t \tag{11.1}$$

$$h2\_revenue_t = storage\_to\_demand_t \cdot h2\_selling\_price \tag{11.2}$$

$$revenue\_total = \sum ee\_revenue_t + \sum h2\_revenue_t \tag{11.3}$$

Costs

The formulas for the *CAPEX* (formula 3.3) and *OPEX* (formula 3.4) presented in chapter 2.8 must now be embedded into the tool. The known power and capacity variables used in previous chapters are needed along with the unknown number variables to calculate the total power of each system component. Furthermore, the specific *CAPEX* and *OPEX* value is needed to calculate the corresponding expenditures. Since the calculation does not differ for the different components, only the calculation steps for the electrolyzer are explained as an example below. The procedure is applied to all components with the corresponding variables.

Formula 11.4 shows the calculation of the *CAPEX* of the electrolyzer (*invest_total_ely*) by multiplying its capacity by the specific *CAPEX* (*capex_ely*). This value is then inserted in the equation 3.3 from chapter 2.8 to obtain the *CAPEX* cost per year (*invest_year_ely*), which depends on the lifetime of the plant, the interest rate and the proportion of equity and debt. To calculate the corresponding *OPEX* cost of the electrolyzer per year, the specific *OPEX* is required. For the electrolyzer, this value (*opex_ely*) is multiplied by the total investment amount *invest_total_ely* (formula 11.5). This results in the *OPEX* cost per year for electrolyzer (*operation_cost_ely*). The sum of all *CAPEX* costs is defined as *invest_system* and the sum of all *OPEX* costs is defined as *operation_cost_system*.

$$invest\_total\_ely = capex\_ely \cdot ely\_p \cdot ely\_number \tag{11.4}$$

$$operation\_cost\_ely = invest\_ely \cdot opex\_ely \tag{11.5}$$

Objective Function

The last step to define for the created concrete model is the objective function. To do this, the corresponding variables are inserted in formula 12. These are the profits generated per year from the sale of electricity and H_2 (*revenue_total*) and the sums of the costs presented above per year for all components. The result of equation 12 should now reach the maximum possible value for which all constraints and variable properties presented above are met. This value (*profit_max*) then corresponds to the maximum possible profit per year for the simulated energy system under all the made assumptions.

$$profit\_max = revenue\_total - invest\_system - operational\_cost\_system \tag{12}$$

In the last step, all variables, and constraints inclusive the objective function are passed to the solver program Gurobi, which returns the solution of the mixed-integer optimization problem.

4 Case Study Rügen

In the following chapter, the location used and the needed assumptions like *CAPEX*, *OPEX*, lifetime, efficiencies, etc. of all the components of the modulated energy system are presented in order to be able to use the previously described optimization tool and perform a techno-economic analysis. The structure of the complete system and the connection of the different technical components can be seen in Figure 3 from chapter three.

The assumptions made in the following chapters are taken from scientific literature and studies or are own assumptions. Simplifications have been also made. These are necessary for the implementation of the tool and in order not to exceed the scope of the work. The simplifications are presented in this chapter as well. Finally, all the parameters used for the case study are summarized in Table 11 at the end of this chapter.

4.1 Location and Grid Connection

The developed optimization tool is applied to an area on the Baltic Sea Island of Rügen. The island is located in the county of Rügen-Stralsund in the federal state of Mecklenburg-Vorpommern. The island has 1,788 hours of sunshine per year, which are 219 hours more than the average in Germany (Effe, 2023). Furthermore, has the advantage of being directly at the Baltic Sea, where high wind speeds occur (Epp et al., 2021). The mean wind speed at a height of 100 m is 8.42 m/s at the selected area (Global Wind Atlas, 2023). Figure 4 shows the selected location and area used for the simulation. The selected area is approximately 50 ha and is located directly on a highway and has an existing access road next to the area (Google Maps, 2023).

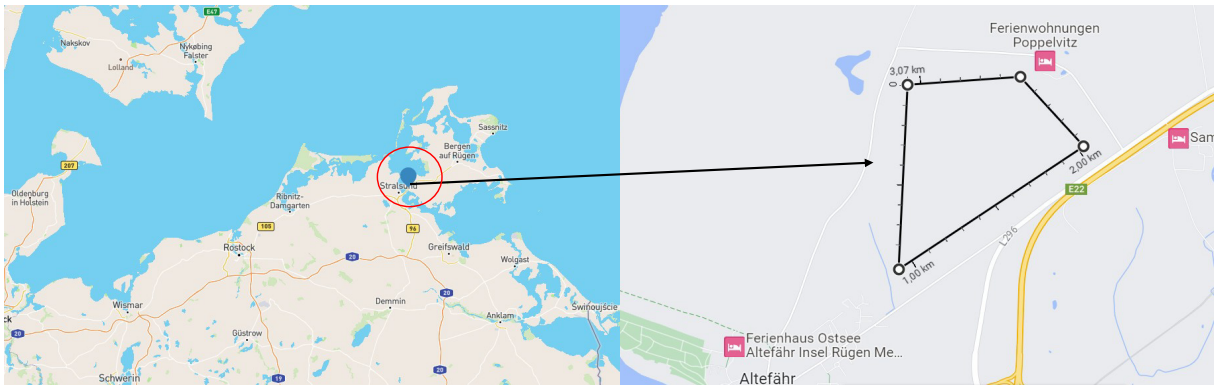

Figure 4: Location of simulated area (Google Maps, 2023)

For the purpose of simplifying the thesis, it is assumed that there is no cost involved in the purchase of the area and grid connection. This means no expenses are incurred in this section of the model. To simulate the extra module of limited grid capacity explained in chapter three, a maximum power capacity of 10 MW is set. If the module remains disabled, there is no limit to the input power, so as much electricity as possible can be fed into the grid. It should be noted that this is a rough assumption to evaluate the tool created and to check the influence of a limited grid capacity on the energy system to be simulated. For more accurate results concerning the site, it is necessary to reach out to the local grid operator who can provide detailed information about the power that can be fed into the grid at the chosen site. This would be E.DIS GmbH for the chosen location (E.DIS Netz GmbH, 2023).

4.2 Electricity Production

To produce electricity, the PV system is one of two options in the model, and the only option if the wind turbine module is disabled. The used assumptions for the electricity production are presented in the next part.

PV System

In the thesis, the PV system consists of the PV system including the required inverters. The assumptions for the inverter will be shown after the ones from the PV system.

The *CAPEX* for PV systems has fallen significantly in recent years. The International Renewable Energy Agency's (IRENA) report states the module costs have dropped by up to 94 % between 2009 and 2022. Overall, the cost of a complete ground-mounted PV system, excluding the inverter, is around 600 €/kW_p. As per IRENA's 2023 report, the current cost in Germany is 605 €/kW_p (IRENA, 2023b). These numbers are also in aligned with other scientific techno-economic studies, such as Sens et al. (2022), which assumed 602 €/kW_p. In this thesis the *CAPEX* is set to 605 €/kW_p. The operating costs of such systems have decreased significantly too, by about 51 % since 2010, according to IRENA (2023b). *OPEX* costs are usually given in either €/kW_p/a or %*CAPEX*/a, which can be converted in each other with the corresponding *CAPEX* values. In the literature, figures between 7 €/kW_p and 10.5 €/kW_p including inverter have been found (IRENA, 2023b; Petkov and Gabrielli, 2020; Vartiainen et al., 2019). For the purposes of this thesis, a cost assumption of 8 €/kW_p (including inverter) was made for the PV system. The PV systems expected lifetime ranges between 27 to 30 years (Petkov and Gabrielli, 2020; Terlouw et al., 2022). In the tool it is set to 30 years.

The capacity factors, which were previously described in section 2.2, are used to represent the energy produced by the PV system. The needed data is provided by the website renewables.ninja, which is based on the two scientific papers from Pfenninger and Staffell (2016) as well as Staffell and Pfenninger (2016) and displayed in Figure 5 and Figure 6. The capacity factors can be easily accessed, and only the location, tilt angle, and orientation of the PV system are required to obtain them. The tilt angle is set to be 35°, and three orientations are utilized: east, south, and west. A combination of orientations can help to give a more constant energy yield over the day and year (Quaschning, 2019). Nonetheless, if this contributes to increased profits is uncertain and will be determined by the results. Figure 5 displays capacity factors from renewables.ninja by orientation, showing the values for the used possible orientations. With the capacity factors on the y-axis and the corresponding hours over the year on the x-axis. The capacity values are highest in summer, and the southern orientation has the highest average value of the three used orientations. The average value for south-facing orientation is 14.87 %, while for east-facing orientation, it is 12.14 %, and for the west-facing orientation, it is 11.72 %. These values all refer to 2019, as those are the most recent values freely available on the renewables.ninja website (renewables.ninja, n. d.).

The tool was designed as a mixed-integer optimization, which means a fixed unit size is required. This is set to 1 kW_p to simulate a small size that is easy to plan with. According to the Umweltbundesamt (2023), the area required to install 1 kW_p is 0.001 hectares. This value will also be used for all orientations to describe the needed area for the PV system.

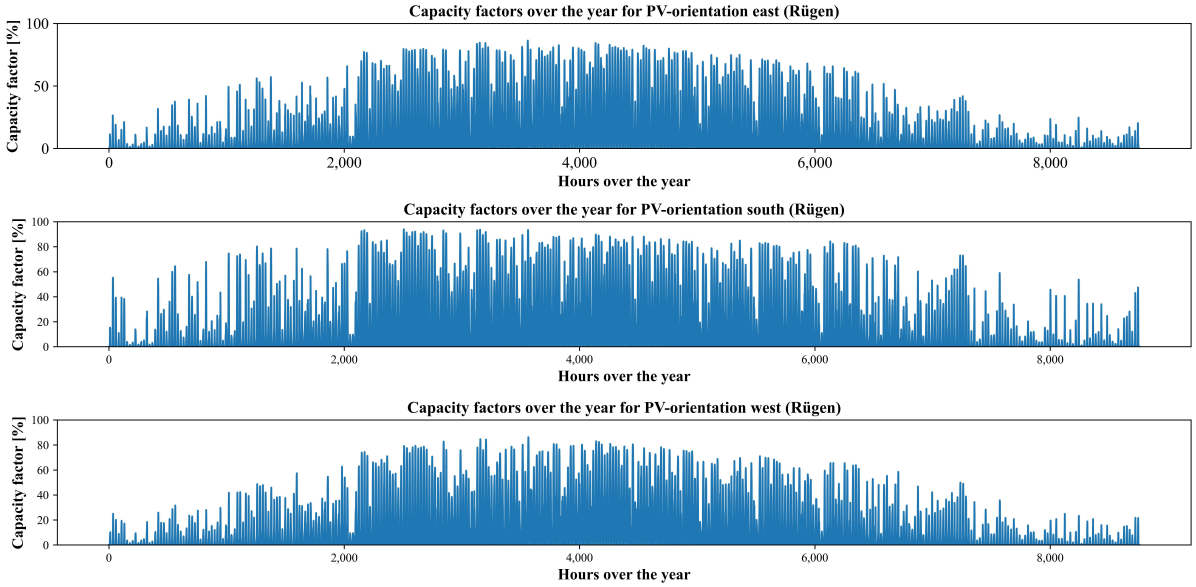

Figure 5: PV capacity factors (own visualization from Pfenninger and Staffell (2016) and Staffell and Pfenninger (2016))

Inverter

Although the *OPEX* for the inverters is assumed to be included in the *OPEX* of the PV system, the *CAPEX* is treated separately here. The costs are 37 €/kW and the lifetime is 20 years (IRENA, 2023b). These values are also assumed in the model. Inverter efficiency varies between 95 to 98 %, depending on the inverter's load (ABB, 2014; Huawei, 2023). For simplification purposes, this thesis assumes a constant efficiency of 97 %, since otherwise the linearity of the MILP would be affected.

Wind Turbine

The *CAPEX* for wind turbines is significantly higher than for PV systems. According to IRENA (2023b) this equates to 1,730 €/kW. In other studies, the values are not quite as high, ranging from 1,298 to 1,462 €/kW (Petkov and Gabrielli, 2020; Sens et al., 2022; Terlouw et al., 2022). The *OPEX* for such systems is higher than that of PV systems as well. The values are ranging from 34 €/kW/a to 53 €/kW/a with a lifetime of 25 to 27 years of the turbines have been reported in the literature (IRENA, 2023b; Petkov and Gabrielli, 2020; Terlouw et al., 2022). A *CAPEX* of 1,500 €/kW, an *OPEX* of 40 €/kW/a and a lifetime of 26 years are set for the use of the optimization tool.

To get the hourly capacity factors required to simulate the electricity generation for the wind turbines, the height of the turbine and the type of rotor must be selected at renewables.ninja. With these values it is possible to generate the needed hourly capacity factors. It is assumed that a Nordex N100/2500 turbine with a hub height of 100 m and a rotor diameter of 100 m is used. The turbine's rated power is 2,500 kW, which serves as the unit size for optimization as well (windpower.net, 2023). The resulting capacity factors are presented in Figure 6 and have an average value of 42.5 % throughout the year. These are higher and more constant over the year than the PV capacity factors. The next needed parameter is the needed area for such wind turbines. According to Lütkehus et al. (2013) they require at least an area four times their rotor diameter to prevent interference with each other. This results with a rotor diameter of 100 m to an area requirement of 12.5 ha/turbine. The area needed for building the wind turbine is way less and depends mostly on the foundation. EnBW (2022) states that normally 0.46 ha is needed for that. These values are also assumed in the thesis.

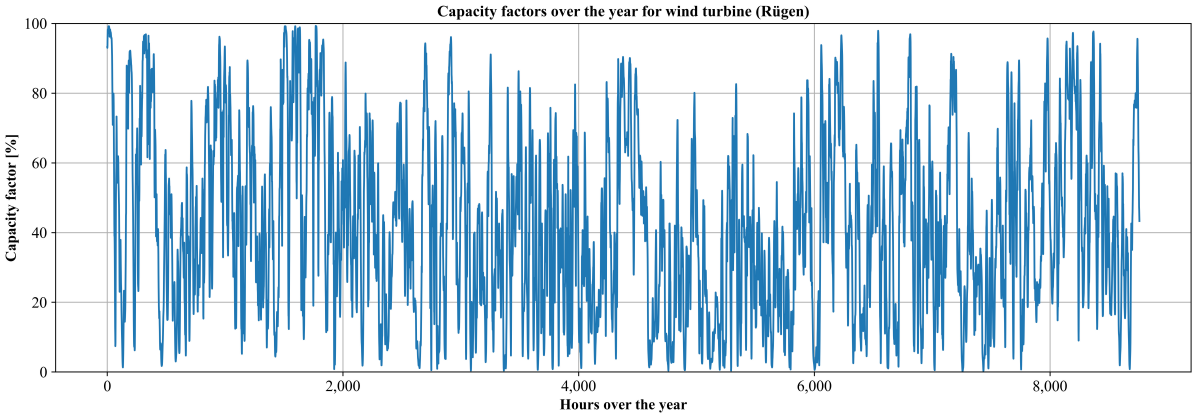

Figure 6: Capacity factors wind (own visualization Pfenninger and Staffell (2016) and Staffell and Pfenninger (2016)

4.3 Battery

As stated in Section 2.3, the battery module in the tool represents a lithium-ion battery. Over the years, the costs of investing in such batteries have drastically decreased (Hannan et al., 2021). However, it is important to differentiate between the expenses of a battery pack and a battery storage system, which is more expensive. In this utilization, a battery storage system is required due to the need for electronic control, safety components, and other features. In the literature, assumptions of 299 €/kWh to 350 €/kWh have been reported for the *CAPEX* for such a system. The *OPEX* is around 2.5 % to 3 % of the *CAPEX* (Cole et al., 2021; Sens et al., 2022; Vartiainen et al., 2019). For the purposes of this thesis, the *CAPEX* is set to 325 €/kWh and the *OPEX* to 2.5 % of *CAPEX* per year. A lithium ion storage system has a lifespan of 13 to 15 years, which is set to 15 years in the tool (Sens et al., 2022; Terlouw et al., 2022).

One of the key technical parameters of a battery is the efficiency. Terlouw et al. (2022) report it to be 91 %, whereas (Sens et al., 2022; Vartiainen et al., 2019) consider lower values of 90 % and 89 %. In the thesis an efficiency of 90 % is assumed. Furthermore, the battery will start already partly charged with a SoC of 50 % to be able to cover any power demand right from the start of the simulation and has a unit size of 20 kWh. In order to maximize the lifetime of the battery system upper and lower limits for the SoC are needed. These limits must be set in a range that still provides enough usable battery capacity without making the total battery system too large. Here the limits are set at 20 and 80 %, which are reasonable values stated by Quaschning (2019).

4.4 Hydrogen Production, Compression and Storage

Now the assumptions for the H_2 module, including the electrolyzer, the compressor, and the H_2 storage system, will be discussed and set.

Electrolyzer

The *CAPEX* of an electrolyzer dependents on the choice of technology (Smolinka et al., 2018). As mentioned in chapter 2.4 the PEMEL has been chosen for this case study. Over the last years, the *CAPEX* has decreased and, according to Fraunhofer ISE (2021), it is for an electrolyzer providing H_2 at 30 bar at 978 €/kW. Other references show different values. For instance, Jarosch et al. (2022) reports 738 €/kW, whereas Petkov and Gabrielli (2020) present 1,295 €/kW. The systems *OPEX* and lifetime fluctuate less, ranging from 2.75 to 3.5 %*CAPEX*/a and lasting 15 years (Gorre et al., 2020; Jarosch et

al., 2022; Petkov and Gabrielli, 2020; Sens et al., 2022). For the utilization of the optimization tool, a *CAPEX* of 1,000 €/kW, an *OPEX* of 3.5 % and a lifetime of 15 years are assumed.

The needed technical assumptions for the electrolyzer unit include efficiency, H_2 output pressure and temperature, and unit size required for the MILP. Efficiency can be specified in either kWh/Nm^3 or as a percentage. If stated as a percentage, it refers to either the lower or the higher heating value, so this should always be included for verification. Gorre et al. (2020) assume 75 % for a 30 bar output based on the HHV. The same value is also given by a manufacturer of PEMEL (H-TEC SYSTEMS) with an output of 20 to 30 bar, who also states the output temperature of produced H_2 with 57 °C (H-TEC SYSTEMS, n.d.). Another scientific paper assumes an efficiency of 60 % (based on LHV), without specifying the pressure (Schütte et al., 2022). In this thesis, an efficiency of 70 % based on the HHV is assumed, along with a H_2 output of 30 bar and an outlet temperature of 57 °C for the H_2. Furthermore, the unit size of 250 kW is set for the electrolyzer.

To simplify the tool and to fulfill the requirements of linear programming, some technical parameters of the electrolyzer were modified which could not be implemented in the limited time available for the thesis. Specifically, the load change is assumed to be more flexible, allowing the electrolyzer to ramp from 0 % load to 100 % nominal power immediately. In addition, only hourly values are calculated in the simulation, which is why a more precise approach is not possible. Moreover, the efficiency is assumed to be constant instead of being determined by the load of the electrolyzer, like it is in the real world (Falcão and Pinto, 2020).

Compressor

The compressors *CAPEX* ranges from 1,780 to 2,500 €/kg_{H2}/h with different pressure limits from 100 to 250 bar (Sens et al., 2022; Terlouw et al., 2022). The annual *OPEX* is between 4 % and 5 % of the *CAPEX*, and it has a lifetime of 10 to 15 years (Neubauer, 2023; Sens et al., 2022; Terlouw et al., 2022). This thesis assumes a *CAPEX* of 2.000 €/kg_{H2}/h, an *OPEX* of 4.5 %CAPEX/a, and a lifetime of 12.5 years. The unit size for the MILP is set to 1 kg_{H2}/h.

In the previously mentioned studies, the assumed efficiency for the H_2 compressor is 79 %, while the H_2 loss during the compression process is 0.005 $kg_{H2}/kg_{comp\ H2}$ (Neubauer, 2023; Sens et al., 2022; Terlouw et al., 2022). The mentioned values for the efficiency and the H_2 loss are used as well in the optimization. To calculate the electricity required for the compressor to compress the H_2, the formula 2 from chapter 2.4 is utilized. This formula requires the mean gas factor for H_2 of 1.05, the polytropic corresponding coefficient of 1.3, the universal gas constant of 8.3145 J/(mol K), the output temperature and pressure of H_2 out of the electrolyzer of 57 °C and 30 bar, the molar mass of H_2 of 2.0159 kg/mol, the efficiency of the compressor of 79 % mentioned above, and the current pressure of the H_2 storage tank (Bouché and Wintterlin, 1968; Wiegleb, 2016). This results in the energy demand as a function of the pressure to be achieved. But for tool implementation purposes the mean value will be used instead, because the specific energy requirement is multiplied by the amount of H_2 to be compressed. With an unknown over the process changeable variable, it would first have to be determined for each point in time by multiplying two unknown variables. This affects the linearity of the MILP and is therefore not possible to implement in the form in which the tool is constructed. Consequently, for the purpose of simplification, the specific energy demand is set to be the constant value 0.02454 kWh_{el}/kWh_{H2}.

Storage

After compressing the H_2, it is stored until a demand requires the withdrawal of it. Steel gas pressure storage tanks are assumed, as they have lower costs compared to other H_2 storage technologies (Barthelemy et al., 2017). While these storage systems require significant space, this is not a criteria for the

storage system in this thesis (Andersson and Grönkvist, 2019). The *CAPEX* of steel gas tank depends on the pressure which the tank needs to withstand. In the literature, the *CAPEX* for 200 bar storage systems is around 350 to 450 €/kg_{H2} according to Elberry et al. (2021). Other studies mention higher costs of 460 €/kg_{H2} (Terlouw et al., 2022) and 490 €/kg_{H2} (Gorre et al., 2020). The *OPEX* is between 2 to 4 %CAPEX/a according to the aforementioned studies. Additionally, the storage system has a lifetime of 20 years (Gorre et al., 2020; Hassan et al., 2021; Terlouw et al., 2022). For the utilization in this thesis, a *CAPEX* of 430 €/kg_{H2}, an *OPEX* of 3 %CAPEX/a and a lifetime of 20 years are assumed, based on the literature just presented.

As stated at Reuß et al. (2017) , there is no loss of H_2 during storage. Further, the required module size is set to 60 kg_{H2} and is able to withstand 200 bar. This size is common for steel storage tanks, which can be purchased in large quantities for 200 bar (Linde GmbH, 2016). In addition, a storage level of 20 % is initially set in order to provide possible H_2 requirements directly at the beginning of the simulation.

4.5 Electricity and Hydrogen Prices

To calculate the profit, prices must be determined for the sale of electricity and H_2. The price of electricity is set to fluctuate throughout the year, while a constant price is assumed for H_2. The exact used values are presented in the following.

Electricity Price

An hourly electricity price must be available, because in the tool the electricity is fed into the grid every hour as well. The "energy-charts.info" website from the Fraunhofer ISE (2023b) provides a diverse range of information on the electricity grid, current generation and consumption data. It also includes electricity prices from the day-ahead market in Germany in recent years. Since the capacity factors used for RE refer to 2019, this year is also used as the reference year for the used electricity prices to sell the produced electricity. Figure 7 illustrates the hourly electricity prices for Germany during 2019 on the day-ahead market. The price is mostly in the range of 25 to 60 €/MWh over the year and the mean value is 37.66 €/MWh. The maximum value is 121.46 €/MWh and in only seven hours over the year, the electricity prices were higher than 100 €/MWh. The minimum value is -90.01 €/MWh and in total, for 211 hours a negative electricity price was reached in 2019. In comparison to 2022, the prices from 2019 are significantly lower as it can be seen in Figure 8. The mean electricity price from 2022 in Germany was 235.44 €/MWh. That means the average price from 2022 was higher than the maximum value from 2019. The minimum value was 69 €/MWh, which is nearly the double amount of the average price from 2019 (Fraunhofer ISE, 2023b). The reason for such a change in electricity prices in Germany occurred due to the war in Ukraine (Leupoldina, 2022). Due to these fluctuations in energy prices and the fact that the used capacity factors for the RE are from 2019, the electricity prices from 2019 were assumed to calculate the different scenarios. Despite that, the prices from 2022 will be used in an additional scenario in the end in order to analyze the effect of high electricity prices on the results. Furthermore, it is important to be mentioned that no EEG compensation is paid on top of the electricity price. This means the RE system relies only on the electricity market and the H_2 production without any subsidies.

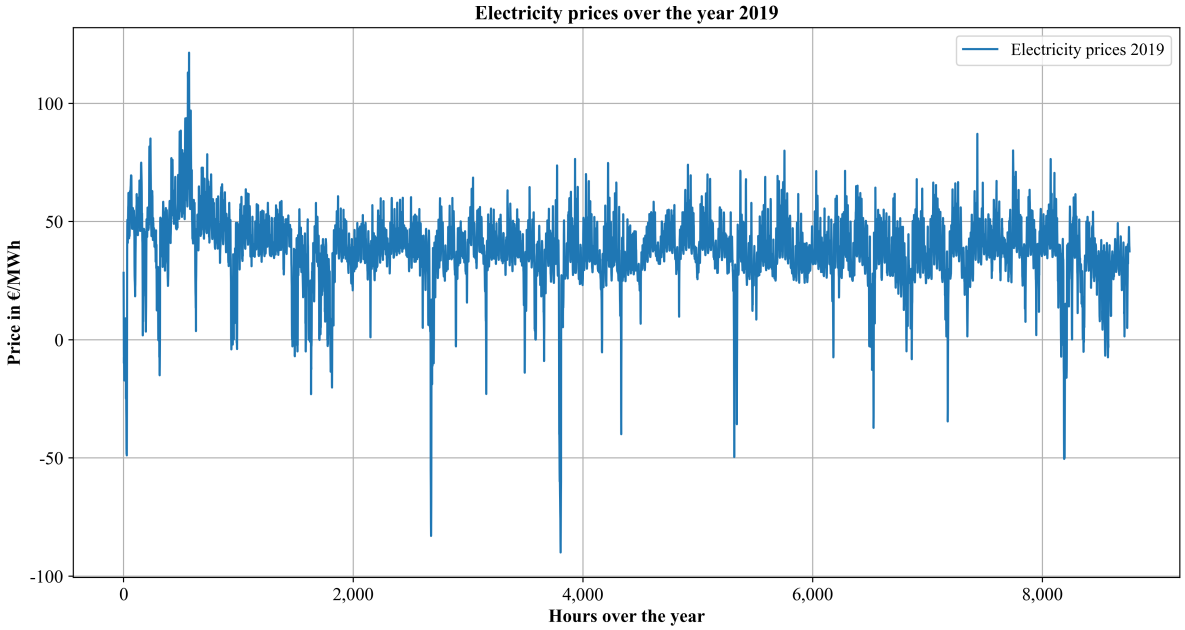

Figure 7: Electricity prices from day-ahead market in Germany 2019 (Fraunhofer ISE, 2023b)

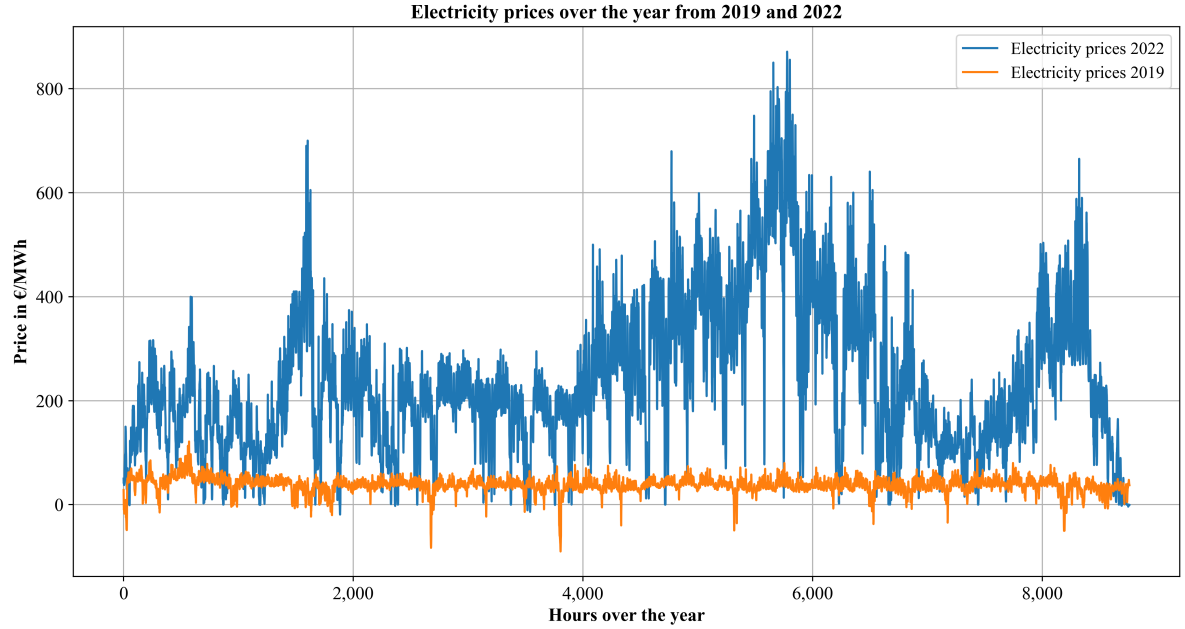

Figure 8: Comparison of the electricity prices from the day-ahead market in Germany from 2019 and 2022 (Fraunhofer ISE, 2023b)

Hydrogen Price

In contrast, the sale of H_2 is assumed to have a constant price. Currently in 2023, renewable H_2 is priced with 9.50 to 13.85 €/kg at filling stations in Germany. The price at filling stations has a dynamic price. Furthermore, it depends on the supply pressure either the H_2 is supplied with 350 or 700 bar (H2 MOBILITY Deutschland GmbH & Co. KG, 2023). Since in the model the H_2 is sold with maximal 200 bar and still has to be transported, for example to a filling station, the selling price assumption must be lower

than the just mentioned values. In the following it is assumed that the H_2 is sold to a filling station operator. The transportation cost for gaseous compressed H_2 by truck is 0.16 €/kg_{H2} for distances up to 1000 kilometers as reported by the Nationaler Wasserstoffrat (2021). Additionally, a profit margin for is needed for the filling station operator as well. Because of the just explained points, the selling price for H_2 out of the storage system to the customer is set to 7.5 €/kg_{H2}. Furthermore, the H_2 price is used to calculate the cost of the already filled H_2 storage tank at the start of the simulation to fulfill a demand right from the start of the simulation if necessary.

4.6 Estimated Hydrogen Demand

To implement module five from Figure 3, a daily H_2 demand is necessary to set. Since the planned energy system is located on the island of Rügen, an appropriate demand estimation for the location is required.

The Rügen-Stralsund district is one of the HyStarter regions. In the future, these regions want to develop into a H_2 hub. To achieve this, multiple aspects related to H_2 are being assessed in additional HyStarter studies. The focus is on the utilization of H_2 in the mobility and heating sectors, electricity storage, and H_2 production (Epp et al., 2021). In order to apply the developed tool, different H_2 demands for mobility are used, which were calculated in the HyStarter study for Rügen-Stralsund. Two different demands are presented in Table 10. The first case assumes that 5 % of passenger cars are fuel cell vehicles in the future. The second case considers a 30 % share of fuel cell vehicles in public transport. The annual demand for the first case is 833 t_{H2} and 394 t_{H2} for the second. This subsequently results in a daily demand of 2,250 kg and 1,080 kg, which must be met by the modeled energy system (Epp et al., 2021). In the following the first case will be named demand high and the second case demand low.

Table 10: Demand scenarios (Epp et al., 2021)

	Demand high	**Demand low**
Yearly demand [t/a]	822	394
Daily demand [kg/d]	2,250	1,080

In Table 11 all assumed values are illustrated as an overview.

Table 11: Overview of used parameters

Component	**Parameter**	**Unit**	**Value**	**Reference**
PV	CAPEX	€/kW_p	605	(IRENA, 2023b; Sens et al., 2022)
	OPEX (incl. inverter)	€/kW_p/a	8	(IRENA, 2023b; Petkov and Gabrielli, 2020; Vartiainen et al., 2019)
	Lifetime	a	30	(Petkov and Gabrielli, 2020; Terlouw et al., 2022)
	Required Area	ha/kW_p	0.001	(Umweltbundesamt, 2023)
	Unit Size	kW_p	1	
Inverter	CAPEX	€/kW	37	(IRENA, 2023b)
	Lifetime	a	20	(IRENA, 2023b)
	Efficiency	%	97	(ABB, 2014; Huawei, 2023)
	Unit Size	kW	500	Own assumptions

Wind Turbine	CAPEX	€/kW	1,500	(IRENA, 2023b; Petkov and Gabrielli, 2020; Sens et al., 2022; Terlouw et al., 2022)
	OPEX	€/kW/a	40	(IRENA, 2023b; Petkov and Gabrielli, 2020; Sens et al., 2022; Terlouw et al., 2022)
	Lifetime	a	26	(IRENA, 2023b; Petkov and Gabrielli, 2020; Sens et al., 2022; Terlouw et al., 2022)
	Required Area	ha/Unit	12.5	(Lütkehus et al., 2013)
	Required Foundation Area	ha/Unit	0.46	(EnBW, 2022)
	Hub Height	m	100	(windpower.net, 2023)
	Rotor Diameter	m	100	(windpower.net, 2023)
	Unit Size	kW	2,500	(windpower.net, 2023)
Battery	CAPEX	€/kWh	325	(Cole et al., 2021; Sens et al., 2022; Vartiainen et al., 2019)
	OPEX	%/CAPEX/a	2.5	(Cole et al., 2021; Sens et al., 2022; Vartiainen et al., 2019)
	Lifetime	a	15	(Sens et al., 2022; Terlouw et al., 2022)
	Efficiency	%	90	(Sens et al., 2022; Terlouw et al., 2022; Vartiainen et al., 2019)
	Start SoC	%	50	Own assumption
	Min SoC	%	20	Own assumption
	Max SoC	%	80	Own assumption
	Unit Size	kWh	20	Own assumption
Electrolyzer	CAPEX	€/kW	1,000	(Fraunhofer ISE, 2021; Jarosch et al., 2022; Petkov and Gabrielli, 2020)
	OPEX	%CAPEX/a	3.5	(Gorre et al., 2020; Jarosch et al., 2022; Petkov and Gabrielli, 2020; Sens et al., 2022)
	Lifetime	a	15	(Gorre et al., 2020; Jarosch et al., 2022; Petkov and Gabrielli, 2020; Sens et al., 2022)
	Efficiency	%	70	(Gorre et al., 2020; H-TEC SYSTEMS, n.d.)
	Pressure Output	bar	30	(Gorre et al., 2020; H-TEC SYSTEMS, n.d.; Schütte et al., 2022)
	Temperature Output	°C	57	(H-TEC SYSTEMS, n.d.)
	Unit Size	kW	250	Own assumption
Compressor	CAPEX	€/kg_{H2}/h	2,000	(Sens et al., 2022; Terlouw et al., 2022)

	OPEX	%/CAPEX/a	4.5	(Sens et al., 2022; Terlouw et al., 2022)
	Lifetime	a	12.5	(Sens et al., 2022; Terlouw et al., 2022)
	Efficiency	%	79	(Sens et al., 2022)
	Losses	$kg_{H2,\ loss}/kg_{H2,\ comp}$	0.005	(Sens et al., 2022)
	Electricity Demand	kWh_{el}/kWh_{H2}	0.02454	Own assumption based on formula 2
	Unit Size	kg_{H2}/h	1	Own assumption
H_2 Storage	CAPEX	€/kg	430	(Elberry et al., 2021; Gorre et al., 2020; Terlouw et al., 2022)
	OPEX	%CAPEX/a	3	(Elberry et al., 2021; Gorre et al., 2020; Terlouw et al., 2022)
	Lifetime	a	20	(Gorre et al., 2020; Hassan et al., 2021; Terlouw et al., 2022)
	Start SoC	%	20	Own assumption
	Maximum Pressure	bar	200	(Linde GmbH, 2016)
	Losses	kg_{H2}/d	0	(Reuß et al., 2017)
General	Interest	%	5	Own assumption
	Share of Debt	%	80	Own assumption
	H_2 sale price	€/kg	7.50	(H2 MOBILITY Deutschland GmbH & Co. KG, 2023)
	Max Grid Capacity	kW	10,000	Own assumption

4.7 Sensitivity Analysis

A sensitivity analysis is performed to test the effect of changes in input parameters on the results. By systematically varying relevant parameters, the variables that have a strong influence on the results are identified. This is a method commonly used in such scientific work (Cormos et al., 2018; Cuisinier et al., 2021; Gorre et al., 2020; Terlouw et al., 2022). The assumptions for the sensitivity analysis are presented in the following.

The values analyzed in the sensitivity analysis are the *CAPEX* of the individual components and the H_2 price. The various *CAPEX* values of the components are varied in 5 % steps. The first value is 75 % and the last 125 % of the actual assumed value. For the H_2 price, the values are varied more in steps of 10 % from 50 % to 150 %. Table 12 shows the highest and lowest values of the varied variables to provide an overview of the range in which the sensitivity analysis is conducted.

Table 12: Highest and lowest assumptions for the sensitivity analysis

Component	Parameter	Unit	Value
PV	$CAPEX_{-25\%}$	€/kW_p	453.75
	$CAPEX_{+25\%}$	€/kW_p	756.25
Inverter	$CAPEX_{-25\%}$	€/kW	27.75
	$CAPEX_{+25\%}$	€/kW	46.25
Wind Turbine	$CAPEX_{-25\%}$	€/kW	1,125

	$CAPEX_{+25\%}$	€/kW	1,875
Battery	$CAPEX_{-25\%}$	€/kWh	243.75
	$CAPEX_{+25\%}$	€/kWh	406.25
Electrolyzer	$CAPEX_{-25\%}$	€/kW	750
	$CAPEX_{+25\%}$	€/kW	1,500
Compressor	$CAPEX_{-25\%}$	€/kg_{H2}/h	1,600
	$CAPEX_{+25\%}$	€/kg_{H2}/h	2,500
H_2 Storage	$CAPEX_{-25\%}$	€/kg_{H2}	322.5
	$CAPEX_{+25\%}$	€/kg_{H2}	537.5
General	H_2 sale $price_{-50\%}$	€/kg_{H2}	3.75
	H_2 sale $price_{+50\%}$	€/kg_{H2}	11.25

5 Results

This chapter presents the generated results of the different scenarios calculated with the optimization tool. Various combinations of the modules described in chapter 3 are discussed. First, scenarios with an exclusive electricity feed in and without H_2 production are presented, followed by those with a combined electricity feed in and a H_2 production, and, thirdly, those with a combined electricity feed in, a H_2 production, and a daily H_2 demand that must be covered. Furthermore, Chapter 5.4 shows the results of the most profitable scenario if the electricity price from 2022 were assumed instead of the prices from 2019. Finally, the results of the sensitivity analysis are presented.

Overall, a battery system is not part of the solution in any of the assumed scenarios. For this reason, the results of the scenarios are identical, with the same modules except for the battery. For example, the scenario consisting of PV, wind turbines, and H_2 production generates the same results in every aspect of the optimization as the scenario with PV, wind turbines, battery, and H_2 production. In order to present the results more readily and to avoid unnecessary duplication, these battery scenarios are not shown separately in the presentation of the results. In addition, all the scenarios include an exclusively southern PV orientation as part of the solution and never a western or eastern orientation. Therefore, PV with a southern orientation is represented as PV in the following.

To improve the flow of reading, not all the individual values shown in the following diagrams are mentioned directly. For this reason, all values for the following figures are summarized in the Appendix A to E.

5.1 Scenario: Exclusive Electricity Feed in

In this chapter, the results of the optimization for the scenarios with exclusive electricity feed in are presented, which are “PV,” “ PV + Wind”, “PV + Grid restriction” and “ PV + Wind + Grid restriction”.

Annual Revenue, Costs, Profits, and ROI

Figure 9 presents on the primary y-axis the revenue from electricity sales per year, in green, and the costs occurring per year, in light blue, and on the secondary y-axis the *ROI* as a black cross for all scenarios that do not include H_2 production (x-axis). The difference between the revenue and cost bars corresponds to the optimized value from the tool's objective function, the profit per year.

The results of the "PV" scenario are identical to the "PV + Wind" scenario, and the "PV + Grid restriction" is identical to "PV + Wind + Grid restriction". The revenues and costs per year are four times higher for the scenarios without grid restriction than for those with restriction. This also applies to the profit per year, which is 76 % lower with than without the restrictions.

The *ROI*, on the other hand, is almost identical for the four scenarios. With 0.8278 % (without grid restriction) and 0.8273 % (with grid restriction) the value differs only in the third decimal point.

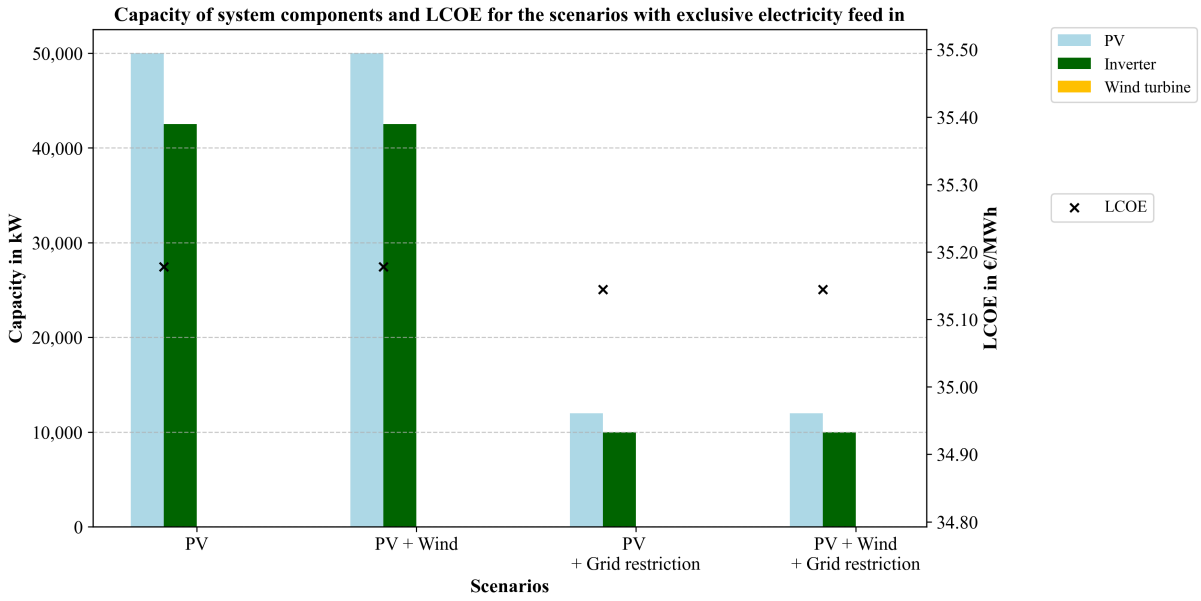

Figure 9: Revenue and costs per year and ROI for scenarios with an exclusive electricity feed in

System Design and LCOE

Figure 10 displays the capacity of the PV system and the inverter in kW on the primary y-axis and the *LCOE* in €/MWh on the secondary y-axis for the four scenarios (x-axis) with exclusive electricity feed in. PV is illustrated as a light blue bar, inverters as a green bar, and wind turbines as a yellow bar, while the *LCOE* is marked as a black cross. As shown in Figure 9, the values for each of the scenarios without and with grid restraint are identical. In none of the four scenarios are wind turbines part of the optimization solution. Without grid restriction, 50 MW PV and 42.5 MW inverters are used. With the grid restrictions, the capacity is reduced by 76 % for PV and by 76.5 % for the inverter. The *LCOE*, on the other hand, only differs by 0.03 €/MWh between the scenarios.

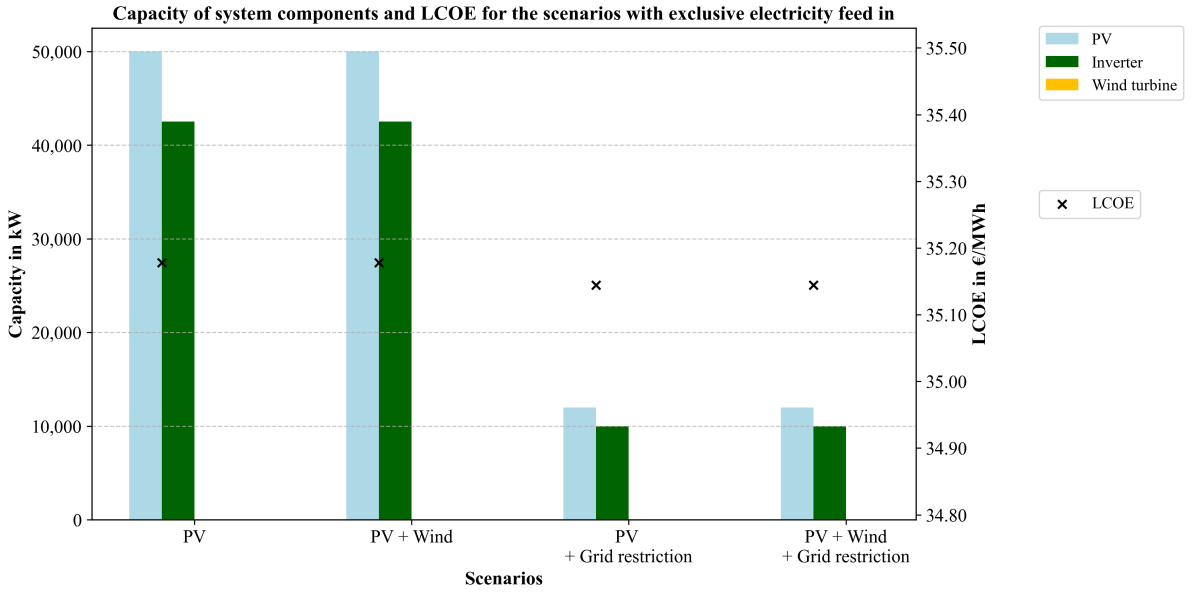

Figure 10: Capacity of system components: PV, inverter, and wind turbine as well as the LCOE for scenarios with exclusive electricity feed in

Total Investment and Payback Time for the Energy System

In Figure 11, the total investment, including the interest and the *PT*, for the different scenarios in this chapter is presented. The investment is divided by each investment in the used system components for all scenarios with exclusive electricity feed in in € and corresponds to the primary y-axis. The bars for the PV are in light blue, and those for the inverter are in green. The corresponding values are stacked on top to represent the total investment in the energy system. The *PT* is marked as a black cross, and the values belong to the secondary y-axis. For the scenarios without grid restrictions, 95.8 % of the total investment is accounted for by the PV system and 4.2 % by the inverter (green). With grid restrictions, the investment is significantly lower as less power is installed, as displayed in Figure 10. Furthermore, the total investment is 76 % less in these scenarios. The ratio from the investment of PV to inverter is almost identical in the scenarios with grid restriction, with 95.9 % to 4.1 %, as is the *PT,* which is at 23.64 and 23.64 years.

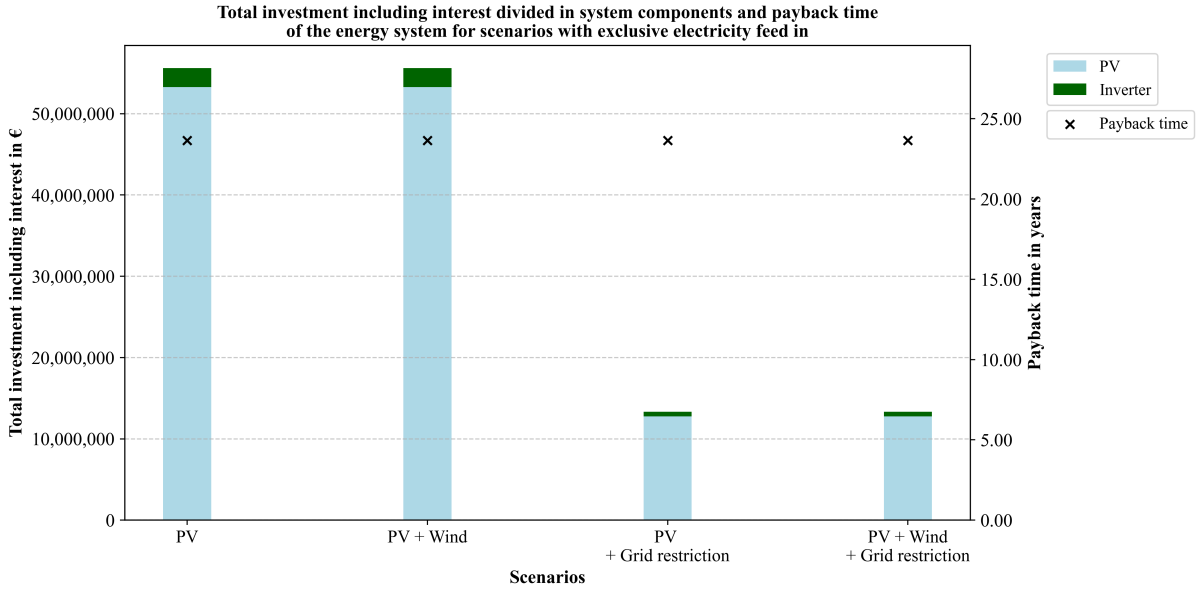

Figure 11: Total investment including interest divided in the system components and the payback time of the energy system for scenarios with exclusive electricity feed in

Electricity usage over the year

Figure 12 illustrates the amount of electricity that is fed into the grid (blue) and the amount that is not used but could be produced (orange) for the scenario without grid restriction (left) and with grid restriction (right) over the simulated year. The left-hand image shows that the feed in limit is around 42.5 MWh. This is the same amount the inverter could handle per hour. So, the feed in depends on the inverter power of 42.5 MW. The right-hand image shows that slightly less than 10 MWh of electricity can be fed into the grid in the scenario with grid restriction. The grid restriction was set to 10 MW. Apart from the magnitude of the power, no difference can be seen in the curves for the electricity feed in and the not-used electricity. In both scenarios, the electricity is generated mostly in the summer, and daily ups and downs in generation over the duration of the year are visible. In addition, three peaks of unused electricity, which lie between the hours 2,200 and 4,000 of the year, are above the capacity of the inverters. This can be observed in the left and right-hand figures. In absolute figures, 61,333 MWh of electricity are fed into the grid, and 1,941 MWh are switched off. If grid restrictions apply, 76 % less electricity is fed into the grid, amounting to 14,688 MWh, and 75 % less electricity is switched off, accounting for 486 MWh.

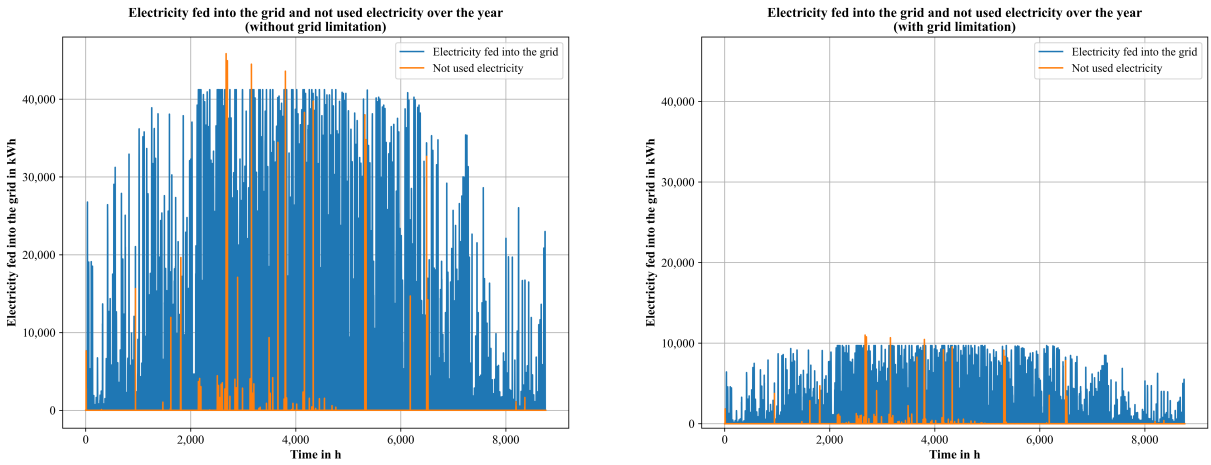

Figure 12: Comparison of electricity fed into the grid and electricity not used without grid limitation (left) and with limitation (right) over the year

Summary of the exclusive electricity feed in scenarios

In summary, the results show how the grid restriction impacts the optimized solution of the analyzed energy systems. The profit per year and the total investment are higher without a grid restriction. Furthermore, the PV and inverter capacities are significantly larger if no grid restrictions exist, while no wind turbines are part of the solution of the optimization tool for all four scenarios. However, the economical key figures like *ROI, LCOE,* or *PT* are almost identical for all scenarios, as is the ratio of PV to inverter capacity. This leads to the conclusion that, based on the assumed values, it is more economically viable to install PV than wind. Moreover, with a grid restriction, less electricity can be fed into the grid, but with an optimized design for this case, almost the same economic efficiency can be achieved.

5.2 Scenario: Combined Electricity Feed in and Hydrogen Production

The optimization results for the scenarios with a combined electricity feed in and H_2 production are provided in this chapter, which are “PV + Ely”, “ PV + Wind + Ely”, “PV + Ely + Grid restriction” and, “ PV + Wind + Ely + Grid restriction”. In contrast to the results from chapter 5.1, module 4, consisting of the electrolyzer, compressor, and H_2 storage, can also be part of the result of the optimization tool.

Annual Revenue, Costs, Profits, and ROI

Figure 13 shows the revenue from electricity and H_2 sales per year, together with the resulting costs per year and the *ROI* for the scenarios with combined electricity and H_2 production without any specific H_2 demand. The orange bar represents the revenue from electricity, and the green bar represents the revenue from H_2 in €/a. The sum of those is the total revenue per year. The light blue bar next to the revenue represents the total costs per year. These values correspond to the primary y-axis. The *ROI* of the scenarios is marked as a cross, with values relating to the secondary axis. The different scenarios for the values are listed on the x-axis. The difference between the bars is the optimized value, the profit per year in euros.

In scenarios including wind turbines, significantly higher revenues from the sale of H_2 appear. The "PV + Wind + Ely" scenario has the highest profit and amounts to 11,401,807 €/a. Moreover, it has the highest *ROI* of the four scenarios as well. The revenue per year for electricity and for H_2 is higher for the two scenarios without grid restriction than for the other two scenarios. However, the revenue for H_2 is significantly higher than for electricity, above 90 % in all scenarios. Module 2 of the tool, which

includes wind turbines, has the greatest influence on revenue. In the results for the two scenarios that allow wind turbines in the optimization, 73 % and 67 % more revenue are generated compared to the scenarios without wind turbines. In contrast, the costs per year for the four different scenarios differ by a maximum of 30 %. These are highest in the "PV + Ely + Grid restriction" scenario and lowest in the "PV + Ely" scenario. These scenarios also have the lowest *ROI* of the four. It can therefore be concluded that wind turbines have a significant positive influence on the economic efficiency of the scenarios analyzed. The influence of grid restriction, on the other hand, on revenue, costs, and, thus, profit per year, is low. The same applies to the *ROI*.

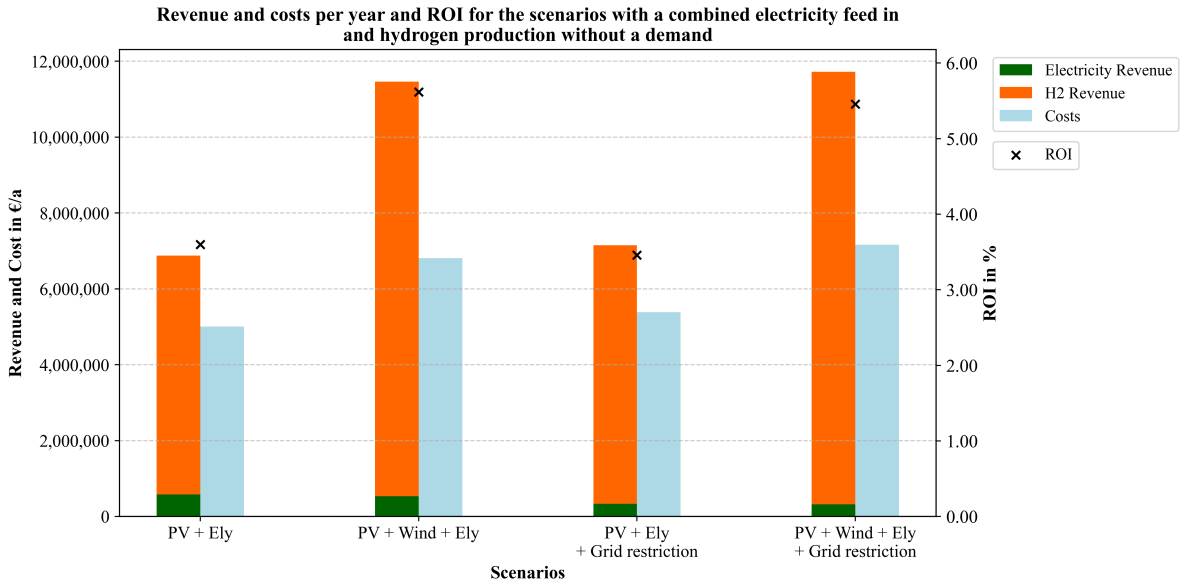

Figure 13: Revenue and costs per year and ROI for the scenarios with a combined electricity feed in and hydrogen production without demand

System Design and $LCOH_2$

The system design for the various scenarios of combined electricity feed in and H_2 production without a specific demand is shown in Figure 14, which is divided in capacity of PV (light blue), inverter (green), wind turbine (yellow), and electrolyzer (blue) (left) and the capacity of the compressor (orange) and the H_2 storage (turquoise) (right). In order to show the entire energy system as a whole, the figures are shown side by side. Individual, larger versions of the two diagrams can be found in Appendix F and G. For both figures, the different scenarios analyzed in the chapter are shown on the x-axis. On the left-hand figure, the primary y-axis shows the output in kW, and the secondary y-axis shows the $LCOH_2$ and the $LCOH_2$, where the revenue from the sale of electricity has been included. The figure on the right shows the capacities on both y-axes, on the primary axis in kg_{H2}/h for the compressor and on the secondary axis in t_{H2} for the H_2 storage.

In scenarios "PV + Ely" and "PV + Ely + Grid restriction," PV power reaches its highest value at 50 MW. In the other scenarios, PV power is slightly lower, but an additional 10 MW from wind turbines is in the solution of the optimization tool. Inverter capacity is highest in the "PV + Ely" scenario, decreases with the addition of the wind module, and drops even further under grid restriction, reaching its lowest in the "PV + wind + Ely + grid restriction" scenario. Despite this, this scenario has the highest electrolyzer and compressor capacity among the four scenarios, being the lowest without wind turbines. H_2 storage capacity follows a similar trend, being higher with wind turbines and reaching its highest with the simultaneous existence of grid restrictions. Notably, electrolyzer and compressor capacities, as well as H_2 storage, have the highest and lowest values within the same scenarios.

The lowest $LCOH_2$ is in the scenario that has the highest profit per year, "PV + Ely + Wind", and is 4.67 €/kg_{H2} and drops to 4.31 €/kg_{H2} by including the electricity revenue. In the scenario with wind turbines and grid restrictions, the $LCOH_2$ is only slightly lower but also decreases less with the income from electricity sales. The two scenarios without wind turbines have a significantly higher $LCOH_2$. Without grid restriction, the value can be reduced by 0.70 €/kg_{H2} through electricity sales, which is the highest reduction due to including electricity revenue in the calculation of $LCOH_2$ in the four scenarios.

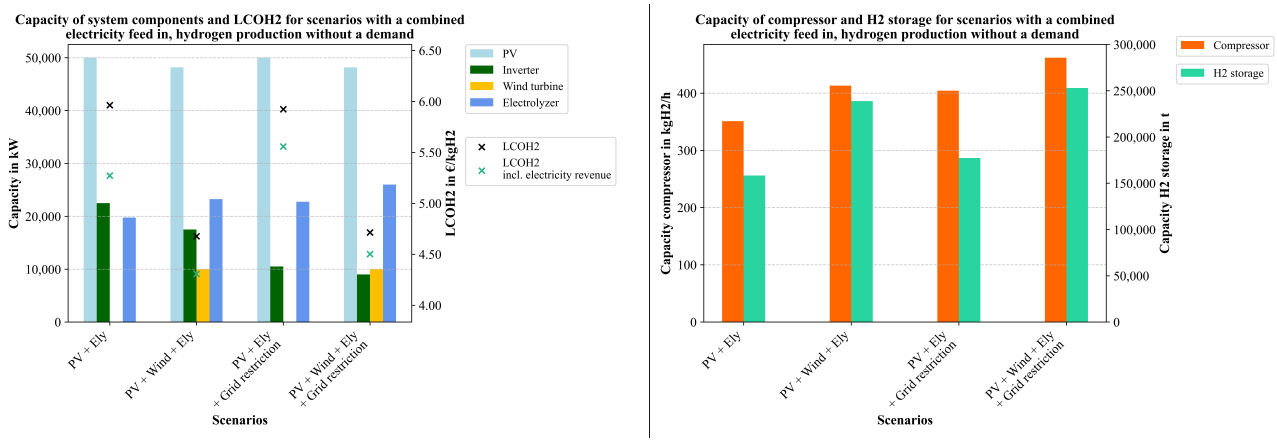

Figure 14: Capacity of the system components: PV, inverter, wind turbine and electrolyzer as well as the $LCOH_2$ and $LCOH_2$ incl. electricity revenue (left) and capacity of compressor and H_2 storage (right) for scenarios without a H_2 demand

Total Investment and Payback Time for the Energy System

Figure 15 shows the total investment of the energy system, including the interest for each of the modeled scenarios with combined electricity feed in and H_2 production without a specific demand, and the corresponding *PT* on the secondary y-axis. The primary y-axis illustrates the total investment, which is divided by each investment for the used system components in euros. The overall investment in the energy system is displayed by stacking the corresponding values of the components on top of each other. The colors for the individual components in the bar for the investment are the same as in Figure 14. The overall investment in the energy system is shown by stacking the corresponding figures on top of each other.

The scenarios with the highest total investment are those including wind turbines, although this value is slightly higher with the addition of grid restrictions. In all four scenarios, the PV system accounts for the largest share of the investment, followed by the electrolyzer and, if part of the scenario, the wind turbines. In general, the total investment for the inverter, compressor, and H_2 storage system is a relatively small part of the total investment in all four scenarios. Furthermore, despite the higher total investment, the *PT* is reached three years earlier for "PV + Wind + Ely" and "PV + Wind + Ely + Grid restriction" than for "PV + Ely" and "PV+ Ely + Grid restriction".

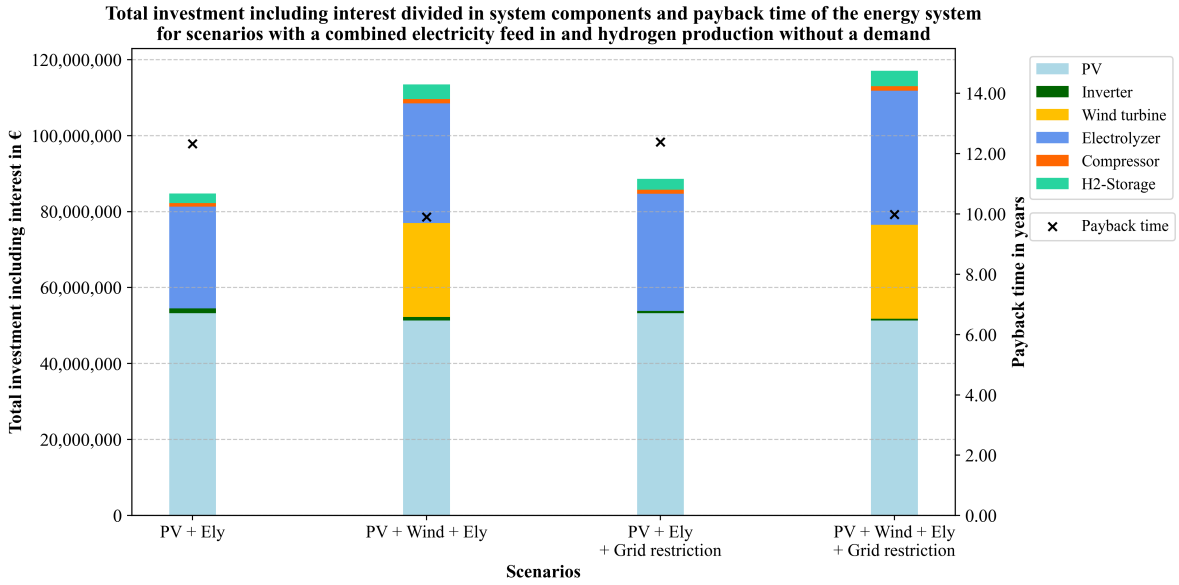

Figure 15: Total investment including interest divided in the system components and the payback time of the energy system for the scenarios without a H_2 demand

Electricity usage over the year

On the left-hand side of Figure 16, the amount of electricity that is fed into the grid (blue) and the amount that is not used but would be available (orange) are shown for the different scenarios analyzed in this chapter over the year. Moreover, the electricity that flows into the electrolyzer to produce H_2 is shown in the figures on the right-hand side.

It can be seen in the left images that the inverter or grid restriction limits the feed in of electricity into the grid. Only in the "PV + Wind + Ely" scenario is not a specific variable that limits the feed in visibly. The electricity flowing into the electrolyzer is limited by its power and is identifiable in all scenarios. In addition, the electrolyzer is operated much more consistently with PV and wind turbines than with only PV. This difference is visible in the figures on the right-hand side.

In general, it can be noted that significantly more electricity remains unused due to the grid restriction, especially in the range between hours 2,000 and 6,000 of the year, even though the electrolyzer is scaled up. This occurs even more with a pure PV power supply. In this case, almost 500 % more electricity is switched off than in the same scenario without grid restrictions. Including wind power, the amount is less, but still 412 % higher than without grid restriction. In addition, there is a peak in electricity feed in and switch-off at the beginning and end, as well as in H_2 production. At all four scenarios, the annual demand from chapter 4.6 is covered, but not the given daily demand.

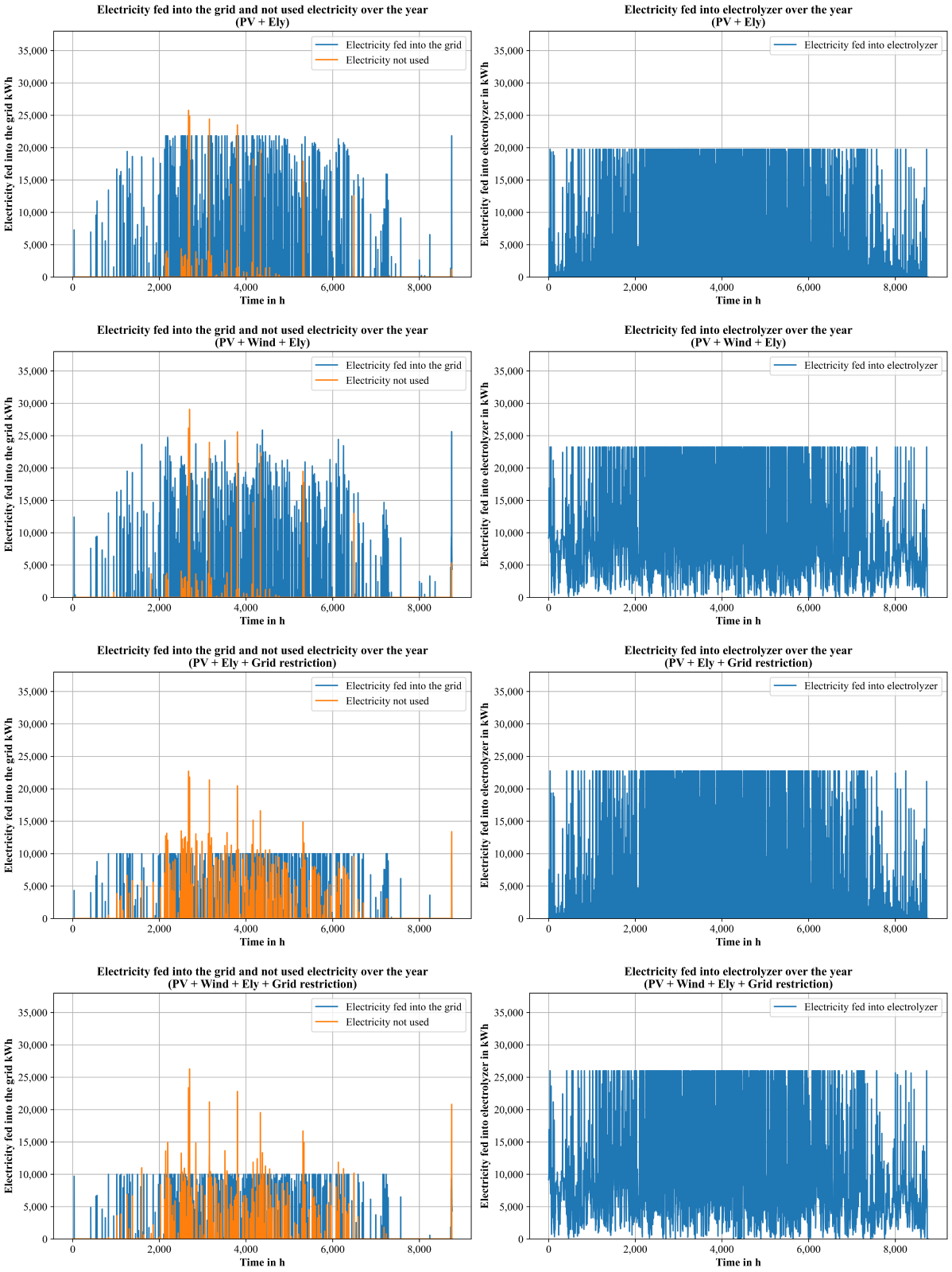

Figure 16: Comparison of electricity fed into the grid, electricity not used (left) and electricity fed into electrolyzer (right) over the year for the scenarios without hydrogen demand

Summary of the Combined Electricity Feed in and Hydrogen Production Scenarios
This chapter delves into the optimization outcomes for scenarios involving combined electricity feed in and H_2 production. The addition of wind turbines shows a positive impact on economic metrics such as *ROI* and $LCOH_2$, although the cost per year rises with wind turbines. Furthermore, the scenario "PV + Ely + Wind," yielding the highest profit per year, also presents the lowest $LCOH_2$ at 4.67 €/kg_{H2}, reducing to 4.31 €/kg_{H2} when incorporating electricity revenue. Total investment peaks in scenarios with wind turbines, yet scenarios with wind power achieve shorter payback times. In total, grid restrictions exhibit a comparatively modest effect on revenue, costs, and annual profit while having a significant effect on the system design.

5.3 Scenario: Combined Electricity and Hydrogen Production with Daily Hydrogen Demand

The optimization results for the scenarios with a combined electricity feed in, H_2 production, and module 5 from the optimization tool, adding the set demands low and high from chapter 4.6, are provided in this chapter. First, the results for demand low are presented, followed by the results for the scenarios where demand high is covered. Due to the uniform structure of the diagrams in the results chapters, the repetitive description of the axis labels and color distinctions is omitted for better readability.

Annual Revenue, Costs, Profits, and ROI (Demand Low)
In general, a similar pattern can be seen in chapter 5.2. If wind turbines can be part of the solution, significantly higher revenues are generated through the sale of H_2 and less through the sale of electricity. Furthermore, the results for the scenarios “PV + Wind + Ely + Demand low” and ”PV + Wind + Ely + Grid restriction + Demand low” are identical to those from Chapter 5.2 without suppling a demand, although a daily H_2 demand is covered.

The analysis of Figure 17 reveals distinct trends in revenue and costs for scenarios with combined electricity and H_2 production. Notably, without the inclusion of wind turbines, H_2 sales are lower, being 41 % less without grid restrictions and 42 % less with grid restrictions compared to scenarios with wind turbines. Similarly, electricity sales revenue declines by 13 % without grid restrictions and by 19 % with grid restrictions when wind turbines are absent. In total, these are, in comparison to the H_2 revenue, only a small part of the total revenue. Costs per year exhibit minimal variation across scenarios, with the highest value in the scenario with wind turbines and grid restrictions.

The scenario "PV + Wind + Ely + Demand low" emerges as the most economically viable, yielding the highest annual profit and *ROI*. In contrast, scenarios covering H_2 demand exclusively with PV electricity supply witness reduced profit and *ROI*. Notably, the impact of grid restrictions on revenue, costs, and profit remains comparatively modest. This underscores the substantial positive influence of wind turbines on economic efficiency within the analyzed scenarios.

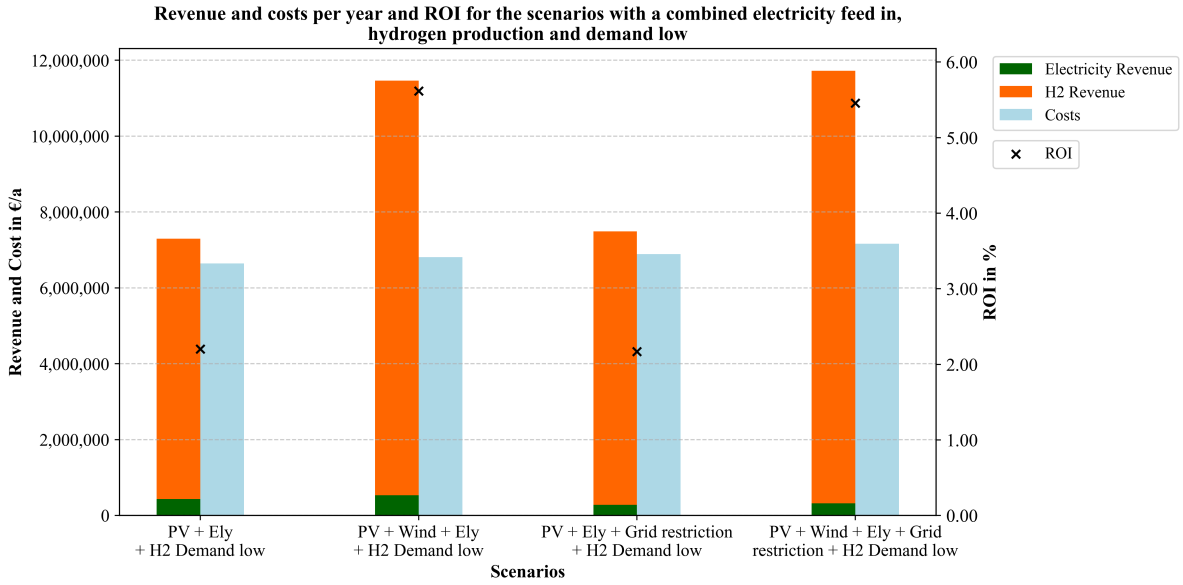

Figure 17: Revenue and costs per year and ROI for the scenarios with a combined electricity feed in and hydrogen production and demand low

System Design and $LCOH_2$ (Demand low)

The system design consisting of PV, wind turbine, and electrolyzer (and grid restriction) has remained the same compared to Chapter 5.2, despite the constraint of supplying daily H_2 demand as well as the corresponding $LCOH_2$. However, the two scenarios without wind turbines have changed, as can be seen in Figure 18. Individual, larger versions of the two diagrams can be found in Appendix H and I. The inverter power has decreased in comparison to the scenarios in 5.2, but the values are still higher than in the same scenarios where wind turbines are added. The electrolyzer capacity is highest with the combination of wind and grid restriction and lowest without the two components. Compared to the previous chapter, however, the electrolyzer capacities no longer differ as much. In the scenarios that allow wind turbines, the capacity of these is 10 MW, and the PV power decreases in order to utilize the area for wind turbines. The most significant difference is observed at H_2 storage. The capacity is more than six times higher if a daily H_2 demand must be covered and no wind turbines are installed. The compressor capacity, on the other hand, has increased by 10-15 % in all the scenarios in comparison to the last chapter.

The $LCOH_2$ also reaches higher values in the results without wind turbines, and the difference between the $LCOH_2$ without the revenue from electricity sales has decreased as well. In general, with exclusive usage of PV, H_2 is produced for less in the scenario with grid restriction, but the $LCOH_2$ is lower without grid restriction if the electricity revenue is included. The values of the other two scenarios are identical to the corresponding scenarios in chapter 5.2.

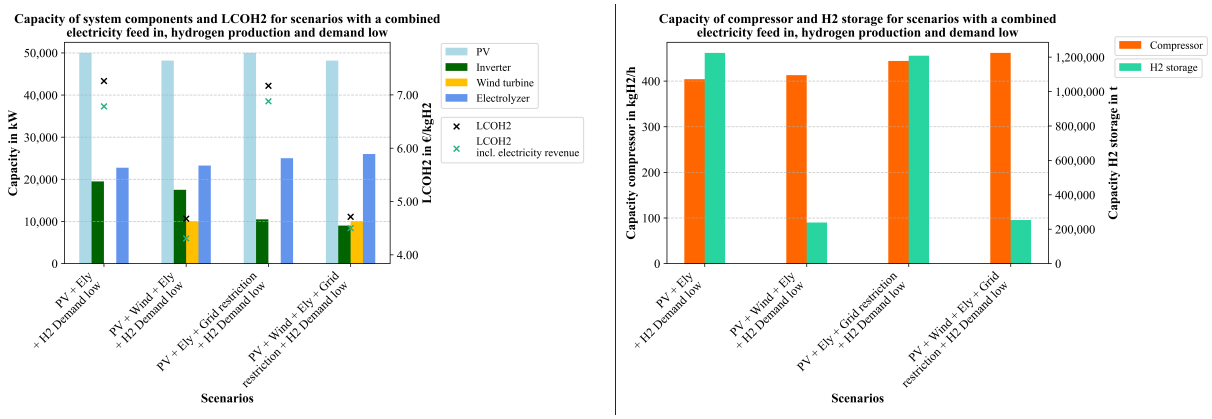

Figure 18: Capacity of the system components: PV, inverter, wind turbine and electrolyzer as well as the LCOH₂ and LCOH₂ incl. electricity revenue (left) and capacity of compressor and H₂ storage (right) for scenarios with H₂ demand low

Total Investment and Payback Time for the Energy System (Demand low)

The difference in the total investment for the optimized energy system, which supplies the "Demand low" is illustrated in Figure 19. The costs for the electrolyzer and the H_2 storage have increased due to the addition of the H_2 demand to be covered in both scenarios with exclusive usage of PV electricity. The sum of the H_2 production and storage components is around 50 % of the total investment in the system, while this value is around 33 % for the other two scenarios. In addition, the *PT* increases by more than two years in comparison to the same scenario from chapter 5.2 without the assumption that the daily H_2 demand must be fulfilled. This means that with wind turbines, the *PT* is reached nearly five years earlier.

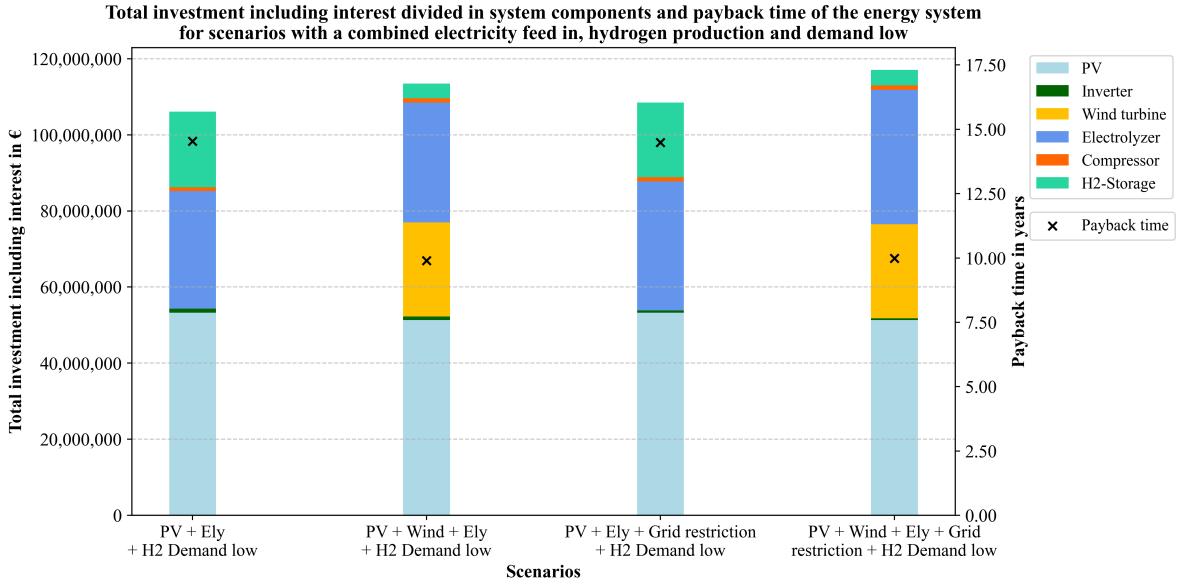

Figure 19: Total investment including interest divided in the system components and the payback time of the energy system for the scenarios with a H_2 demand low

Electricity usage over the year (Demand low)

Figure 20 shows the same limitations of the usage of electricity by inverters and electrolyzer power as well as the electricity grid restriction as in Figure 16 from Chapter 5.2. In addition, it can be seen that in scenarios without wind energy, more electricity flows into the electrolyzer in the winter of the year. This also results in less unused electricity in the system. In the case of "PV + Ely + demand low", 618 MWh remain unused, while four times more electricity remain unused with additional electricity grid

limitation. These are 16 % and 35 % less electricity losses than in Chapter 5.2, but only 9 % and 6 % more H_2. The scenarios with wind turbines producing the same amount of H_2 as in chapter 5.2, with 1,457 t_{H2} and 1,520 t_{H2} can supply around 300 % more H_2 than needed in the year due to the given demand. Furthermore, the most electricity is fed into the grid and the electrolyzer, as well as shut off in the middle of the year.

Summary of the Combined Electricity Feed in and Hydrogen Production Scenarios (Demand low)
In summary, the daily H_2 demand can be covered without losses in profit if wind turbines can be part of the solution, as the results are identical to the previous ones. Without wind turbines, the profit decreases significantly. The electrolyzer' s power and storage capacity increase. As a result, the total investment in the energy system increases significantly without significantly higher revenues. As in the previous scenarios, the difference between grid restriction and those without them in profit is less than 10 %. Furthermore, the constraint of the demand that has to be supplied per day helps to design the energy system in a way to use more of the electricity instead of shutting RE down.

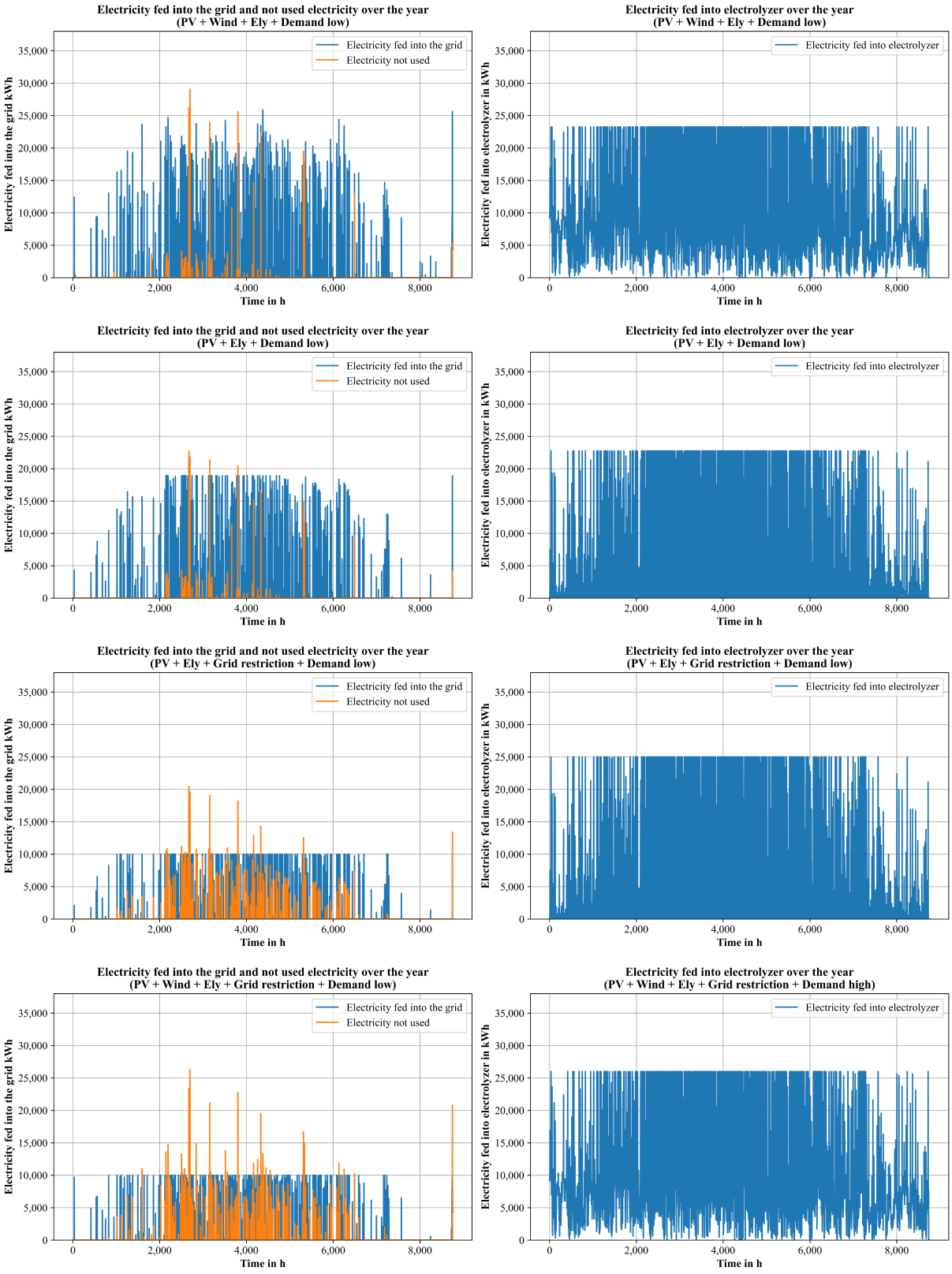

Figure 20: Comparison of electricity fed into the grid, electricity not used (left) and electricity fed into electrolyzer (right) over the year for the scenarios with H_2 demand low

Annual Revenue, Costs, Profits, and ROI (Demand high)

Figure 21 shows the results of the optimization tool for the scenarios that must cover the set "Demand high". Notable distinctions emerge compared to previous scenarios. Here, the absence of wind turbines results in a negative profit, showing a slight difference of only 0.1 % between the scenarios. Conversely, scenarios with wind turbines maintain a positive profit, albeit with a marginal 2 % reduction due to higher daily H_2 demand compared to the same scenarios with "Demand low". Figure 21 illustrates that annual costs are roughly twice as high as the total revenue in scenarios with negative profit, resulting in a negative *ROI*. The revenue from H_2 sees an increase in all scenarios, selling an average of 57 % more than required over the year. However, revenue from electricity experiences a decrease, reaching its lowest point among all simulated scenarios, with some declining by over 50 %. The *ROI* for profitable scenarios remains comparable to the most lucrative scenarios in previous chapters, standing at 5.44 % and 5.32 %.

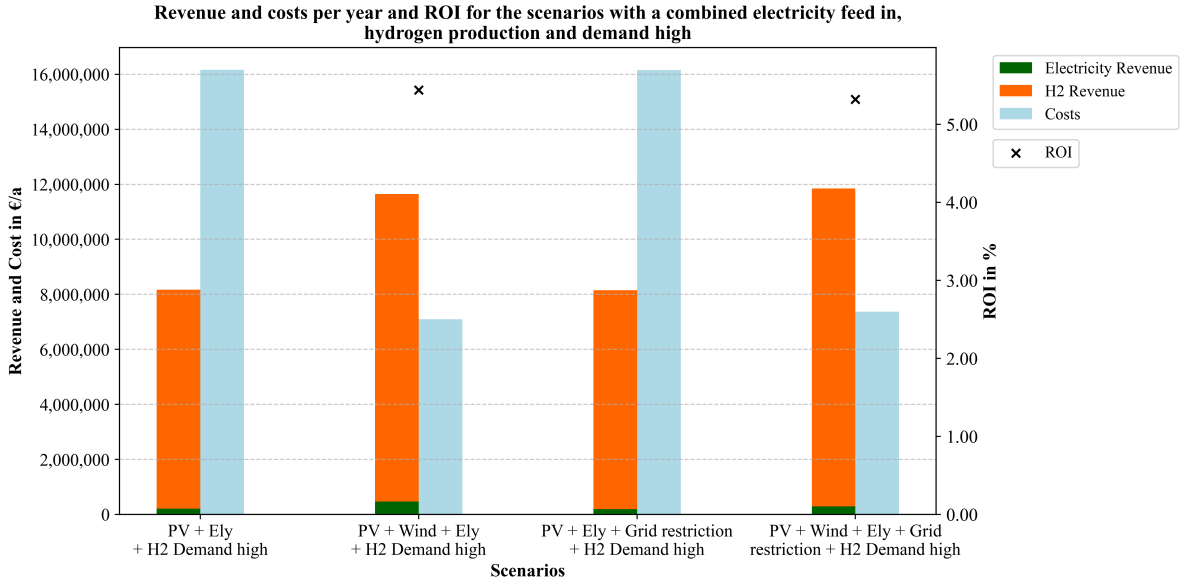

Figure 21: Revenue and costs per year and ROI for the scenarios with a combined electricity feed in, hydrogen production and H_2 demand high

System Design and $LCOH_2$ (Demand high)

For the different system designs, Figure 22 shows how the H_2 storage size increases significantly with PV only electricity generation. The secondary axis is limited to 1,500 kt_{H2}, but the actual storage capacity is 8,699 kt_{H2} for these two scenarios. Individual, larger versions of the two diagrams can be found in Appendix J and K. This means that the values are over 2,400 % higher than the scenario with wind turbines. The compressor capacity does not increase as much but still reaches the highest values of the analyzed scenarios. In addition, the *$LCOH_2$* increases significantly and is over 15 €/kg_{H2} for both scenarios, even when including the revenue from electricity sales. This is more than three times higher than the other two scenarios that cover the demand. Furthermore, the inverter power is lower if no wind turbines are added. The electrolyzer power, on the other hand, has the same value for these scenarios and is the highest of the four. In general, it is observed that higher electrolyzer capacity is needed to supply the "demand high". Moreover, the inverter power decreases and the compressor and H_2 storage must increase, whereby this effect is significantly higher with exclusive PV use.

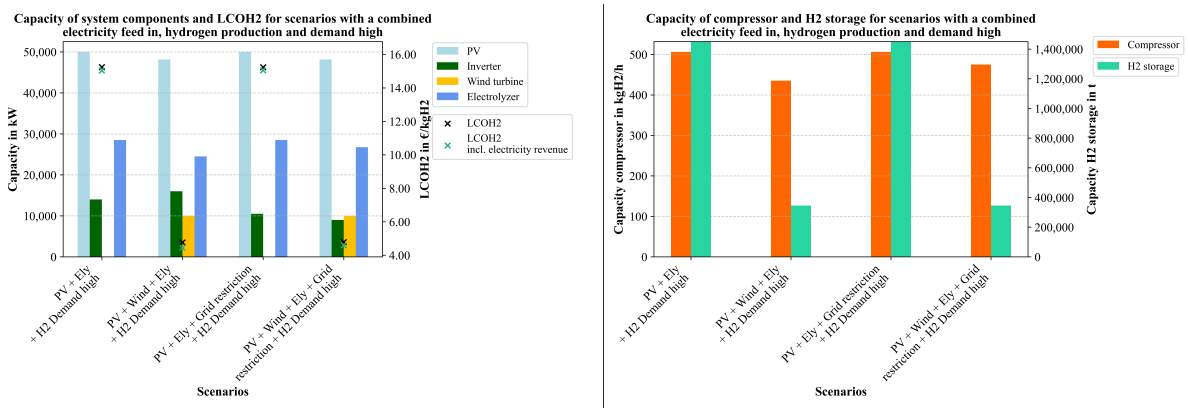

Figure 22: Capacity of the system components: PV, inverter, wind turbine and electrolyzer as well as $LCOH_2$ and $LCOH_2$ incl. electricity revenue (left) and capacity of compressor and H2 storage (right) for scenarios with H_2 demand high

Total Investment and Payback Time for the Energy System (Demand high)

Figure 23 illustrates the impact of the large H_2 storage system on the total investment for the PV-only scenarios. 60 % of the investment is caused by the storage system alone. The complete H_2 system, consisting of electrolyzer, compressor, and storage unit, is responsible for 77 % of the investment. This results in a *PT* of around 30 years. Without such a large storage system, as in the other two scenarios, the H_2 system contributes 35 % to the total investment. In total, it can be analyzed that, if wind turbines can be part of the solution of the optimization tool, the total investment is half as high as without wind, turbines and the *PT* is reached three times faster.

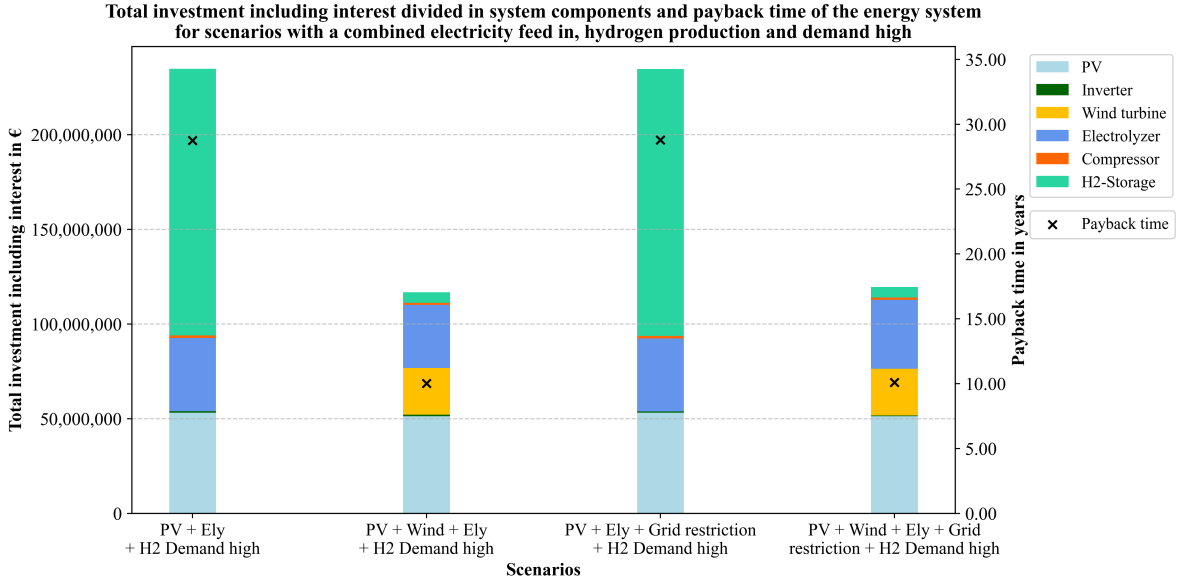

Figure 23: Total investment including interest divided in system components and the payback time of the energy system for the scenarios with a H_2 demand high

Electricity usage over the year (Demand high)

The amount of electricity fed in, switched off, and fed into the electrolyzer in Figure 24 shows that less electricity remains unused than in the results presented above. Particularly in the scenarios with electricity grid restrictions and without wind turbines, the unused quantity falls by 72 % to 1,007 MWh compared to the same scenario without the H_2 demand to be covered. With wind turbines, the amount of unused electricity falls by 12 % to 2,857 MWh. The amount of electricity fed into the grid also decreases when the daily demand increases, but to a lesser extent than the unused amount of electricity,

and again, primarily in scenarios with pure PV electricity use and without grid restrictions. Compared to the feed in quantity of 15,700 MWh from Chapter 5.2, 61 % less electricity is fed into the electricity grid. As in all of the figures for electricity feed in and shutdown, there is a peak in the amount of unused electricity and the amount flowing into the electrolyzer at the end of the year.

Summary of the Combined Electricity Feed in and Hydrogen Production Scenarios (Demand high)

In summary, the prescribed daily demand covered in the four scenarios examined here has a significant impact. While the annual profit, *ROI*, and *PT* decrease slightly in scenarios with wind turbines, they decline markedly in scenarios without wind turbines, even reaching negative values for annual profit and achieved *ROI*. Grid restrictions have the least influence on results among the scenarios examined thus far. Additionally, it is observed that in scenarios with a higher daily H_2 demand, the inverter capacity decreases as more electricity is directed to the electrolyzer to meet the demand.

Overall, the results from this chapter show that only through the additional use of wind turbines can such a daily amount of H_2 be produced profitably, whether with or without grid restrictions. It is also possible to supply the demand with PV, but it is not economically efficient and only has a much larger H_2 storage capacity.

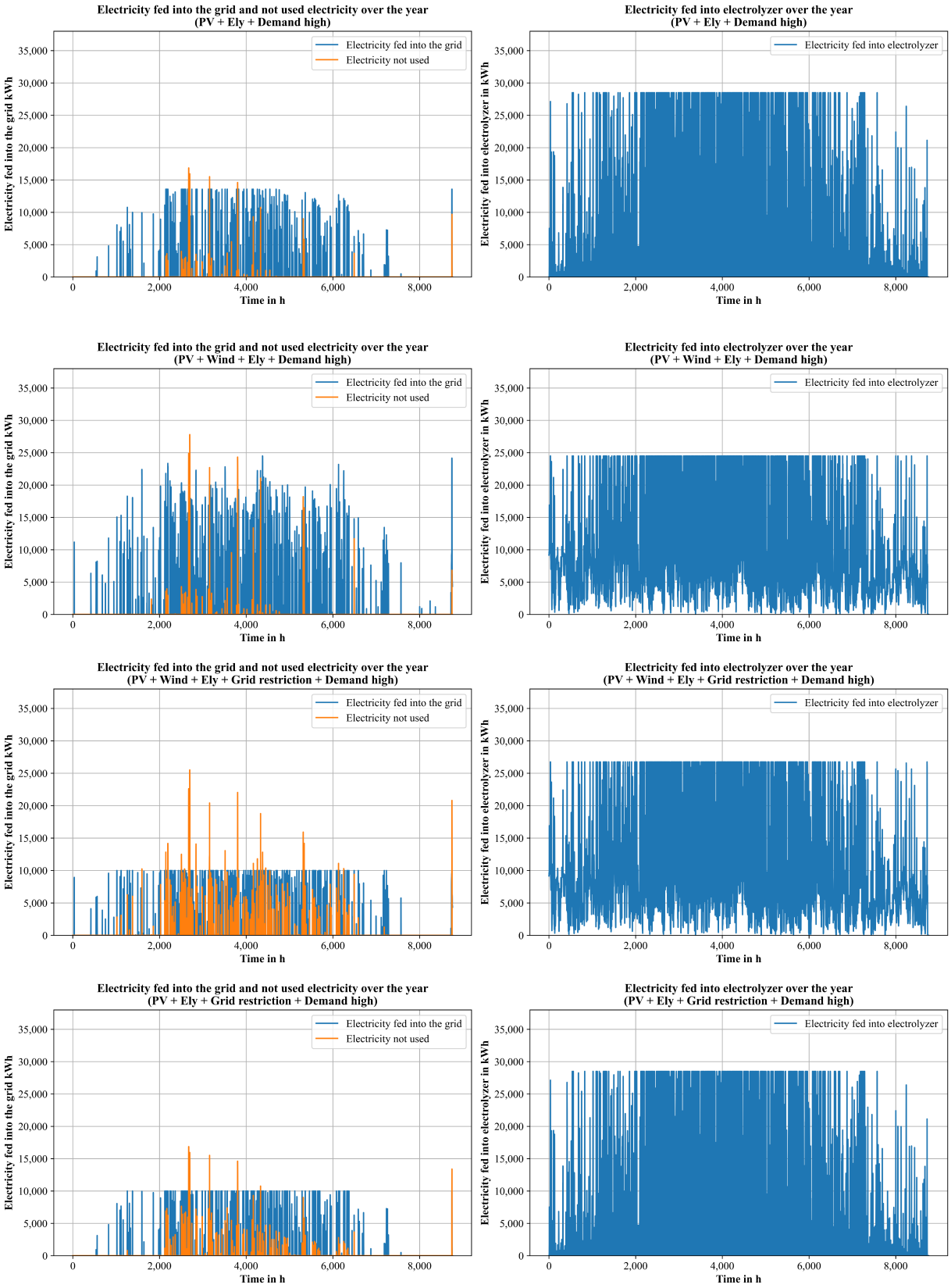

Figure 24: Comparison of electricity fed into the grid, electricity not used (left) and electricity fed into electrolyzer (right) over the year for the scenarios with H_2 demand high

5.4 Scenario: Electricity prices from 2022

This chapter presents how the electricity price influences the results of the designed optimization tool. To analyze this, all assumptions have remained the same except for the electricity prices over the year, which are from 2022 instead of 2019 (Figure 8). In order to see how the assumed grid restriction and a daily H_2 demand influence the solution with the increased electricity price, a total of four different scenarios are simulated. These are "without grid restriction and demand low", "without grid restriction and with demand low", "with grid restriction and without demand" and "with grid restriction and demand low", and the impact on profit, revenue, and costs per year as well as the system design are discussed.

Annual Revenue, Costs, Profits, and ROI (Electricity Prices from 2022)

Figure 25 shows the annual revenue from electricity and H_2 sales together with the annual costs and the *ROI* for the respective scenarios. The content of the diagram differs from the previous ones. The share of revenue from electricity sales has increased significantly and contributes to at least two-thirds of the total revenue. Without grid restrictions and H_2 demand to be met, it is 100 %. This scenario also has the lowest costs per year. In addition, the *ROI* is the highest as well, at 25 % and therefore 343 % higher than in the most profitable scenario previously. In the scenario “without grid restriction + demand low”, the annual revenue is only slightly lower, and the annual costs are only slightly higher. However, the *ROI* decreases to 20 %. In scenarios with grid restrictions, the annual profit significantly decreases and the annual costs increase. Meanwhile, the influence of the daily H_2 demand constraint is less significant.

Overall, all four achieve a higher profit and a higher *ROI* than the most profitable scenario from the previous chapters. Only the revenue from H_2 decreases. If the daily demand “low” has to be covered and there are no grid restrictions, only one percent more H_2 is produced than is required annually. With grid restrictions, however, the amount of H_2 sold increases.

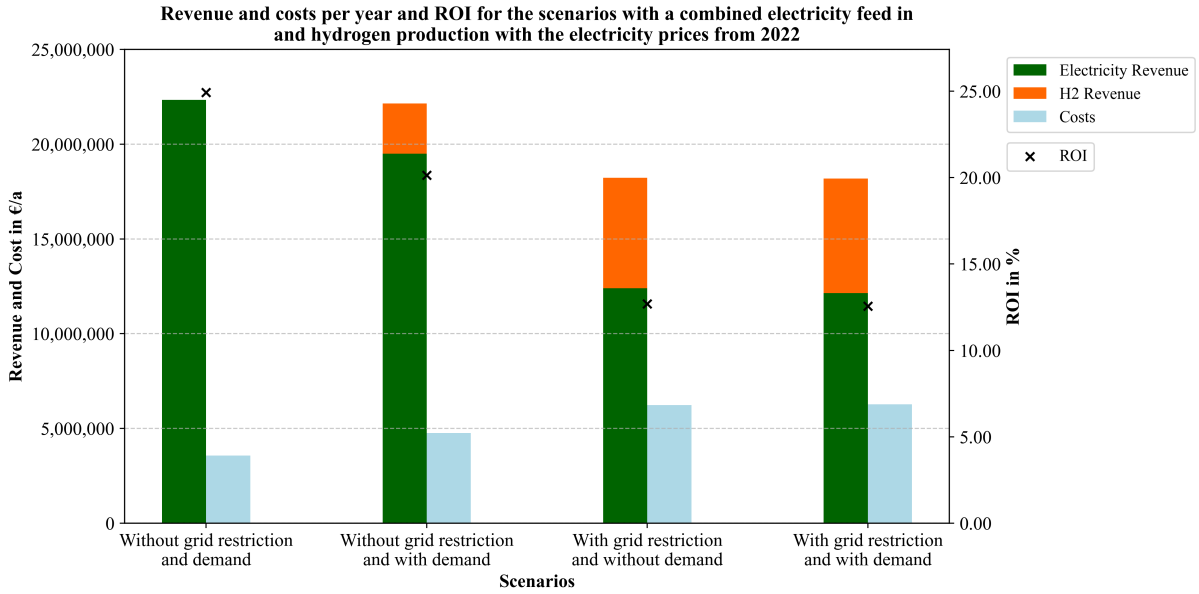

Figure 25: Revenue and costs per year and ROI for the scenarios with a combined electricity feed in and hydrogen production (electricity prices from 2022)

System Design and $LCOH_2$ (Electricity Prices from 2022)

The system design of the scenarios in Figure 26 also differs significantly from the previous ones. Although H_2 production is enabled in the tool, it is not part of the optimized solution when there is no grid restriction or a H_2 demand to be met. With H_2 demand to be covered, the electrolyzer has a capacity of 7 MW, and the inverter capacity is reduced to 39 MW. Including grid restriction, the power of the electrolyzer increases by about 180 %. The compressor capacity also increases by 180 % in the scenarios with grid restrictions, although the storage capacity is half of the capacity in the scenario without restrictions.

If H_2 is produced, the $LCOH_2$ is almost 100 % higher than in the 2019 electricity price scenarios. The $LCOH_2$, including the revenue from electricity sales, is in the negative range at -41.5 €/kg_{H2} without grid restrictions and at -7.9 €/kg_{H2} with restrictions. The *LCOE* for the scenario without H_2 production is only 2 % higher than the results from Chapter 5.1, where no H_2 production was possible.

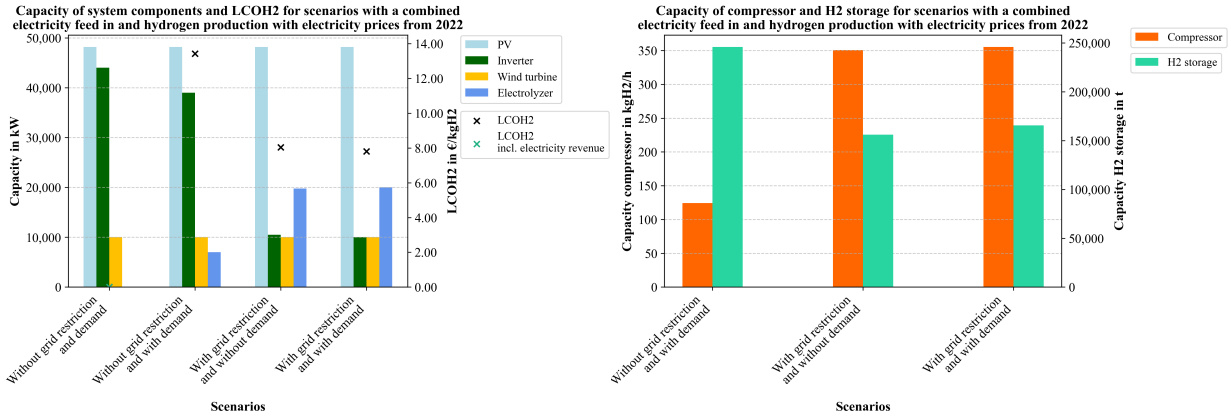

Figure 26: Capacity of PV, inverter, wind turbines and electrolyzer as well as $LCOH_2$ and $LCOH_2$ incl. electricity revenue (left) and capacity of compressor and H2 storage with electricity prices from 2022

Summary of the Combined Electricity Feed in and Hydrogen Production Scenarios (Electricity Prices from 2022)

In summary, this chapter examines the influence of higher electricity price on the outcomes of the optimization tool. Notably, the scenario yielding the highest annual profit relies exclusively on electricity feed in, achieving a 25 % *ROI*, which is 3.433 % higher than the previously most profitable scenario. H_2 production is only integrated into the system when there is a daily H_2 demand or a grid restriction. However, all four scenarios exhibit significant variations in system design, with grid restrictions having the greatest impact and the constraint of H_2 demand being less. Overall, under the 2022 electricity prices, the optimized energy systems demonstrate increased profits and a system design tendency that can increase electricity feed in.

5.5 Sensitivity Analysis

The last part of the results chapter is the sensitivity analysis. The influence of the *CAPEX* of the individual components and the H_2 price on the optimized profit and *ROI* is examined. In addition, the change in the system design of the components due to the variation of the variables in the sensitivity analysis is presented as well. The "PV + Wind + Ely" scenario is assumed as the initial scenario for the analysis.

Profit per Year and ROI (CAPEX Variation)

Figure 27 and Figure 28 present the sensitivity analysis results for profit per year (top) and *ROI* (bottom). The x-axis reflects variations in the considered variable, while the y-axis indicates the corresponding changes in the analyzed variable (profit per year and *ROI*). Notably, among all *CAPEX* variables for the modeled energy system components, the electrolyzer *CAPEX* has the most substantial impact on the profit per year, as can be seen at the dotted turquoise line. A 25 % decrease in electrolyzer *CAPEX* results in a 18 % profit increase, while a 25 % increase leads to a 14 % profit decrease. The PV system's *CAPEX* (purple line) has the second biggest influence on profit per year by a maximum of 10 %, followed by the wind turbine *CAPEX* (blue dashed line).

For the *ROI*, the PV system's *CAPEX* exerting the greatest influence. A 20 % increase in *ROI* is observed when the *CAPEX* of the PV system decreases by 20 %. The electrolyzers impact on *ROI* is less significant than on profit. Overall, reducing *CAPEX* across components has a more pronounced effect on profit and *ROI* than increasing *CAPEX*.

A look at the remaining values shows that they have a minor influence on both, profit per year and *ROI*.

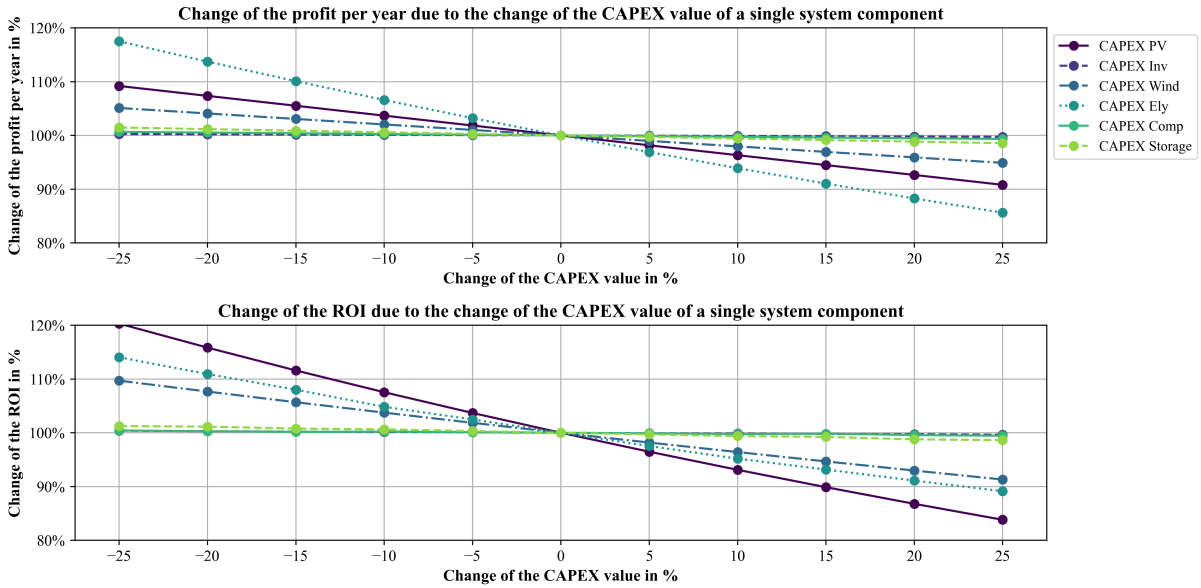

Figure 27: Results sensitivity analysis (Profit per year and ROI) with change of CAPEX of energy system components

Profit per Year and ROI (H_2 Price Variation)

As can be seen in Figure 28, the influence of the H_2 price (purple line) is significantly higher than that of the *CAPEX* of the components. With a reduction of 10 %, the profit per year already decreases by 23 % and with a reduction 20 % by 44 %. At a reduction of 50 %, the profit per year is only 7 % of the base scenario. With an increase in the H_2 price, the profit increases even more steeply than it decreases with a reduction. With a 20 % higher price, 49 % more profit is achieved and with a 50 % increase, profit rises by 123 %. In general, the profit increases exponentially with a linear increase in the H_2 price. For the *ROI*, the curve showing the influence of the H_2 price looks more linear and does not have the same high influence as the profit per year, but still has significantly more influence at the analyzed economic values than the *CAPEX* of the individual components.

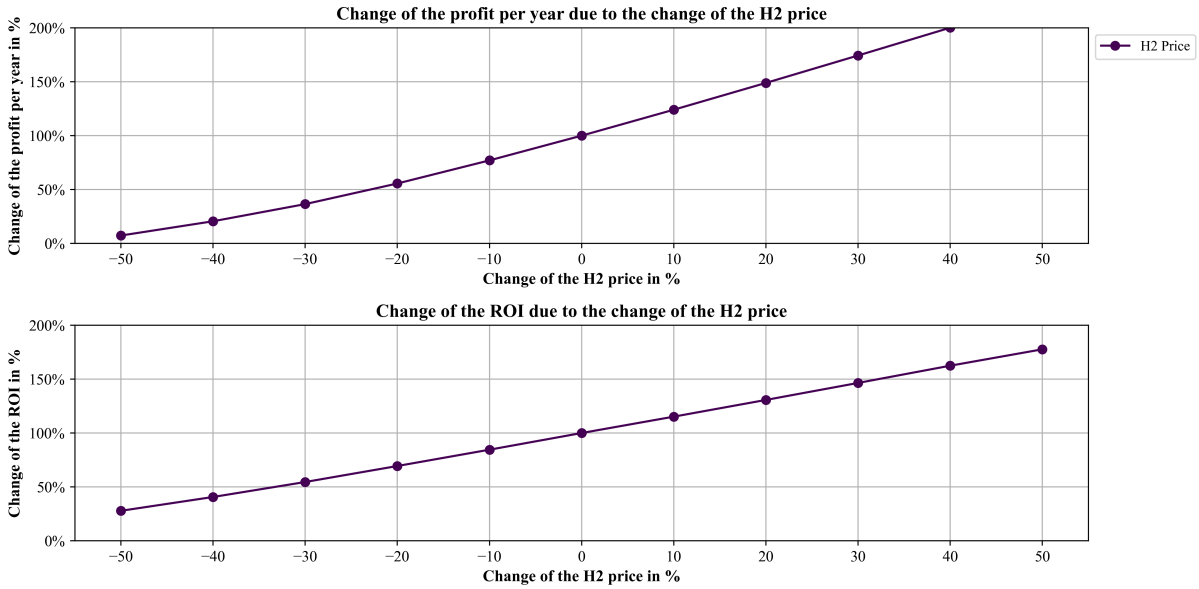

Figure 28: Results sensitivity analysis (Profit per year and ROI) with change of hydrogen selling price

System Design (CAPEX Variation)

Figure 29 shows the change in the system design of the individual components required for H_2 production due to the variation of the *CAPEX* values. The colors for the different *CAPEX* values of the components are the same as in Figure 27. As previously stated for the profit per year, the *CAPEX* of the electrolyzer has also the greatest influence on the results of the optimization tool in the system design among the components. However, a less linear graph can be seen here, especially when *CAPEX* is reduced. The power of the electrolyzer increases more steeply, with 10.7 % in the first two 5 % reductions, only 2.2 % in the next 5 % step, and then again significantly by 11 %. In the opposite direction, the electrolyzer power decreases constantly by 3 to 5 % per 5 % increase. The other *CAPEX* variables have almost no influence on the sensitivity analysis conducted regarding the system design. Looking at the compressor power in the middle image, it is also visible that the *CAPEX* of the electrolyzer has the biggest influence as well on the compressor. The curve is almost identical to that of the electrolyzer capacity. The storage capacity in the bottom image has the same curve, but the change is less pronounced and increases by a maximum of 12 % and decreases by 11 %, which is significantly less than of the other two components.

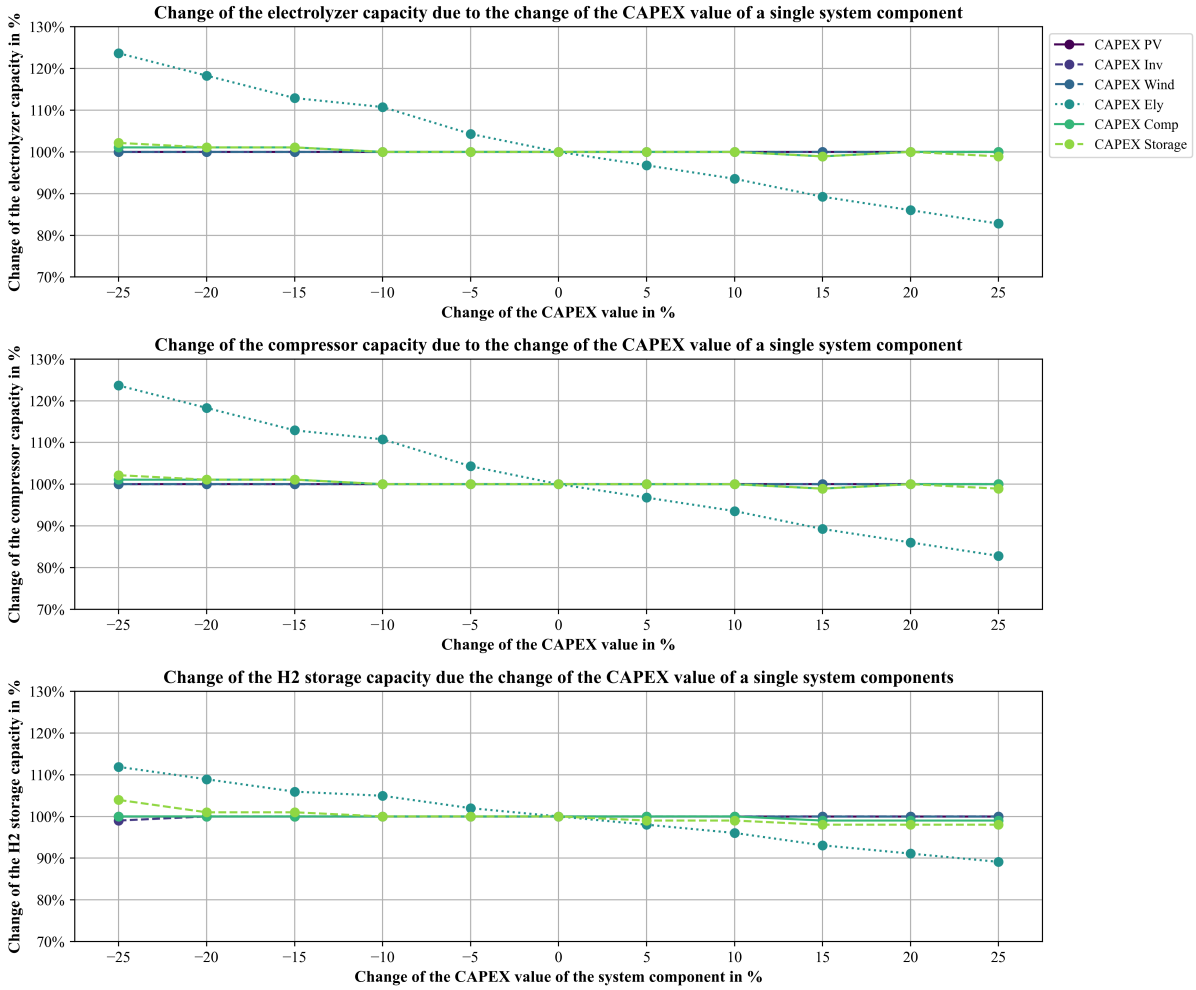

Figure 29: Results sensitivity analysis (Change of component system design) with change of CAPEX of energy system components

System Design (H_2 Price Variation)

Figure 30 shows the change in the system design of the individual components required for H_2 production due to variations in the H_2 selling price. As with the profit per year and the *ROI*, the change in the H_2 price has a much stronger influence on the system design of the components than the change in the *CAPEX* of the components. It is noticeable that when the price of H_2 is reduced, the design of the components decreases significantly more than they increase when the price of H_2 increases. For example, the power of the electrolyzer is only 25 % of the original power when the H_2 price decreases by 50 %, but when the price increases by 50 % the power only increases by 37 %. This is almost identical for the compressor, but the power of the compressor increases even less than that of the electrolyzer. The largest increase for both is with a change in the H_2 price of -40 % to -10 %, which is over 50 % for both components. The storage system, on the other hand, has a similar curve, but the values rise and fall less steeply and range between 42 % less and 234 % more capacity than in the base scenario "PV + Wind + Ely".

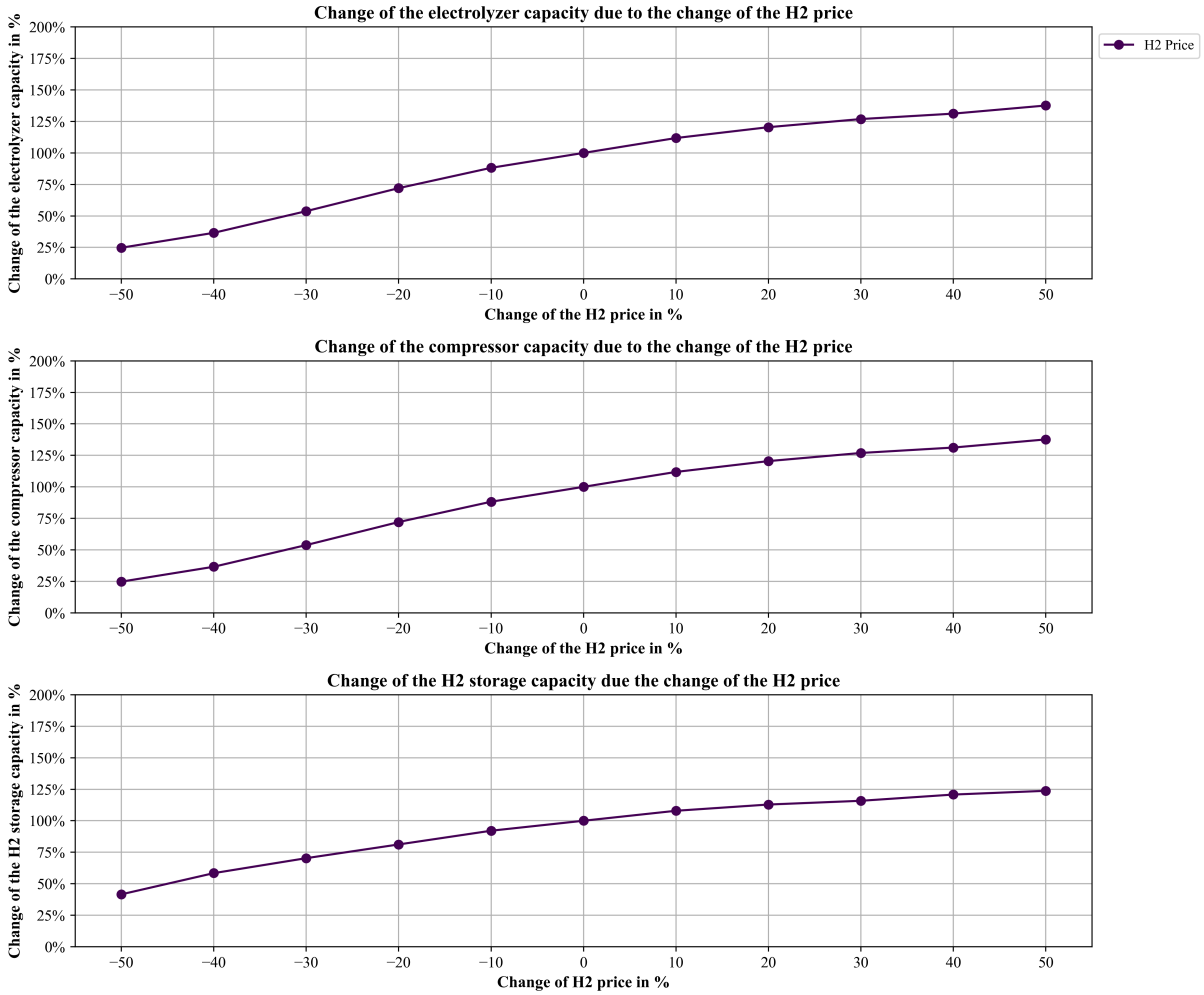

Figure 30: Results sensitivity analysis (Change of component system design) with change of hydrogen price

Summary of Sensitivity Analysis

The sensitivity analysis explores how changes in the *CAPEX* of individual components and the H_2 price impact the optimized outcomes, including profit and *ROI*, as well as the overall system design of the energy system. The findings indicate that the *CAPEX* of the electrolyzer influences the profit per year the most across various *CAPEX* values, whereas the inverter, compressor, and H_2 storage exhibit the least impact. In terms of *ROI*, the *CAPEX* of the PV system exerts the most major influence, while the inverter, compressor, and H_2 storage have minimal effects. Notably, the H_2 price demonstrates a more substantial effect on both profit and *ROI* compared to the *CAPEX* of individual components and the system design. This highlights the essential role of the H_2 price in designing the optimal system configuration to maximize annual revenue.

6 Discussion

The following is a chronological presentation of the findings based on each of the research questions in Chapter 1.2, as well as the limitations and weaknesses of the thesis.

Research Question 1

One objective of the thesis was to investigate the extent to which it makes economic sense to integrate electricity feed in with H_2 production in a single energy system. The results of chapters 5.1 to 5.3 show that it makes economic sense under the assumptions made. A higher profit per year, a higher *ROI*, and a lower *PT* are achieved when RE electricity is combined with H_2 production. This is the case for all of the combined generation scenarios presented, except for the two scenarios where the daily set H_2 "high demand" is met only with PV electricity. The "PV + Wind + Ely" scenario, which has the highest annual profit among the scenarios examined in chapters 5.1 to 5.3, has a 77 times higher annual profit, which illustrates the positive influence of H_2 production. However, it cannot be concluded that the combination is more economical in all cases. By changing the electricity price to 2022 prices, the optimization tool generates significantly different results. The highest profit per year is achieved by a scenario without H_2 production and is more than three times higher than the most profitable scenario with electricity prices. Therefore, there is no general answer to the research question investigated here. The results depend on the assumptions used to run the optimization tool. The influence of the electricity price and other parameters on the results is further discussed in Research Question 3.

Research Question 2

A further objective of the thesis was to investigate how the integration of wind turbines and/or batteries into the exclusive use of PV, together with the constraints of grid limitation and/or daily H_2 demand, affects the economic viability and system design of an energy system combining renewable electricity feed in and H_2 production.

First, it can be concluded from the results that the battery has no impact on the energy system under the assumptions made. Although the integration of a battery system in an energy system with H_2 production can ensure a more constant operation of the electrolyzer (Benghanem et al., 2023). However, a battery system was not part of the solution of the optimization tool in any of the scenarios of the results and sensitivity analysis. This leads to the conclusion that the cost of battery systems is too high to have a positive economic impact on the analyzed energy system. This statement is also supported by other studies that focus specifically on the combined use of electrolyzer and battery (Abomazid et al., 2022; Srinivasan, 2021). Even with a 25 % reduction in battery *CAPEX*, the battery was not part of any of the energy systems modeled. This indicates that despite a possible cost reduction in the near future, the battery does not appear to be economically relevant in the context considered unless the cost reduction is greater than 25 %. Cole et al. (2021) expect this reduction by 2030 at the latest. This aspect would need to be further investigated to find the parameters where the battery has a positive impact.

The results show that the integration of wind turbines has a positive impact on the economics of combined electricity and H_2 production. In all scenarios where wind turbines could be considered as part of the solution, the maximum available wind power was always installed. This observation shows that wind turbines are considered economically advantageous in the scenarios examined and contribute to higher annual profits. Furthermore, in all scenarios, the *ROI* is higher and the *PT* and $LCOH_2$ are lower with wind turbines than in the scenarios without wind turbines. This supports the above statement. This gives the impression that with a larger available area, more wind turbines would have been installed, and the ratio of wind to PV would also change. However, according to Hofrichter et al. (2023), this statement mainly depends on the chosen location and decreases with the higher availability of wind and solar irradiation. This shows that the results of the optimization tool would change significantly if a different location had been investigated. This highlights the importance of site selection for the results

of the optimization tool. In further research, the optimization tool could be used to examine different sites to further investigate the impact of site selection. In addition, this finding shows that current site-related values such as wind speed and solar irradiation should always be taken into account when planning similar energy systems in practice, as they have a major impact on annual profit and optimal system design.

In terms of system design, the use of wind turbines has reduced inverter power. However, this should be viewed critically, as the inverters in this system only relate to the PV systems, and the wind systems use their own inverters, which are included in their *CAPEX* and were therefore not directly considered in their design. As a result, the inverter power was partially reduced due to a decrease in PV power. In addition, the wind turbines in the optimization tool use their own inverters to feed power into the grid, which also affects this aspect. In addition, the results showed that the increase in wind turbines resulted in significantly more revenue from H_2 sales. Therefore, more H_2 was produced and sold over the year, even though in some scenarios the electrolyzer power is lower than in scenarios without wind turbines. This implies that more H_2 was produced and sold over the year despite the lower electrolyzer capacity. This observation indicates that the integration of wind turbines leads to more constant H_2 production over the year. This is also confirmed by observing the electricity usage over the year. The addition of wind turbines also has an impact on the compressor and H_2 storage. However, this depends on whether there is a daily H_2 demand to be met or not. If no daily demand was specified as a condition in the optimization, the compressor power and H_2 storage capacity increase compared to the scenarios without the possibility of wind turbines. One reason for this could be that there is a higher total RE capacity, and therefore more H_2 can be produced and therefore stored per hour. This is because the H_2 must first be compressed and stored before it can be sold once a day. Based on the assumptions made and with respect to the Rügen site, it can generally be said that the addition of wind turbines has a significant positive economic impact. However, the capacity factors used to model the possible amount of wind energy must be critically questioned. They are only for a single reference year, and if another reference year were used, the result would be different. Wind fluctuates not only over one year but over several years, so it is recommended to simulate over several years to get more robust results. The same aspect is true for PV electricity, which is directly dependent on the selected solar irradiation.

The assumed electricity grid restriction of 10 MW, on the other hand, has a major influence on the system design and the profit per year, but less on the economic efficiency key values of the energy system. The results have shown that the profit decreases significantly, but on the other hand, the costs also decrease. However, the *ROI* decreased only slightly due to the addition of limited grid feed in. This indicates that without the reduction of the RE plants, but with the reduction of the inverter power together with the increase of the electrolyzer power, the losses due to the grid restrictions are almost completely compensated by a change in the system design. This phenomenon can be seen in all results with a combined electricity feed in and H_2 production under the assumptions made with the electricity price from 2019. This points to the fact that at locations without a connection to the high-voltage or medium-voltage grid or in locations with frequent grid overloads, it can be possible to compensate electricity revenue losses by producing H_2. However, as mentioned above, the magnitude of this influence depends on the location of the energy system. In addition, electricity and H_2 prices affect how much the grid constraint affects the results of the optimization tool. This will be further discussed in the answer to the third research question.

The implementation of the daily H_2 demand has almost no influence on economic profitability in scenarios with electricity from PV systems and wind turbines. With the assumption of the scenario “Demand low”, there is even no difference in the results for the scenarios without a daily H_2 demand. This means that a constant daily demand can be covered by the combination of PV and wind systems together with a H_2 storage system without any economic losses. Even the daily "demand high", which is more than twice as high, could be covered over the year with an *ROI* that is only 0.2 % points lower than the

“Demand low”. However, a different result can be seen with the exclusive use of PV electricity. While the scenario "Demand low" still achieves a positive profit, the profit for "Demand high" is significantly negative. The H_2 storage capacity had to be increased, as well as the electrolyzer and compressor capacities. This is the only way to meet the increased demand. The exclusive use of PV electricity shows that it is possible to produce enough H_2 throughout the year, despite considerably fewer hours of sunshine in winter, but only with a loss of economic feasibility. It also shows that optimal system design is a key factor in the planning of H_2 production systems, which must provide a constant supply of H_2 with regard to the fluctuating generation of electricity from RE. In general, the question arises as to whether an even higher daily demand could be supplied in the examined area. Moreover, in further research, it could be investigated what would be the maximum daily demand that could be covered by the energy system while still making a reasonable economic profit. For this, the optimization objective needs to be changed. For example, a constraint that implies a set profit per year that must be reached or another economic key value as the *ROI*.

Adding the constraint of a daily H_2 demand that must be supplied to the optimization tool is another way to provide more practical results. In most cases of H_2 use, such as industry or mobility, a certain demand must usually be available within a certain period of time (hourly, daily, etc.) (Apostolou et al., 2019; Schütte et al., 2022). Otherwise, switching to the use of H_2 is not economically viable for customers (Staiger and Tanțău, 2020).

Research Question 3

The final objective of the thesis was to investigate the extent to which the prices of electricity and H_2, as well as the *CAPEX* of individual system components, influence the economic efficiency and system design of the analyzed energy systems that combine electricity feed in to the grid and H_2 production. All the aspects mentioned before are strongly dependent on the selected electricity and H_2 price, which is demonstrated by the results from chapters 5.3 and 5.4. With the change to the much higher electricity prices from 2022, the optimization tool generates significantly different results. The scenario with the highest profit per year has an over three hundred times higher annual profit than the optimized result from Chapter 5.1 for pure electricity feed in, although H_2 production is also excluded here. Compared to the highest profit per year from combined electricity and H_2 production, with the electricity prices from 2019, a profit four times higher is still realized with the assumption of the electricity prices from 2022. However, the increase in profit per year is due to the lower costs and higher revenue per year. This is because H_2 production can be excluded, which in every system otherwise contributes at least 30 % of the total investment. In addition, more revenue can be generated through the increased electricity price. A look at the electricity market data in Figure 8 explains why there is such a significant increase in revenue. The average selling price of electricity over the year 2022 per MWh was 235.44 € and 37.77 € for 2019. The *LCOE* in the results for electricity is on average around 35 €/MWh for all simulated scenarios. With the average price of 2022, 7,000 % more revenue could therefore be generated per MWh than with the average price of 2019. This data indicates why H_2 production is not part of the solution in the most profitable 2022 scenario. The sales price of H_2 is set at a constant 7.50 €/kg_{H2}, which corresponds to 190.35 €/MWh_{H2} (based on HHV). The lowest value for the $LCOH_2$ is 4.67 €/kg_{H2} and therefore 118.52 €/MWh_{H2}. This means that the sale of H_2 generated a maximum profit of 71.82 €/MWh_{H2}. This represents a reduction of 64 % compared to the profit generated by selling electricity in 2022 at the average day-ahead market prices.

If the conditions of electricity grid restriction and/or daily H_2 demand are added to the 2022 scenarios, the results change again. These change the system design of the energy system in order to integrate H_2 production. So, producing only electricity would be more profitable, but even in the scenarios with H_2 production, the profit per year and the *ROI* are higher than in all simulated scenarios with 2019 electricity prices. The reason for that is that the power of the electrolyzer, the compressor, and the

capacity of the H_2 storage are relatively minor compared to the scenarios in chapters 5.1 to 5.3. This is done to have lower cost, but to still have large enough capacities to use as much available electricity that would otherwise be switched off due to the grid restriction. In general, it can be stated that, with the assumptions made, H_2 production is a way to profitably use surplus electricity in the event of grid restrictions. A statement derived from these results is that electricity prices are an essential factor for the system design and the economic outcome. This fact suggests that modeled energy systems should not only be simulated over one year, as done in the thesis. In order to achieve more accurate and robust results, a simulation period of several years with different electricity prices and strong changes in these should be chosen instead. Furthermore, the use of different price forecasts could be possible to reduce the impact of this uncertainty factor. But this will always be an uncertainty factor, as the electricity prices for 2022 were influenced by unpredictable global political events (Leupoldina, 2022), which could occur in the future as well.

The sensitivity analysis conducted shows that, in addition to the electricity price, the assumed H_2 price has the greatest influence on the results of the optimization tool created. In contrast, the change in the *CAPEX* of the components has less impact on the results. Only that of the electrolyzer and the PV system, but this effect is significantly smaller than for the H_2 price. In general, it can be stated that the economic viability of the combined electricity feed in and H_2 production depends largely on the relation of the H_2 selling price to the $LCOH_2$ and the electricity sales price to the *LCOE*. Regarding the price of renewable H_2 in the future, this aspect is crucial for the economic feasibility of real H_2 projects. This is because the price must fall considerably in order to replace non-renewable H_2. Non-renewable H_2, also known as grey H_2, has production costs of 0.80 to 2.10 €/kg_{H2} (Ajanovic et al., 2022). This clear price advantage over renewable H_2 means that potential customers are more likely to act in their economic interest and use grey H_2, which in turn prevents the development of the infrastructure for renewable H_2 (Ajanovic et al., 2022). In the performed sensitivity analysis, the minimum analyzed value for the H_2 price was 3.75 €/kg_{H2}, which decreases the profit per year close to zero. In conclusion, if renewable H_2 were sold for the same price as grey H_2, nearly no profit at all would be made. Which is a limitation in the whole thesis as the profitability of all simulated systems depends on the price assumptions, which is indicated by the performed sensitivity analysis and the results in chapter 5.3. Possible options to reduce the price gap between renewable H_2 and grey H_2 include targeted support measures to reduce costs, tax incentives or the implementation of mechanisms that consider the externalization of environmental costs, such as a CO2 price (IRENA, 2023a).

General Limitations and Weaknesses of the Optimization Tool

In addition to the limitations and weaknesses explained in the previous paragraphs, the further limitations and weaknesses of the optimization tool are now presented. In general, the modeling of energy systems is associated with many challenges. A fundamental limitation is the need to simplify complex systems in order to implement them mathematically in the desired depth, and simplifications are essential to doing this (Pieper, 2017). A key point in relation to this work is that the optimization method used is MILP. Although this provides efficient optimization, it is based on being described by linear equations (Klemm and Vennemann, 2021). However, energy systems do not function under linear constraints. For this reason, parameters such as the load-dependent efficiencies of the electrolyzer and the inverter were assumed to be linear or constant. The linear assumptions cannot exactly describe the actual physical relationships and dynamics but offer the possibility of reducing the required computing power and complexity in order to generate useful results (Urbanucci, 2018).

Another limitation relates to the generation of RE and therefore impacts the results of the optimization tool. The shading of the wind turbines on the PV systems. In the thesis, the wind turbines are located close to the PV systems. This would result in the towers, nacelles, and rotating rotor blades shading the PV panels throughout the day. This leads to lower power generation of the PV systems (Mamia and

Appelbaum, 2016). To include this effect in the optimization tool, a detailed and accurate representation of the shading impact caused by wind turbines on PV panels would be necessary. Another option would be to add a factor that estimates the losses. Moreover, in all simulated scenarios, the solution of the optimization tool included only south-facing orientation for the PV panels. This implies that the other two orientations were not economically advantageous. However, the assumption was made that PV panels with west and east orientations require the same area as those with a south orientation. This assumption, as indicated by Khatib and Deria (2022), is not accurate. Khatib and Deria (2022) state that the required area per kW is lower due to the higher tilt angle that is used, and the *CAPEX* for such systems is lower since less mounting structure is needed. Therefore, with adjusted assumptions for area requirements and *CAPEX*, the optimization tool would generate different results.

Furthermore, there is no maximum amount of H_2 that can be sold per day. This leads to a significant overproduction, which is also visible in the results. This is rather unusual in the real world, as industry or filling stations usually need a specific demand within a certain period of time (Apostolou et al., 2019; Schütte et al., 2022). Moreover, with a limited demand of H_2 per day or a changing demand over the year, the results of the optimization tool would probably differ significantly from the results generated in this thesis. This aspect could be investigated in further research.

The last point to mention regarding the limitations and weaknesses of the thesis is the fact that no inflation or reinvestment is included in the economic evaluation. This is a critical aspect as it would directly affect the results of the optimization tool if added. Therefore, this should be added to the optimization tool or similar tools in the future to provide more realistic data.

7 Conclusion

This section begins with a summary of the thesis, followed by an exploration of potential directions for advancing the optimization tool created and further research, ultimately concluding the work.

7.1 Summary

As part of the master's thesis, a Python-based optimization tool that optimizes the profit per year for energy systems was built. The tool has various modules to simulate different scenarios. Overall, it is specified that PV and inverters can always be part of the optimized energy system. There are five additional modules that provide the optimization tool with more options for the solution. These are grid limitations, additional wind turbines, battery storage, H_2 generation, and the requirement to cover a daily H_2 demand. In addition, there is a limited area available on which the RE can be built, which limits power generation of RE. The approach of a Mixed-Integer-Linear-Problem (MILP) is used for the implementation of the tool. This helps to generate realistic design sizes for the single components instead of, for example, generating a three-quarter wind turbine as part of the solution. This option offers added value, particularly in terms of practical aspects. Furthermore, the techno-economic parameters required for the optimization tool were presented and discussed, and current values were taken from scientific literature and official reports from energy associations or calculated and adopted. Subsequently, the optimization tool is applied to a case study for a 50-hectare area on the Baltic Sea island of Rügen.

From the results, it can be concluded that the combination of electricity feed in and H_2 production can be more economical than an exclusive electricity feed in to the power grid. The thesis illustrates that the most cost-effective renewable H_2 production is through the supply of continuous electricity, which is achieved through a combination of PV and wind power generation. For this reason, wind turbines are always part of the result if the wind turbine module in the tool is enabled. The use of exclusively PV electricity for H_2 production is only economically viable when there is no requirement to cover daily demand. The optimal system design yielded a substantial profit with an *ROI* of over 5 %. This system consisted of a PV system, inverters, wind turbines, an electrolyzer, a compressor, and an H_2 storage tank. The system could also supply a constant daily demand of H_2 throughout the year. The constraint of the limited grid capacity does have only a slight effect on the economic key figures like the *ROI* and the payback time of the energy system, while the system design changes are significant. More electrolyzer, compressor, and H_2 storage capacity is installed while the inverter power decreases. However, the results also show how fluctuations in electricity and H_2 prices have a considerable influence on the results of the optimization tool and, thus, on the design and economic viability of such energy systems. With the change to the electricity exchange market data from 2022, the scenario with the highest profit is an exclusive electricity feed in scenario. This indicates the importance of conducting simulations that cover multiple years, ideally including multiple price forecasts for electricity and H_2. In addition, simulations should cover the entire life of the energy system to provide more accurate and reliable results. Furthermore, it is shown that battery systems have not yet reached the price range to improve the economic viability of such systems, as in all simulated scenarios, the battery system is excluded from the energy system. PV with a west and east orientation were also not part of the solutions of the tool, as they did not lead to a more economical result.

In conclusion, the results show how electricity feed in can be combined with H_2 production through economic optimization and operated with a positive profit. However, despite an optimized plant design and an *ROI* of over 5 %, the energy system can only be profitable if either the electricity price generates high revenues, as in chapter 5.3, or the renewable H_2 is sold for a significantly higher price than grey H_2

as in chapter 5.2. The sensitivity analysis indicates that as the H_2 sales price decreases to 3.75 €/kg_{H2}, which is still higher than the prices for grey H_2, both the annual profit and the *ROI* in the analyzed energy system converge to zero.

7.2 Outlook

To give an outlook, further research options are presented. These include extending the level of detail of the developed optimization tool. One option would be to transform the tool from a MILP to an MIP, which would allow modeling nonlinear properties that previously had to be assumed as such, which is possible with the PYOMO library used (Bynum et al., 2020). Another aspect, as mentioned above, would be to simulate the tool with data over a longer period of time to reduce the uncertainties of a one-year simulation, such as fluctuating electricity prices, wind speeds, and solar irradiance. In addition, ways to improve the overall economics of similar energy systems should be explored. There are many options that could be analyzed to improve this. For example, the electrolyzer could provide grid services to have another source of revenue. A different possibility is to examine how much money from subsidies would be needed to compete with grey H_2, or whether it is possible to operate an electrolyzer economically by using electricity that would have been switched off by redispatch measures. In 2021, this amounted to 10.8 TWh of curtailed electricity in Germany as part of the redispatch process (Bundeskartellamt and Bundesnetzagentur, 2022), which could have been used for H_2 production, offering an opportunity to utilize surplus electricity.

References

ABB (2014) *ABB Zentral-Wechselrichter: PVI-500.0-CN* [Online]. Available at https://www.fimer.com/sites/default/files/PVI-500.0_BCD.00451_DE.pdf (Accessed 21 November 2023).

Abomazid, A. M., El-Taweel, N. A. and Farag, H. E. Z. (2022) 'Optimal Energy Management of Hydrogen Energy Facility Using Integrated Battery Energy Storage and Solar Photovoltaic Systems', *IEEE Transactions on Sustainable Energy*, vol. 13, no. 3, pp. 1457–1468.

Ajanovic, A., Sayer, M. and Haas, R. (2022) 'The economics and the environmental benignity of different colors of hydrogen', *International Journal of Hydrogen Energy*, vol. 47, no. 57, pp. 24136–24154.

Almutairi, K., Hosseini Dehshiri, S. S., Hosseini Dehshiri, S. J., Mostafaeipour, A., Jahangiri, M. and Techato, K. (2021) 'Technical, economic, carbon footprint assessment, and prioritizing stations for hydrogen production using wind energy: A case study', *Energy Strategy Reviews*, vol. 36, pp. 1–17.

Andersson, J. and Grönkvist, S. (2019) 'Large-scale storage of hydrogen', *International Journal of Hydrogen Energy*, vol. 44, no. 23, pp. 11901–11919.

Androniceanu, A. and Sabie, O. M. (2022) 'Overview of Green Energy as a Real Strategic Option for Sustainable Development', *Energies*, vol. 15, no. 22, p. 8573.

Apostolou, D., Enevoldsen, P. and Xydis, G. (2019) 'Supporting green Urban mobility – The case of a small-scale autonomous hydrogen refuelling station', *International Journal of Hydrogen Energy*, vol. 44, no. 20, pp. 9675–9689.

Barthelemy, H., Weber, M. and Barbier, F. (2017) 'Hydrogen storage: Recent improvements and industrial perspectives', *International Journal of Hydrogen Energy*, vol. 42, no. 11, pp. 7254–7262.

Benghanem, M., Mellit, A., Almohamadi, H., Haddad, S., Chettibi, N., Alanazi, A. M., Dasalla, D. and Alzahrani, A. (2023) 'Hydrogen Production Methods Based on Solar and Wind Energy: A Review', *Energies*, vol. 16, no. 2, p. 757.

BMWi (2020) *Was ist eigentlich grüner Wasserstoff?* [Online]. Available at https://www.bmwk-energiewende.de/EWD/Redaktion/Newsletter/2020/07/Meldung/direkt-erklaert.html (Accessed 13 October 2023).

BMWK (2023) *Fortschreibung der Nationalen Wasserstoffstrategie*.

Bormann, D. and Johannsmann, S. (2000) *Technische Betriebswirtschaft*, München, Hanser.

Bouché, C. and Wintterlin, K. (1968) 'Energieumsatz im Kolbenverdichter', in Bouché, C. and Wintterlin, K. (eds) *Kolbenverdichter,* Berlin, Heidelberg, Springer Berlin Heidelberg, pp. 28–42.

Bundeskartellamt and Bundesnetzagentur (2022) *Monitoringbericht 2022: Monitoringbericht gemäß § 63 Abs. 3 i.V.m. § 35 EnWG und § 48 Abs. 3 i.V.m. § 53 Abs. 3 GWB,*

Bundesnetzagentur (2023) *SMARD | So funktioniert der Strommarkt* [Online]. Available at https://www.smard.de/page/home/wiki-article/446/384 (Accessed 16 October 2023).

Bynum, M. L., Hackebeil, G. A., Hart, W. E., Laird, C. D., Nicholsen, B. L., Siirola, J. D., Watson, J. and Woodruff, D. L. (2020) *Pyomo: Optimization Modeling in Python*.

Cole, W., Frazier, W. and Augustine, C. (2021) *Cost Projections for Utility-Scale Battery Storage: 2021 Update*.

Cormos, A.-M., Szima, S., Fogarasi, S. and Cormos, C.-C. (2018) 'Economic Assessments of Hydrogen Production Processes Based on Natural Gas Reforming with Carbon Capture', *Chemical Engineering Transactions*, no. 70.

Cuisinier, E., Bourasseau, C., Ruby, A., Lemaire, P. and Penz, B. (2021) 'Techno-economic planning of local energy systems through optimization models: a survey of current methods', *International Journal of Energy Research*, vol. 45, no. 4, pp. 4888–4931.

E.DIS Netz GmbH (2023) *Netzanschluss* [Online]. Available at https://www.e-dis-netz.de/de/energie-anschliessen/stromnetz/netzanschluss.html (Accessed 6 December 2023).

Effe, M. (2023) *Klimatabelle & Klima Rügen | Temperaturen, Sonnenstunden, Regentage* [Online]. Available at https://www.klimatabelle.de/klima/europa/deutschland/klimatabelle-ruegen.htm (Accessed 18 December 2023).

Elberry, A. M., Thakur, J., Santasalo-Aarnio, A. and Larmi, M. (2021) 'Large-scale compressed hydrogen storage as part of renewable electricity storage systems', *International Journal of Hydrogen Energy*, vol. 46, no. 29, pp. 15671–15690.

EnBW (2022) *Windkraft im Wald* [Online]. Available at https://www.enbw.com/unternehmen/eco-journal/wind-im-wald.html (Accessed 26 November 2023).

Epp, J., Scheidler, V., Schmidt, A. and Steiger, P. (2021) *HYSTARTER-REGION RÜGEN-STRALSUND: Die Rolle von Wasserstoff in der regionalen Energie- und Verkehrswende* [Online]. Available at https://www.hy.land/wp-content/uploads/2021/06/HYStarter-Ruegen-Stralsund-WEB.pdf (Accessed 6 June 2023).

European Commission (2023) *Commission Delegated Regulation (EU) 2023/1184,* European Commission [Online]. Available at https://ec.europa.eu/info/law/better-regulation/have-your-say/initiatives/7046068-Produktion-erneuerbarer-Kraftstoffe-Anteil-des-Stroms-aus-erneuerbaren-Energietragern-Vorgaben-_de.

Falcão, D. S. and Pinto, A. (2020) 'A review on PEM electrolyzer modelling: Guidelines for beginners', *Journal of Cleaner Production*, vol. 261, p. 121184.

Fraunhofer ISE (2021) *Cost Forecast for Low-Temperature Electrolysis - Technology Driven Bottom-Up Prognosis for PEM and Alkaline Water Electrolysis Systems*.

Fraunhofer ISE (2023a) *Aktuelle Fakten zur Photovoltaik in Deutschland* [Online]. Available at https://www.ise.fraunhofer.de/de/veroeffentlichungen/studien/aktuelle-fakten-zur-photovoltaik-in-deutschland.html (Accessed 6 June 2023).

Fraunhofer ISE (2023b) *energy-charts.info* [Online]. Available at https://energy-charts.info/ (Accessed 26 November 2023).

Ghaib, K. (2017) *Das Power-to-Methane-Konzept: Von den Grundlagen zum gesamten System*, Wiesbaden, Germany, Springer Vieweg.

Global Wind Atlas (2023) *Global Wind Atlas* [Online]. Available at https://globalwindatlas.info/en (Accessed 18 December 2023).

Google Maps (2023) *Altefähr* [Online]. Available at https://www.google.de/maps/@54.3382738,13.1425292,15.05z?entry=ttu.

Gorre, J., Ruoss, F., Karjunen, H., Schaffert, J. and Tynjälä, T. (2020) 'Cost benefits of optimizing hydrogen storage and methanation capacities for Power-to-Gas plants in dynamic operation', *Applied Energy*, vol. 257, pp. 1–14.

Gurobi Optimization LLC (2023) *Mixed-Integer Programming (MIP) – Gurobi Optimization* [Online]. Available at https://www.gurobi.com/resources/mixed-integer-programming-mip-a-primer-on-the-basics/ (Accessed 30 October 2023).

H2 MOBILITY Deutschland GmbH & Co. KG (2023) *H2 Tanken* [Online]. Available at https://h2.live/ (Accessed 25 November 2023).

Hannan, M. A., Wali, S. B., Ker, P. J., Rahman, M. A., Mansor, M., Ramachandaramurthy, V. K., Muttaqi, K. M., Mahlia, T. and Dong, Z. Y. (2021) 'Battery energy-storage system: A review of technologies, optimization objectives, constraints, approaches, and outstanding issues', *Journal of Energy Storage*, vol. 42, pp. 1–22.

Harris, C. R., Millman, K. J., van der Walt, S. J., Gommers, R., Virtanen, P., Cournapeau, D., Wieser, E., Taylor, J., Berg, S., Smith, N. J., Kern, R., Picus, M., Hoyer, S., van Kerkwijk, M. H., Brett, M., Haldane, A., Del Río, J. F., Wiebe, M., Peterson, P., Gérard-Marchant, P., Sheppard, K., Reddy, T., Weckesser, W., Abbasi, H., Gohlke, C. and Oliphant, T. E. (2020) 'Array programming with NumPy', *Nature*, vol. 585, no. 7825, pp. 357–362.

Hassan, I. A., Ramadan, H. S., Saleh, M. A. and Hissel, D. (2021) 'Hydrogen storage technologies for stationary and mobile applications: Review, analysis and perspectives', *Renewable and Sustainable Energy Reviews*, vol. 149, pp. 1–27.

Hernández-Callejo, L., Gallardo-Saavedra, S. and Alonso-Gómez, V. (2019) 'A review of photovoltaic systems: Design, operation and maintenance', *Solar Energy*, vol. 188, pp. 426–440.

Hofrichter, A., Rank, D., Heberl, M. and Sterner, M. (2023) 'Determination of the optimal power ratio between electrolysis and renewable energy to investigate the effects on the hydrogen production costs', *International Journal of Hydrogen Energy*, vol. 48, no. 5, pp. 1651–1663.

H-TEC SYSTEMS (n.d.) *H-TEC SYSTEMS PEM-Elektrolyseur: ME450* [Online]. Available at https://www.h-tec.com/fileadmin/user_upload/produkte/produktseiten/ME450-1400/spec-sheet/H-TEC-Datenblatt-ME450-DE-23-08.pdf (Accessed 23 November 2023).

Huawei (2023) *Huawei SUN2000L-2KTL FusionSolar PV Wechselrichter* [Online]. Available at https://ske-solar.com/produkt/huawei-sun2000-10ktl-m1-wechselrichter-high-current-version/ (Accessed 21 November 2023).

Hunter, J., Dale, D., Firing, E. and Droettboom, M. (2023) *Matplotlib 3.8.2 documentation* [Online]. Available at https://matplotlib.org/stable/api/index.html (Accessed 6 December 2023).

IEA (2023) *Global Hydrogen Review 2023*.

IRENA (2023a) *Creating a global hydrogen market: Certification to enable trade: Certification to enable trade*.

IRENA (2023b) *Renewable power generation costs in 2022,* International Renewable Energy Agency.

Jarosch, C., Jahnke, P., Giehl, J. and Himmel, J. (2022) 'Modelling Decentralized Hydrogen Systems: Lessons Learned and Challenges from German Regions', *Energies*, vol. 15, no. 4, p. 1322.

JetBrains (2023) *PyCharm: the Python IDE for Professional Developers by JetBrains* [Online]. Available at https://www.jetbrains.com/pycharm/ (Accessed 5 December 2023).

Khan, M. A., Young, C., MacKinnon, C. and Layzell, D. (2021) 'The Techno-Economics of Hydrogen Compression', *Transition Accelerator Technical Briefs*, vol. 1, no. 1, pp. 1–36 [Online]. Available at https://transitionaccelerator.ca/wp-content/uploads/2023/04/TA-Technical-Brief-1.1_TEEA-Hydrogen-Compression_PUBLISHED.pdf.

Khatib, T. and Deria, R. (2022) 'East-west oriented photovoltaic power systems: model, benefits and technical evaluation', *Energy Conversion and Management*, vol. 266, p. 115810.

Klemm, C. and Vennemann, P. (2021) 'Modeling and optimization of multi-energy systems in mixed-use districts: A review of existing methods and approaches', *Renewable and Sustainable Energy Reviews*, vol. 135, pp. 1–16.

Kurzweil, P. and Dietlmeier, O. K. (2018) *Elektrochemische Speicher*, Wiesbaden, Springer Fachmedien Wiesbaden.

Leupoldina (2022) *Welche Auswirkungen hat der Ukrainekrieg auf die Energiepreise und Versorgungsicherheit in Europa? (Impuls)* [Online]. Available at https://www.leopoldina.org/fileadmin/redaktion/Publikationen/Nationale_Empfehlungen/2022_ESYS_Sonderimpuls_Versorgungssicherheit_web.pdf.

Linde GmbH (2016) *Produkdatenblatt: Wasserstoff 3.0* [Online]. Available at https://static.prd.echannel.linde.com/wcsstore/DE_REC_Industrial_Gas_Store/datasheets/pds/wasserstoff_3.0.pdf.

Lütkehus, I., Salecker, H. and Adlunger, K. (2013) *Potenzial der Windenergie an Land: Studie zur Ermittlung des bundesweiten Flächen-und Leistungspotentials der Windenergie an Land*.

Mamia, I. and Appelbaum, J. (2016) 'Shadow analysis of wind turbines for dual use of land for combined wind and solar photovoltaic power generation', *Renewable and Sustainable Energy Reviews*, vol. 55, pp. 713–718.

Nationaler Wasserstoffrat (2021) 'Wasserstofftransport' [Online]. Available at https://www.wasserstoffrat.de/fileadmin/wasserstoffrat/media/Dokumente/2021-07-02_NWR-Grundlagenpapier_Wasserstofftransport.pdf (Accessed 25 November 2023).

Neubauer, N. (2023) *Model–Based Techno–Economic Optimization of a Grid Serving Electrolyzer on an Industrial Scale*, Master Thesis, HAW Hamburg [Online]. Available at https://reposit.haw-hamburg.de/bitstream/20.500.12738/14404/1/Grid_Serving_Electrolyzer.pdf.

Pandas development team (2023) *API reference — pandas 2.1.3 documentation* [Online]. Available at https://pandas.pydata.org/pandas-docs/stable/reference/index.html (Accessed 6 December 2023).

Petkov, I. and Gabrielli, P. (2020) 'Power-to-hydrogen as seasonal energy storage: an uncertainty analysis for optimal design of low-carbon multi-energy systems', *Applied Energy*, vol. 274, pp. 1–25.

Pfenninger, S. and Staffell, I. (2016) 'Long-term patterns of European PV output using 30 years of validated hourly reanalysis and satellite data', *Energy*, vol. 114, pp. 1251–1265.

Pieper, M. (2017) *Mathematische Optimierung: Eine Einführung in die kontinuierliche Optimierung mit Beispielen*, Wiesbaden, Heidelberg, Springer Fachmedien Wiesbaden GmbH.

Ponitka, J. and Boettner, S. (2020) 'Challenges of future energy landscapes in Germany — a nature conservation perspective', *Energy, Sustainability and Society*, vol. 10, no. 17.

Quaschning, V. (2019) *Regenerative Energiesysteme: Technologie - Berechnung - Klimaschutz*, 10th edn, München, Hanser.

renewables.ninja (n. d.) *renewables.ninja* [Online]. Available at https://www.renewables.ninja/ (Accessed 21 December 2023).

Reuß, M., Grube, T., Robinius, M., Preuster, P., Wasserscheid, P. and Stolten, D. (2017) 'Seasonal storage and alternative carriers: A flexible hydrogen supply chain model', *Applied Energy*, vol. 200, pp. 290–302.

Schmidt, O., Gambhir, A., Staffell, I., Hawkes, A., Nelson, J. and Few, S. (2017) 'Future cost and performance of water electrolysis: An expert elicitation study', *International Journal of Hydrogen Energy*, vol. 42, no. 52, pp. 30470–30492.

Schuster, T. and Rüdt von Collenberg, L. (2017) *Investitionsrechnung: Kapitalwert, Zinsfuß, Annuität, Amortisation*, Berlin, Heidelberg, Springer Berlin Heidelberg.

Schütte, C., Neubauer, N., Röben, F., Hölling, M., Genz, L., Edens, T., Henne, H.-C. and Schweininger, K. (2022) *Decarbonization of the Metal Industry in Hamburg - Demand, Efficiency and Costs of Green Hydrogen*.

Sens, L., Piguel, Y., Neuling, U., Timmerberg, S., Wilbrand, K. and Kaltschmitt, M. (2022) 'Cost minimized hydrogen from solar and wind – Production and supply in the European catchment area', *Energy Conversion and Management*, vol. 265, p. 115742.

Short, W., Packey, D. and Holt, T. (1995) *A Manual for the Economic Evaluation of Energy Efficiency and Renewable Energy Technologies*.

Smolinka, T., Wiebe, N., Sterchele, P., Fraunhofer-Institut für Solare Energiesysteme ISE / Freiburg – Deutschland, Franz Lehner, E4tech Sàrl / Lausanne – Schweiz, Steffen Kiemel, Robert Miehe, Sylvia Wahren, Fabian Zimmermann and (Fraunhofer-Institut für Produktionstechnologie und Automatisierung IPA -Stuttgart – Deutschland) (2018) *Studie IndWEDe Industrialisierung der Wasser-elektrolyse in -Deutschland: -Chancen und -Herausforderungen für nachhaltigen Wasserstoff für Verkehr, Strom und -Wärme*.

Srinivasan, R. (2021) *Feasibility Study of Green Hydrogen Production Using a Battery-Assisted Solar Photovoltaic System in Germany*, Master Thesis, Hamburg, HAW Hamburg.

Staffell, I. and Pfenninger, S. (2016) 'Using bias-corrected reanalysis to simulate current and future wind power output', *Energy*, vol. 114, pp. 1224–1239.

Staiger, R. and Tanțău, A. (2020) *Geschäftsmodellkonzepte mit grünem Wasserstoff*, Wiesbaden, Springer Fachmedien Wiesbaden.

Statista (2021) *Wind-Volllaststunden nach Standorten für WEA in Deutschland 2021* [Online]. Available at https://de.statista.com/statistik/daten/studie/224720/umfrage/wind-volllaststunden-nach-standorten-fuer-wea/ (Accessed 29 October 2023).

Terlouw, T., Bauer, C., McKenna, R. and Mazzotti, M. (2022) 'Large-scale hydrogen production via water electrolysis: a techno-economic and environmental assessment', *Energy & Environmental Science*, vol. 15, no. 9, pp. 3583–3602.

Umweltbundesamt (2023) *Photovoltaik* [Online]. Available at https://www.umweltbundesamt.de/themen/klima-energie/erneuerbare-energien/photovoltaik#freifl%C3%A4chen (Accessed 2 November 2023).

Urbanucci, L. (2018) 'Limits and potentials of Mixed Integer Linear Programming methods for optimization of polygeneration energy systems', *Energy Procedia*, vol. 148, pp. 1199–1205.

van Rossom, G. (2023) *The Python Language Reference (3.11)* [Online]. Available at https://docs.python.org/3/reference/index.html (Accessed 6 December 2023).

Vartiainen, E., Masson, G., Breyer, C., Moser, D. and Román Medina, E. (2019) 'Impact of weighted average cost of capital, capital expenditure, and other parameters on future utility-scale PV levelised cost of electricity', *Progress in Photovoltaics: Research and Applications*, vol. 28, no. 6, pp. 439–453.

Weimann, L., Gabrielli, P., Boldrini, A., Kramer, G. J. and Gazzani, M. (2021) 'Optimal hydrogen production in a wind-dominated zero-emission energy system', *Advances in Applied Energy*, vol. 3, p. 100032.

Wiegleb, G. (2016) 'Physikalische Eigenschaften von Gasen', in Wiegleb, G. (ed) *Gasmesstechnik in Theorie und Praxis,* Wiesbaden, Springer Fachmedien Wiesbaden, pp. 7–118.

windpower.net (2023) *Nordex N100/2500* [Online]. Available at https://www.thewindpower.net/turbine_de_224_nordex_n100-2500.php.

Statutory Declaration

I herewith declare that I have composed the present thesis myself and without using any other than the cited sources and aids. Sentences or parts of sentences quoted literally are marked as such; other references with regard to the statement and scope are indicated by full details of the publications concerned. The thesis in the same or similar form has not been submitted to any examination body or published. This thesis was not yet, even in part, used in another examination or as a course performance. Furthermore, I declare that the submitted written (bound) copies of the present thesis and the version submitted on a data carrier are consistent with each other in contents.

Date, Max Lüdemann

Appendix

A Results of exclusive electricity feed in

	Total Profit in €/a	Sold electricity in kWh/a	Electricity revenue in €/a	Sold H2 in t/a	H2 revenue in €/a	Costs per year in €/a	PT in years	ROI in %	Total investment in €	Depreciation in €/a	OPEX in €/a
PV	60,323	61,332,373	2,352,905	-	-	2,292,582	23.63	0.83	31,822,500	1,892,582	400,000
PV + Wind	60,323	61,332,373	2,352,905	-	-	2,292,582	23.63	0.83	31,822,500	1,892,582	400,000
PV + Grid restriction	14,316	14,688,150	563,595	-	-	549,279	23.64	0.83	7,624,555	453,351	95,928
PV + Wind + Grid restriction	14,316	14,688,150	563,595	-	-	549,279	23.64	0.83	7,624,555	453,351	95,928

	Power PV South in kW	Power Inverter in kW	Power Wind in kW	Power Electrolyzer in kW	Capacity compressor in kgH2/h	Capacity H2-Storage in t	LCOH2 in €/kg	LCOH2 incl. Electricity revenue in €/kg	LCOE in €/kWh	Electricity not used in kWh
PV	50,000	42,500	-	-	-	-	0.00	0.00	0.035	1,941,750
PV + Wind	50,000	42,500	-	-	-	-	0.00	0.00	0.035	1,941,750
PV + Grid restriction	11,991	10,000	-	-	-	-	0.00	0.00	0.035	486,886
PV + Wind + Grid restriction	11,991	10,000	-	-	-	-	0.00	0.00	0.035	486,886

B Results of combined electricity feed in and hydrogen production

	Total Profit in €/a	Sold electricity in kWh/a	Electricity revenue in €/a	Sold H2 in t/a	H2 revenue in €/a	Costs per year in €/a	PT in years	ROI in %	Total investment in €	Depreciation in €/a	OPEX in €/a
PV + Ely	1,869,866	15,702,816	579,749	839	6,295,018	5,004,902	12.33	3.60	52,561,147	3,824,183	1,180,719
PV + Wind + Ely	4,649,646	14,865,114	537,476	1,457	10,925,296	6,813,125	9.90	5.62	70,640,170	5,089,654	1,723,471
PV + Ely + Grid restriction	1,766,561	8,957,183	332,506	909	6,820,304	5,386,248	12.39	3.46	55,323,552	4,088,821	1,297,428
PV + Wind + Ely + Grid restriction	4,558,389	8,870,853	322,434	1,520	11,401,807	7,165,852	9.99	5.46	73,230,474	5,336,549	1,829,303

	Power PV South in kW	Power Inverter in kW	Power Wind in kW	Power Electrolyzer in kW	Capacity compressor in kg_{H2}/h	Capacity H2-Storage in t	LCOH2 in €/kg	LCOH2 incl. Electricity revenue in €/kg	LCOE in €/kWh	LCOE in €/kWh	Electricity not used kWh
PV + Ely	50,000	22,500	-	19,750	351	158,388	5.96	5.27	0.034	34.34	733,167
PV + Wind + Ely	48,160	17,500	10,000	23,250	413	238,764	4.68	4.31	0.035	35.04	789,195
PV + Ely + Grid restriction	50,000	10,500	-	22,750	404	177,300	5.92	5.56	0.034	33.83	3,662,940
PV + Wind + Ely + Grid restriction	48,160	9,000	10,000	26,000	462	252,948	4.71	4.50	0.035	34.81	3,253,300

C Results of combined electricity feed in and hydrogen production (demand low)

	Total Profit in €/a	Sold electricity in kWh/a	Electricity revenue in €/a	Sold H2 in t/a	H2 revenue in €/a	Costs per year in €/a	PT in years	ROI in %	Total investment in €	Depreciation in €/a	OPEX in €/a
PV + Ely + Demand low	654,855	11,899,671	434,980	915	6,861,607	6,641,733	14.54	2.20	67,086,261	4,961,544	1,680,189
PV + Wind + Ely + H2-Demand low	4,649,646	14,865,114	537,476	1,457	10,925,296	6,813,125	9.90	5.62	70,640,170	5,089,654	1,723,471
PV + Ely + Grid restriction + H2-Demand low	595,425	7,606,734	278,764	961	7,208,286	6,891,625	14.49	2.17	68,822,656	5,135,137	1,756,489
PV + Wind + Ely + Grid restriction + H2-Demand low	4,558,389	8,870,853	322,434	1,520	11,401,807	7,165,852	9.99	5.46	73,230,474	5,336,549	1,829,303

	Power PV South in kW	Power Inverter in kW	Power Wind in kW	Power Electro-lyzer in kW	Capacity compres-sor in kg_{H2}/h	Capacity H2-Stor-age in t	LCOH2 in €/kg	LCOH2 incl. Electricity reve-nue in €/kg	LCOE in €/kWh	LCOE in €/kWh	Electric-ity not used kWh
PV + Ely + Demand low	50,000	19,500	-	22,750	404	1,224,552	7.26	6.78	0.034	34.21	618,450
PV + Wind + Ely + H2-De-mand low	48,160	17,500	10,000	23,250	413	238,764	4.68	4.31	0.035	35.04	789,195
PV + Ely + Grid re-striction + H2-Demand low	50,000	10,500	-	25,000	444	1,208,004	7.17	6.88	0.034	33.83	2,379,594
PV + Wind + Ely + Grid re-striction + H2-Demand low	48,160	9,000	10,000	26,000	462	252,948	4.71	4.50	0.035	34.81	3,252,908

D Results of combined electricity feed in and hydrogen production (demand high)

	Total Profit in €/a	Sold electricity in kWh/a	Electricity revenue in €/a	Sold H2 in t/a	H2 revenue in €/a	Costs per year in €/a	PT in years	ROI in %	Total investment in €	Depreciation in €/a	OPEX in €/a
PV + Ely + Demand high	- 7,991,738	6,082,805	216,850	1,061	7,954,418	16,163,006	28.75	-1.43	154,214,561	11,540,339	4,622,667
PV + Wind + Ely + H2-Demand high	4,546,722	13,058,174	469,621	1,490	11,174,491	7,097,390	10.03	5.44	72,995,702	5,289,289	1,808,101
PV + Ely + Grid restriction + H2-Demand high	- 8,001,533	5,507,232	197,447	1,061	7,954,418	16,153,398	28.79	-1.44	154,085,061	11,530,731	4,622,667
PV + Wind + Ely + Grid restriction + H2-Demand high	4,472,261	8,201,722	295,953	1,540	11,548,529	7,372,221	10.10	5.32	74,986,702	5,481,772	1,890,449

	Power PV South in kW	Power Inverter in kW	Power Wind in kW	Power Electrolyzer in kW	Capacity compressor in kg_{H2}/h	Capacity H2-Storage in t	LCOH2 in €/kg	LCOH2 incl. Electricity revenue in €/kg	LCOE in €/kWh	LCOE in €/kWh	Electricity not used kWh
PV + Ely + Demand high	50,000	14,000	-	28,500	506	8,699,520	15.24	15.04	0.034	33.98	414,445
PV + Wind + Ely + H2-Demand high	48,160	16,000	10,000	24,500	435	345,144	4.76	4.45	0.035	35.00	757,717
PV + Ely + Grid restriction + H2-Demand high	50,000	10,500	-	28,500	506	8,699,520	15.23	15.04	0.034	33.83	1,007,819
PV + Wind + Ely + Grid restriction + H2-Demand high	48,160	9,000	10,000	26,750	475	345,144	4.79	4.60	0.035	34.81	2,857,283

E Results of combined electricity feed in and hydrogen production (electricity prices 2022)

	Total Profit in €/a	Sold electricity in kWh/a	Electricity revenue in €/a	Sold H2 in t/a	H2 revenue in €/a	Costs per year in €/a	PT in years	ROI in %	Total investment in €	Depreciation in €/a	OPEX in €/a
Without grid restriction and demand	18,766,360	96,466,461	22,333,142	-	-	3,566,782	3.51	24.93	45,764,800	2,781,502	785,280
Without grid restriction and with demand low	17,391,161	76,831,810	19,490,202	398	2,657,770	4,756,811	4.15	20.14	55,263,072	3,625,480	1,131,331
With grid restriction and without demand	11,986,683	46,433,015	12,400,588	777	5,825,359	6,239,264	5.86	12.69	65,978,146	4,674,130	1,565,135
With grid restriction and demand low	11,899,567	45,056,426	12,144,552	805	6,036,691	6,281,676	5.90	12.56	66,312,849	4,703,936	1,577,740

	Power PV South in kW	Power Inverter in kW	Power Wind in kW	Power Electrolyzer in kW	Capacity compressor in kg_{H2}/h	Capacity H2-Storage in t	LCOH2 in €/kg	LCOH 2 incl. Electricity revenue in €/kg	LCOE in €/kWh	Electricity not used kWh
Without grid restriction and demand	48,160	44,000	10,000	-	-	-	-	-	0.036	1,391,294
Without grid restriction and with demand low	48,160	39,000	10,000	7,000	124	245,856	13.42	- 41.58	0.036	1,030,323
With grid restriction and without demand	48,160	10,500	10,000	19,750	351	156,024	8.03	- 7.93	0.035	8,017,994
With grid restriction and demand low	48,160	10,000	10,000	20,000	355	165,480	7.80	- 7.28	0.035	7,789,856

F Capacity of System Components and $LCOH_2$ for Scenarios with a Combined Electricity Feed in, Hydrogen Production Without a Demand

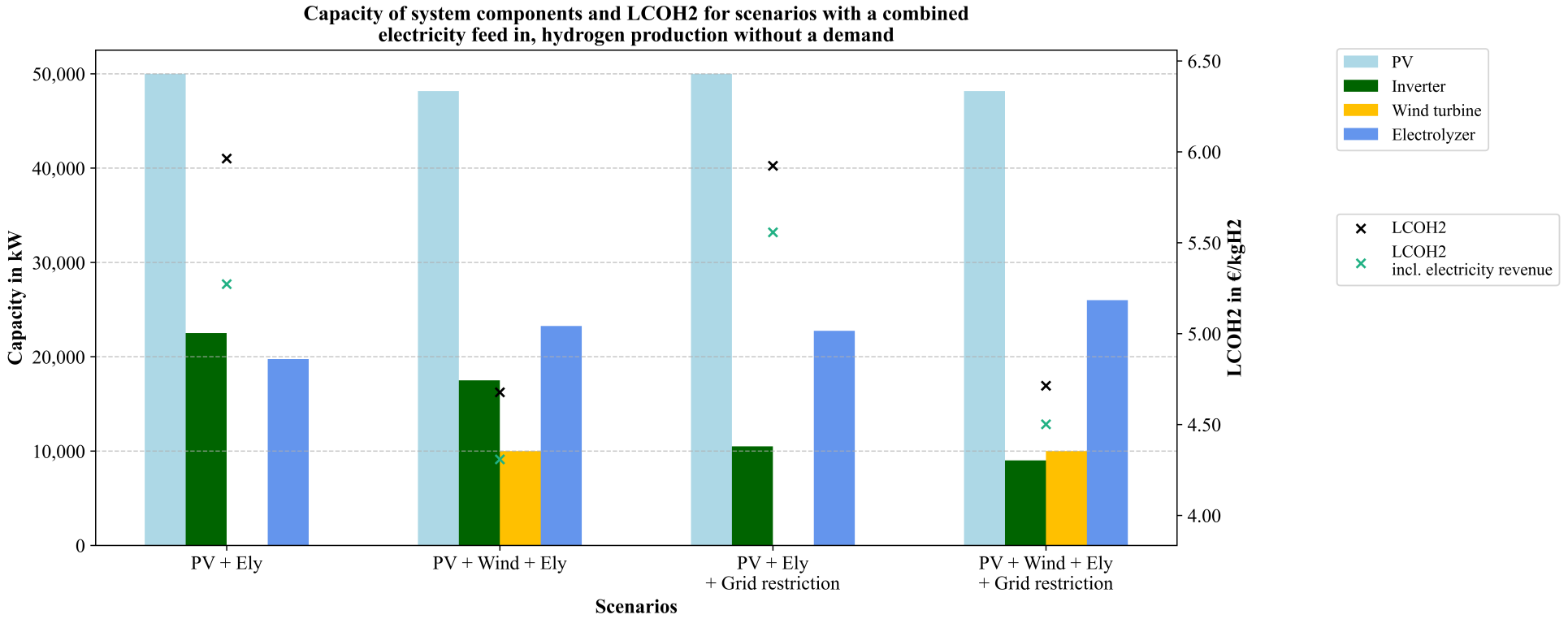

G Capacity of Compressor and H_2 Storage for Scenarios with a Combined Electricity Feed in, Hydrogen Production Without a Demand

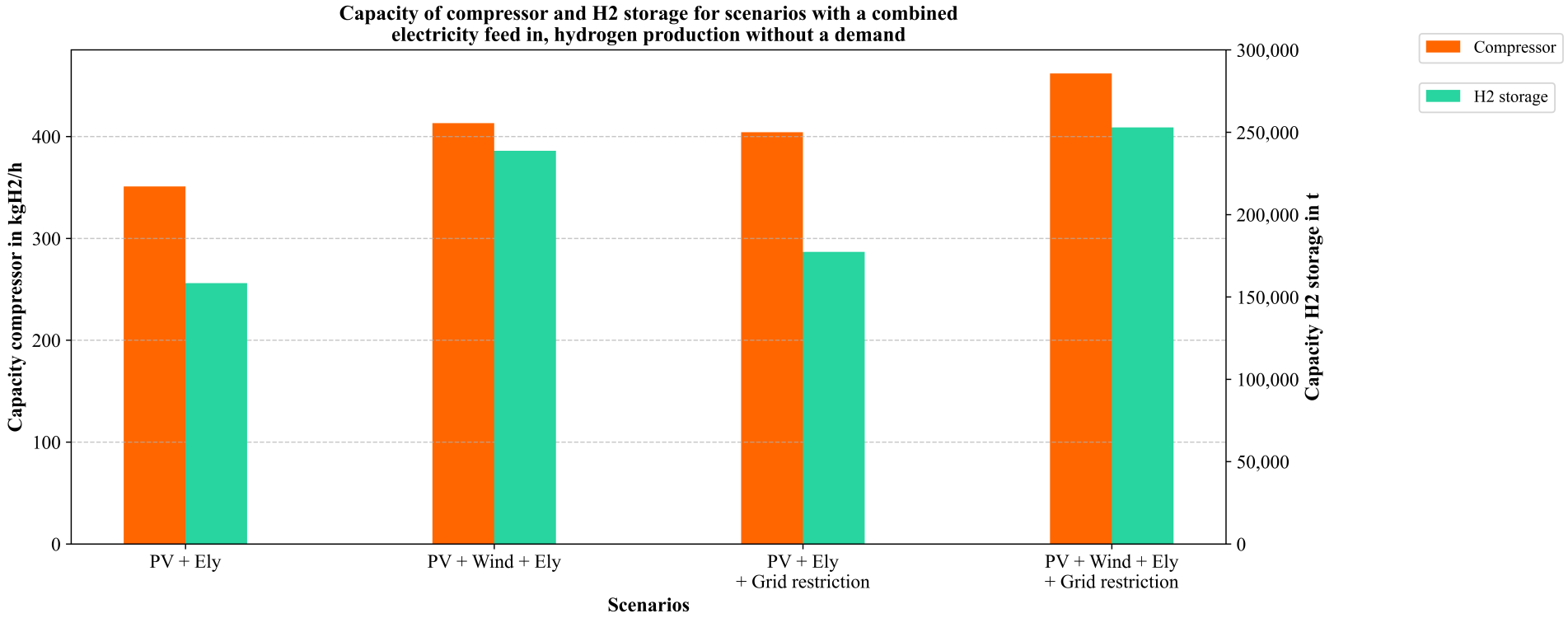

H Capacity of System Components and $LCOH_2$ for Scenarios with a Combined Electricity Feed in, Hydrogen Production and Demand low

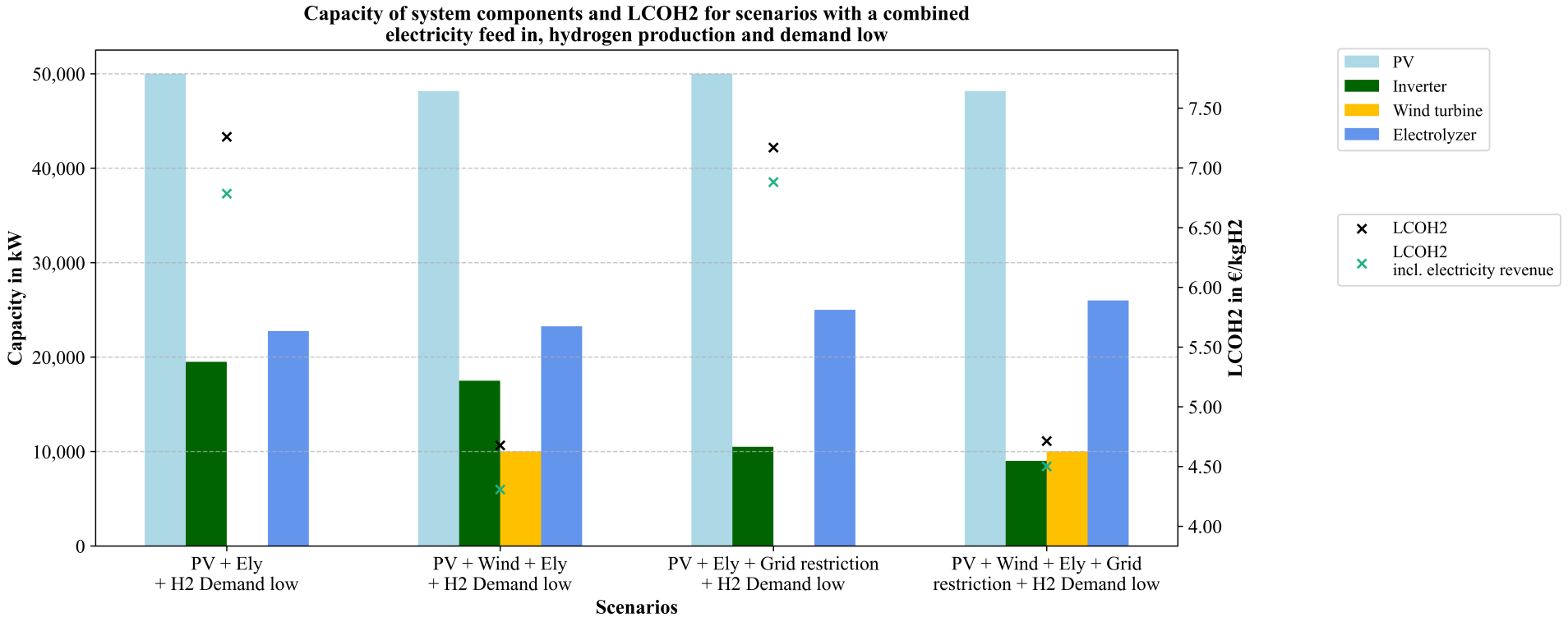

I Capacity of Compressor and H_2 Storage for Scenarios with a Combined Electricity Feed in, Hydrogen Production Without and Demand low

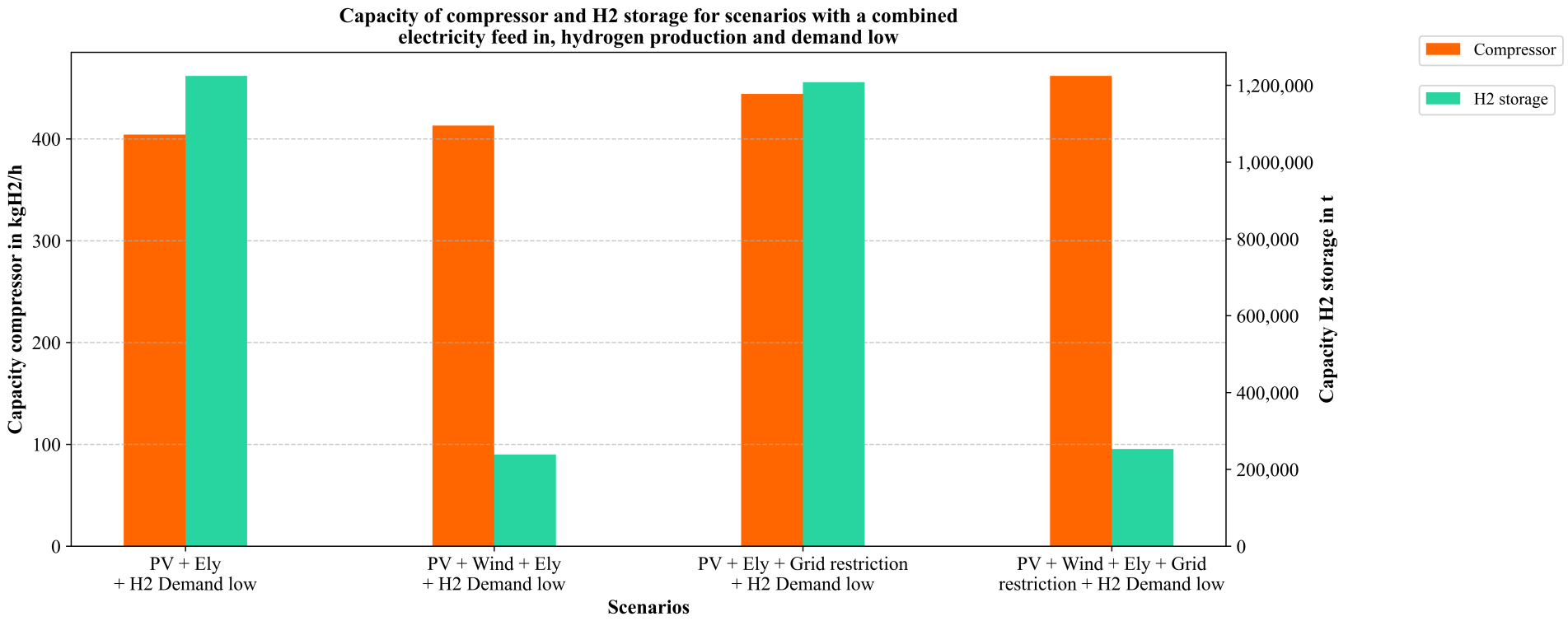

J Capacity of System Components and $LCOH_2$ for Scenarios with a Combined Electricity Feed in, Hydrogen Production and Demand high

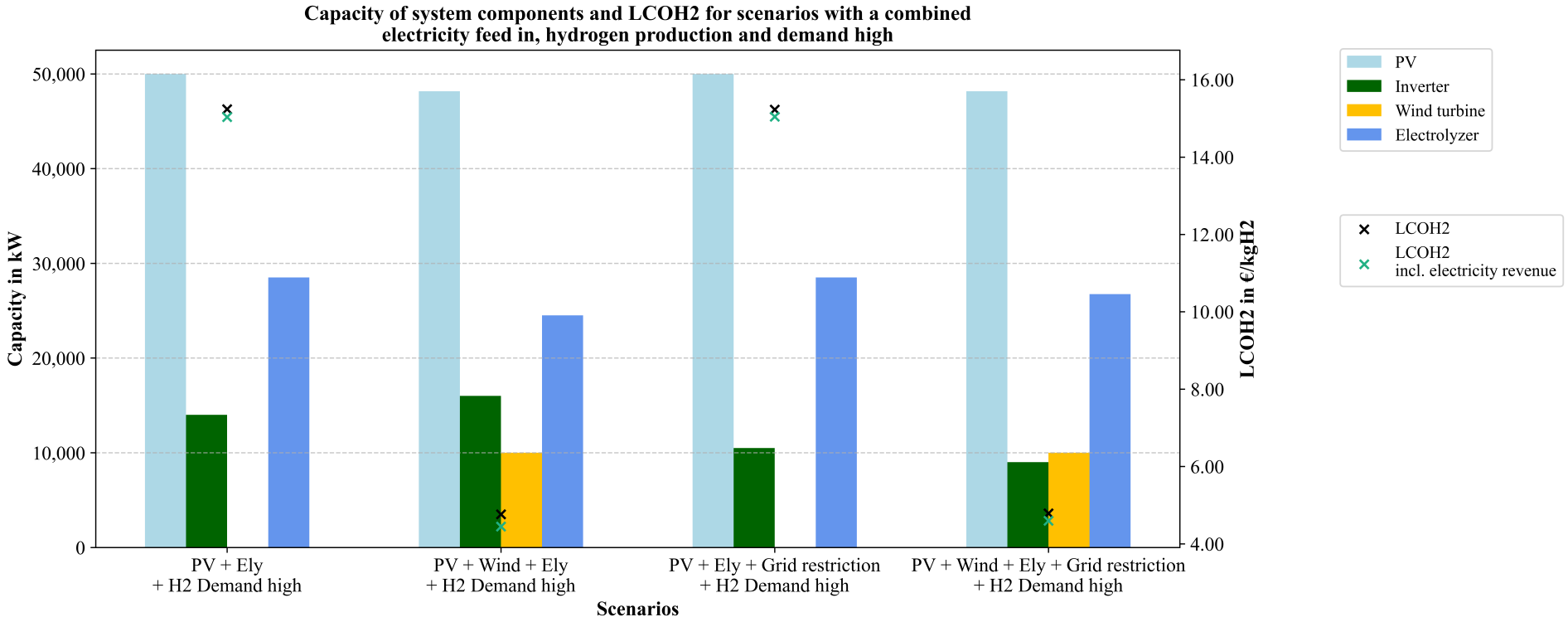

K Capacity of Compressor and H_2 Storage for Scenarios with a Combined Electricity Feed in, Hydrogen Production Without and Demand High

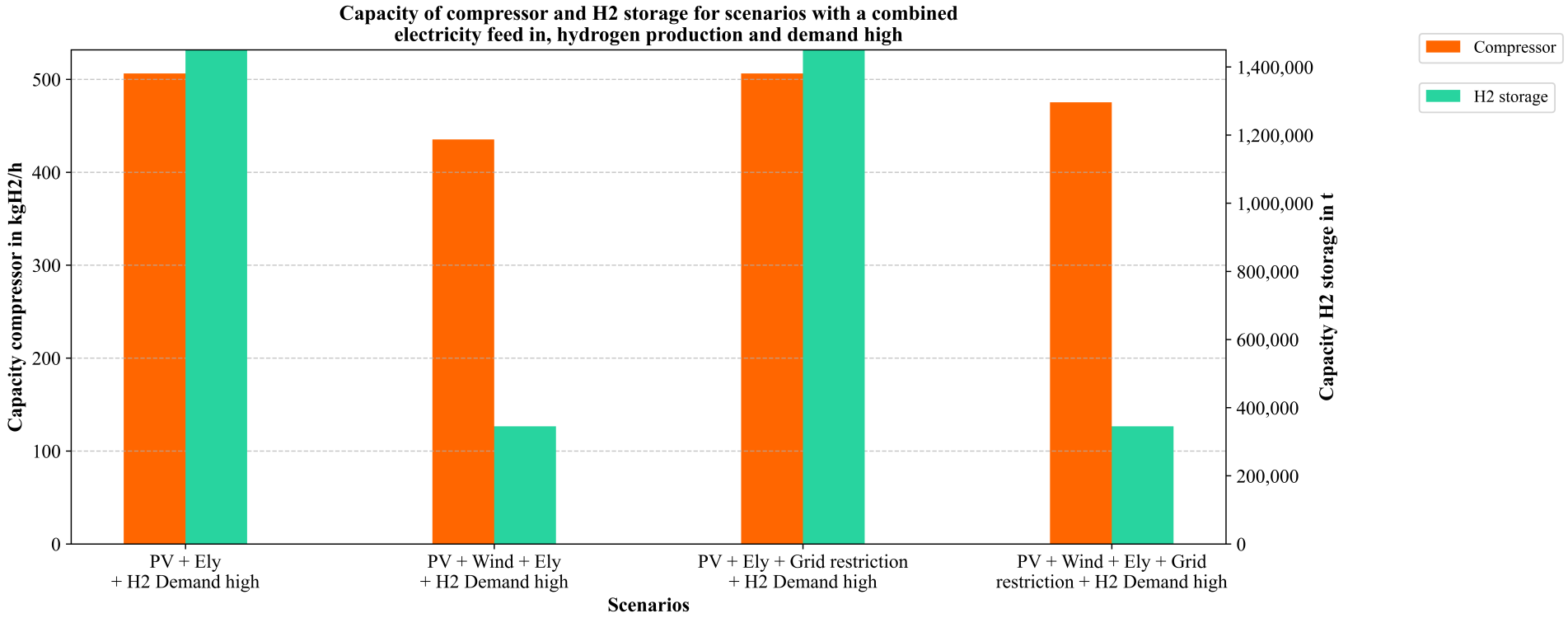

L Capacity of System Components and $LCOH_2$ for Scenarios with a Combined Electricity Feed in and Hydrogen Production with Electricity Prices from 2022

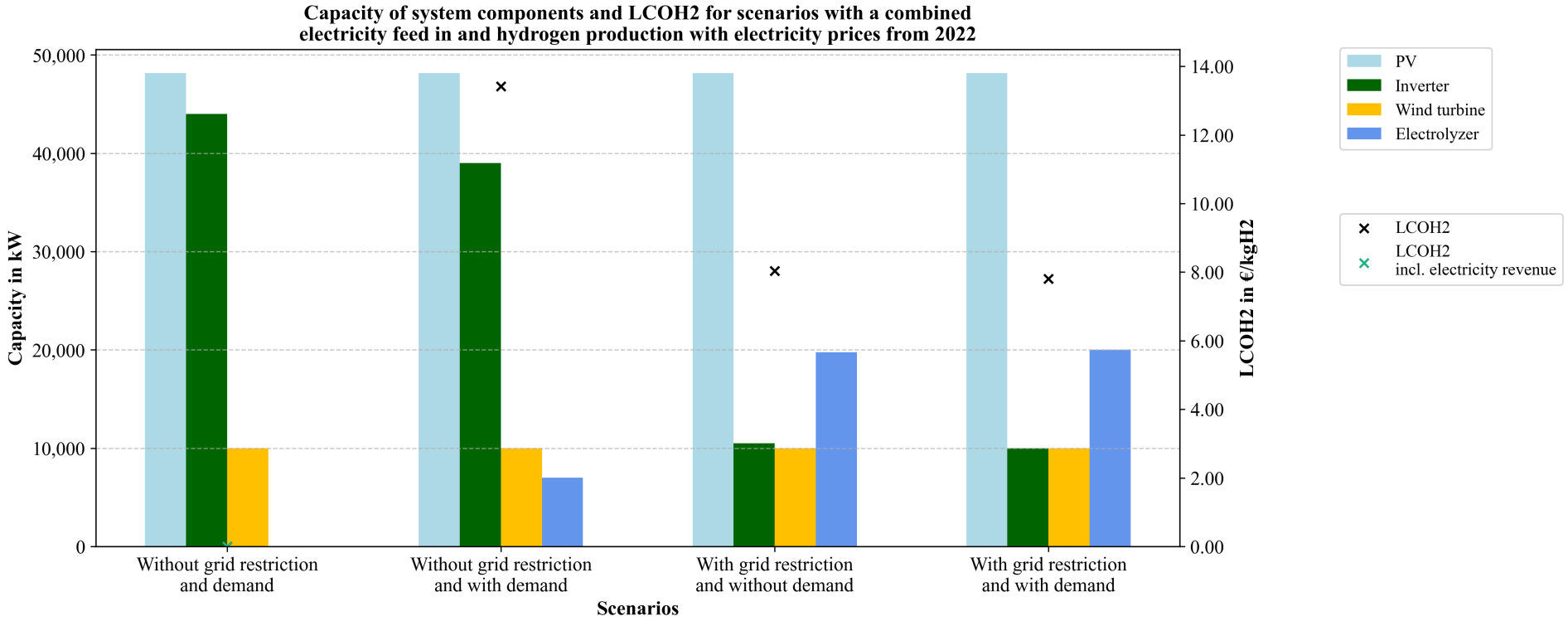

M Capacity of Compressor and H_2 Storage for Scenarios with a Combined Electricity Feed in and Hydrogen Production with Electricity Prices from 2022